Selective Catalytic Reduction of NO_x by hydrocarbon using bimetallic Ag-Au supported on alumina catalyst

Thesis Submitted to AcSIR for the Award of the degree of

DOCTOR OF PHILOSOPHY

In Chemical Science

by

Pavan Manohar More

Enrollment No- 10CC11J26060

Under the guidance of

Dr. Shubhangi B. Umbarkar

Catalysis & Inorganic Chemistry Division
CSIR - National Chemical Laboratory
Pune - 411 008, India

2015

राष्ट्रीय रासायनिक प्रयोगशाला
(वैज्ञानिक तथा औद्योगिक अनुसंधान परिषद)
डॉ. होमी भाभा मार्ग पुणे - 411 008, भारत
NATIONAL CHEMICAL LABORATORY
(Council of Scientific & Industrial Research)
Dr. Homi Bhabha Road, Pune - 411 008, India.

Certificate of the Guide

Certified that the work incorporated in the thesis, ***"Selective Catalytic Reduction of NO_x by hydrocarbon using bimetallic Ag-Au supported on alumina catalyst"***submitted by ***Pavan More,*** for the Degree of ***Doctor of Philosophy,*** was carried out by the candidate under my supervision in the Catalysis & Inorganic Chemistry Division, National Chemical Laboratory, Pune – 411 008, India. Such material as has been obtained from other sources has been duly acknowledged in the thesis.

(**Dr. S. B. Umbarkar**) Date:

Research Guide

Communication Channels
NCL Level DID : 2590
NCL Board No. : +91-20-25902000
EPABX : +91-20-25893300
+91-20-25893400
FAX
Director's Office : +91-20-25893355
COA's Office : +91-20-25893619
COS&P's Office : +91-20-25893008
WEBSITE
www.ncl-india.org

Certificate of the Guide

Certified that the work incorporated in the thesis, ***"Selective Catalytic Reduction of NO_x by hydrocarbon using bimetallic Ag-Au supported on alumina catalyst"*** submitted by ***Pavan More,*** for the Degree of ***Doctor of Philosophy,*** was carried out as a part of "International Associated Laboratory" program under collaboration between CSIR-NCL, Pune, India and UCCS, Lille University, CNRS, France.

(Dr. S. B. Umbarkar) (Prof. Pascal Granger)

Declaration by the Candidate

I, hereby declare that the thesis entitled ***"Selective Catalytic Reduction of NO_x by hydrocarbon using bimetallic Ag-Au supported on alumina catalyst"*** submitted by me for the degree of ***Doctor of Philosophy*** to the ***Academy of Scientific and Innovative Research (AcSIR)***, is the record of work carried out by me at ***Catalysis & Inorganic Chemistry Division, National Chemical Laboratory*** under the guidance of ***Dr. S. B. Umbarkar*** and has not formed the basis for the award of any degree or diploma to this or any other University. I further declare that the material obtained from other sources has been duly acknowledged in the thesis.

(Pavan More) Date:

Signature of the Candidate

Dedicated to His holiness Nirankari Babaji and my Mom.....

The best True master and Mother a son could have…

Acknowledgements

Several people have been instrumental in the completion of this thesis work & I take this opportunity to express my gratitude towards them.

It gives me immense pleasure to sincerely acknowledge my research guide ***Dr. S. B. Umbarkar*** *for her invaluable guidance, patience and support given throughout the course of this investigation. Where others see obstacles she sees opportunities, and where others see failure she sees potential. Her constant encouragement and insight have led to the successful completion of this work. She will always continue to be an inspiring influence for the rest of my life.*

I take this opportunity to express my deepest sense of gratitude and indebtedness to ***Dr. Mohan Dongare*** *for his guidance and suggestions throughout my research work. Without his patience and moral support it would have been difficult for me to complete this work. His friendly nature ensured that I never felt any hesitations in approaching him for scientific discussions. I shall remain grateful to him forever.*

I am grateful to ***Prof. Pascal Granger and Prof. Christophe Dujardin, Lille university, France*** *for for providing me facilities to carry out my Ph. D. work as a part of "International Associated Laboratory" program under collaboration between CSIR-NCL, Pune, India and UCCS, Lille University, CNRS, France. I am thankful to CNRS France for financial support during my stay at lille.*

I express my thanks to ***Dr. Ankush Biradar*** *for his help and efforts during difficult time in the course of Ph.D..*

I extend my thanks to Dr. Vinod, Dr. C.S. Gopinath, Dr. C.V.V. Satyanarayana, Dr. T. Raja, Dr. Shrinivas, Dr. Dhepe, Dr. Nandini Devi and all other scientific & non-scientific staff of Catalysis Division, National Chemical Laboratory, Pune for the help they rendered during my tenure as a research student.

I would like to extend a very special thank you to three individuals, Mr. Purushothaman, Madhu from the Catalysis Division, Mr. Chaudhary, Nair, Gosavi, Lokesh, from the Glass Blowing Section and Mr. Prashant Mane from Organic Chemistry Division, Mr. S. M. Mane, Mr. A. Patil, Mr. S. Jogdand, Mr. Rajopaddhay from Civil section and Mr. Sharaque Inamdar from account section for helping me in their own ways during my stay at N.C.L.

My sincere thanks to Dr. Sourav Pal, Director, National Chemical Laboratory, Pune for providing the infrastructure to carry out the research work and utilize the facilities.

The financial assistance in the form of Research Fellowship from University Grant Commission, New Delhi, is duly acknowledged.

Special thanks to my postgraduate teacher Dr. P. Sonawane, Dr. (Mrs.) Kale, Mr. H. Pawar, Dr. Chikate, Dr. A. Natu, Dr. (Mrs.) Bivare, Dr. (Mrs.) Waghmode who introduced me to the field of research. Without their initiative all this would not have happened.

I attribute very little of my success to myself, because it is the people around me who give me the ability to do what I do.

I take this opportunity to thank my friends in the laboratory, Rajni and Luan, from Lille University France for their cheerful co-operation and affection. I will cherish the happy moments we shared together for a long time to come. I also thank Trupti, Vaibhav, Swati, Prakash, Rajesh, Vidhya, Atul, Reshma, and Dhananjay for their co-operation and help.

It is a pleasure to thank Dr. Ajeet, Ashok, Hanmant, Atul and Prasenjit for their timely assistance and friendly support.

I owe my deepest gratitude to my Mom & Babaji, for their unfailing love that has helped me throughout my life. His holiness is the constant inspiring source for me throughout my life. He always enlightens me with positive thought.

I have no words to express my gratitude to my brothers Sunny, without his support its difficult to complete my post graduation. Thanks a lot for being so understanding & supportive throughout the course of this thesis period. His unstinted love & support is warmly acknowledged.

Finally, I thank Shital for being my best friend and for being there for me in times of need.

Pavan More

Content

Chapter 1: Introduction

1. Introduction

J. J. Berzelius introduced a word catalyst in 1836 as a compound which increases the rate of a chemical reaction, without getting consumed in the reaction [1]. Mitscherlich first discovered this phenomenon through contact process and later Berzelius coin the word "catalyst". A catalyst accelerates a chemical reaction by forming bonds with the reacting molecules and by allowing these to react to form a product. Product detaches from the catalyst and leaves the catalyst unaltered such that it is available for the next reaction. Catalysis is a widely occurring process in nature. For example, living matter relies on enzymes which catalyse numerous biological transformations and involve complex large molecular weight structures that are evolved in nature over millions of years to carry out particular reactions very selectively. The role of the catalyst is to provide an alternate reaction pathway between reactants and products by lowering the activation energy of the reaction.

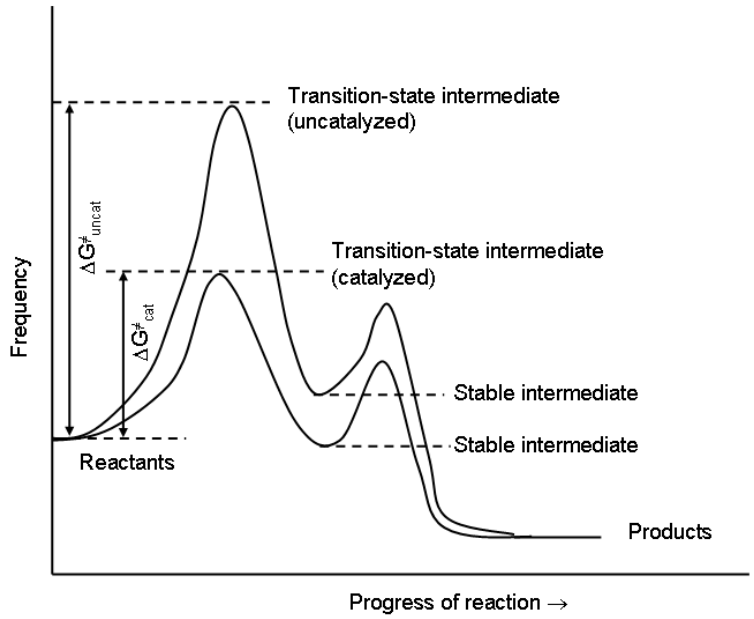

Fig. 1. Transformation of reactant into product

Effect of the catalysts on a thermodynamically favourable reaction

Transformations of reactants into product through intermediate require activation energy as shown in Fig 1. Without catalyst reaction require high activation energy. A catalyst decreases the activation energy of a reaction ($\Delta G^{\neq}$ is lowered), thereby increasing the rate of the reaction but has no effect on the chemical equilibrium of the reaction (ΔG remains the

same). The action of a catalyst can be very specific, which under ideal conditions results in selective formation of the desired product and avoid side reactions.

Catalysis is ubiquitous to life as well as society. Catalytic processes occur everywhere, i.e. in production of food, clothes, energy and enzymatic biotransformation occurring via biological processes within our body. Catalysts are used in 60% of chemicals synthesized and 90% of chemical processes occurring in industry. This accounts for 20% of gross GDP of USA per annum. Catalyst manufacture alone accounts for $10 billion sale worldwide and spread out in four major sectors: refinery, chemicals, polymerization and exhaust emission control. The overall impact of catalysts is $10 trillion per year. The intermediates synthesized by catalyst find applications in production of materials, chemicals and control devices for various industries including chemical, petroleum, pharmaceuticals, automotives, electronic materials, food and energy [2].

Applications of catalysis are well known in many fields which include energy, industry, environment and life sciences. Whether it is homogeneous or heterogeneous (or even enzymatic), catalysis primarily is a molecular phenomenon since it involves the chemical transformation of molecules into other molecules. This distinction is related to the fact that when catalyst operates in same phase where the reaction occurs is called homogeneous catalysis, whereas when it operations under distinct phases is called heterogeneous catalysis. Inspite of many modern analytical techniques the level of understanding of the heterogeneous catalysis is still limited, especially when compared to molecular solid state chemistry and homogeneous catalysis. A concept was introduced in 1926 by H. S. Taylor in heterogeneous catalysis with small number of active sites to solve the problem in obtaining structure-activity relationship. To the date none of the physico-chemical characterisation techniques give clear insight about the structure of active sight and role played by it or any description of mechanistic aspects of reactions occurring at active site. Mechanistic aspects here mean bond breaking and bond making at so called active site. Heterogeneous catalysis is of paramount importance in many areas of the chemical and energy industries. It also plays a key role in the manufacture of essential products in key areas of agriculture and pharmaceuticals but also in the production of polymers and numerous essential materials. Heterogeneous catalysis plays an important role in the general life of the public; not only with respect to an economic viewpoint but it also provides the necessary infrastructure for the well being of society. Heterogeneous catalysis is an integral part of the

modern technology, since about 80% of all industrial chemicals are manufactured by catalytic reactions. Table 1 shows a brief list of some most important catalytic processes developed in the 20th century.

Table 1. Important catalytic process developed in 20th century [3]

Process	Catalysts	Inventor, year
Nitric acid by NH_3 oxidation	Pt/Rh nets	Ostwald, 1906
Ammonia synthesis from N_2, H_2	Fe, Mo	Mittasch, Haber, Bosch, 1908; Production, 1913 (BASF)
Methanol synthesis from CO/H_2	ZnO/Cr_2O_3	Mittasch, 1923
Hydrocarbons from CO/H_2 (motor fuels)	Fe, Co, Ni	Fischer, Tropsch, 1925
Oxidation of ethylene to ethylene oxide	Ag	Lefort, 1930
Cracking of hydrocarbons	Al_2O_3/SiO_2	Houdry, 1937
Hydroformylation of ethylene to propanal	Co	Roelen, 1938 (Ruhrchemie)
Cracking in a fluidized bed	Aluminosilicates	Lewis, Gilliland, 1939 (Standard Oil)
Ethylene polymerization, low-pressure	Ti compounds	Ziegler, Natta, 1954
Hydrogenation, isomerization, hydroformylation	Rh-, Ru complexes	Wilkinson, 1964
Asymmetric hydrogenation	Rh/chiral phosphine	Knowles, 1974; L-Dopa (Monsanto)
Three-way catalyst	Pt, Rh/monolith	General Motors, Ford, 1974

Methanol conversion to hydrocarbons	Zeolites	Mobil Chemical Co., 1975
α-olefines from ethylene	Ni/chelate phosphine	Shell (SHOP process) 1977
Polymerization of olefins	zirconocene/MAO	Sinn, Kaminsky, 1985
Selective catalytic reduction SCR (power plants)	V, W, Ti oxides/ monolith	~1986

Environmental catalysis consists of the study of catalysts and catalytic reactions that impact the environment which provide an effective solution for the removal of various types of pollutants. Environmental catalysis also deals with applications for new eco-compatible refinery, chemical or non-chemical catalytic processes, catalytic technologies for minimization of waste, and new catalytic routes to valuable products without formation of undesirable pollutants. It is mainly concern with abatement of soil, water or air pollution.

Soil pollution is caused due to the use of pesticide, fertilizer or pharmaceutical industrial waste which is major contributor in the last century. Treated sewage sludge which contains hazardous organic matter and heavy metal contaminate the soil. These pollutants degrade the soil and make it non-fertile. Water pollution is also one of major problem studied in environmental catalysis. It is contamination of natural water bodies by chemical, physical, radioactive or pathogenic microbial substances. The specific contaminants leading to pollution in water include a wide spectrum such as elevated temperature and discoloration. It also increases the chemical oxygen demand (COD) of water which affects the aquatic life by lowering the dissolved oxygen in water. Air pollution is another major part of environmental catalysis, which is caused due to the release of harmful gases in atmosphere. The substances like solid particles, liquid droplets, or gases, from natural origin or man-made can create the air pollution.

Air pollution caused by emission of hazardous gases like chlorofluorocarbon released from air conditioners, refrigerators, aerosol sprays. This chlorofluorocarbon is responsible for depletion of ozone layer in stratosphere. Emission of radioactive pollutant by nuclear explosion, nuclear events, and natural decay of radioactive material such as radon etc are

harmful to human health. Various types of pollutants are also emitted from vehicle. Transportation is increasing exponentially all over the world. In 2012 for the first time in history, over 60 million passenger cars were produced in a single year and production of car is increasing rapidly every year [4, 5]. Road transport also remains the main source of many local emissions including benzene, 1,3-butadiene (HCs), carbon monoxide (CO), nitrogen oxides (NO_x) and particulates (PMs), SO_2. Total emissions of NO_x in Asia were 27.3 Mt in 2000, where China at 11.2 Mt (65%) and India at 4.7 Mt (17%) were high-emission countries, as was the case for SO_2 emissions. Japan (7%), South Korea (6%) and Indonesia (6%) also made relatively large contributions to air pollution due to transportation [6]. Today on-road vehicles release the carbon monoxide and nitrogen oxides contributing over twenty percent of the global warming pollution. This air pollution carries significant risks for human health and the environment [7]. The emission from petrol and diesel engines are different due to difference in operating condition. Gasoline (petrol) cars produce more CO and HC than diesel cars, although exhaust emissions of NO_x and particulates are much lower than diesel cars. In fact particulate emissions from petrol cars are so low that they are not routinely measured. The emissions from automobile engines depend on air/fuel (AFR) ratio [8]. This is the mass ratio of air to fuel present during combustion. When all the available oxygen is used to burn the fuel and all the fuel is burnt completely within a vehicle's combustion chamber, the mixture is chemically balanced and this AFR is called the stoichiometric mixture as shown in Fig. 2. For gasoline engine air/fuel ratio is approximately 14.7 [9]. Any mixture with air/fuel ratio less than 14.7 is considered to be a rich (fuel rich) and more than 14.7 is a lean (lean fuel). In presence of excess O_2 three-way catalyst is more selective for CO and HC oxidation rather than NO_x reduction to N_2, hence maintaining the air to fuel ratio (14.7) is crucial for three-way catalyst to perform the NO_x reduction to N_2. When the engine is operated rich of stoichiometric, the CO and HC emissions are highest while the NO_x emissions are lowest. This is because complete burning of gasoline is prevented by the deficiency in O_2. The level of NO_x is reduced because the adiabatic flame temperature is reduced. Commercial “three-way catalyst” (TWCs) is used in catalytic converter for petrol engine to control the emission namely H_2, H_2O, O_2, NO_x, CO, CO_2 and HC (alkane, alkene and aromatics containing 1-8 C atoms).

Three-way catalyst consist of Pt, Pd or Rh on Al_2O_3 support coated on ceramic or metallic honeycomb/monolith [10, 11]. The composition and operating conditions of three-

way catalyst is shown in table 2. It simultaneously converts NO_x, CO and HCs into N_2, CO_2 and H_2O (table 3).

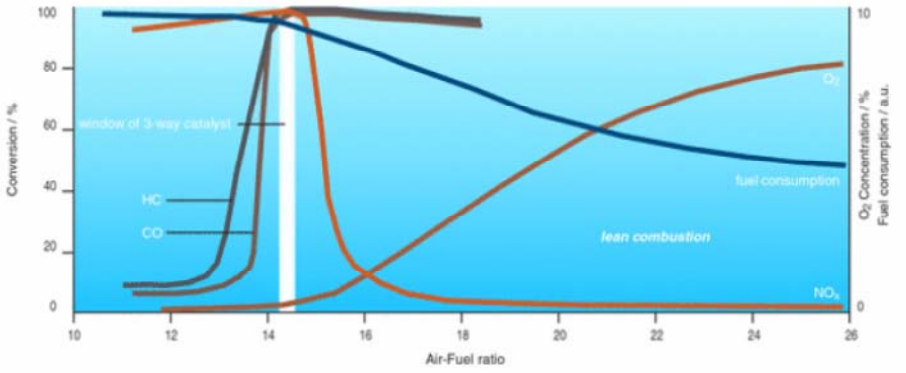

Fig. 2. Fuel consumption and 3-way function of petrol engine as function of air/fuel ratio.

Three-way catalyst was first installed in 1979 in large number of vehicles. To improve the catalytic activity, catalyst has been modified by adding different elements like, Ni, Ce, La, Ba, Zr, Fe and Si to the alumina wash coat. Ni, Fe and Ce can increases the activity of Pt and Pd for reduction of NO_x [12]. This catalyst performs three functions at a time and hence the name. The literature reports that platinum and palladium exhibit relatively high selectivity for CO to CO_2 and NO_x to NH_3 formation during the catalytic reduction of NO by H_2 under reducing conditions whereas Rh is used for reduction of NO_x to N_2 [13-16]. There are many factors affecting the working of three-way catalyst like fuel content, air to fuel ratio, sintering of active components etc. The fuel quality also plays major role in the choice of catalyst formulation due to presence of residual Pb levels, phosphorous and sulphur in fuel and lubricant which can poison the catalyst. Support of three-way catalyst is modified with various metal oxides to avoid the sintering [17].

The decisions regarding the choice of the noble metal and loading are based on cost factors and fuel quality. In order to reduce pollution the thickness of the washcoat containing the noble metals has to be increased consequently increasing the cost of catalyst [11, 18]. Therefore to reduce the cost researchers are trying to use only Pd based three-way catalyst for petrol engine [8, 19-20]. Diesel engine working under high air to fuel ratio (lean fuel mixture) is more efficient due to the less consumption of fuel. Diesel engine produces more NO_x due to the presence of excess of air with considerable particulate matter (PMs). Fig. 3 shows vehicular NO_x emission from 2000 to 2015.

Table 2. Composition and operating condition of three-way catalyst

Composition	
Carrier	Monolith: cordierite ($2MgO.2Al_2O_3.5SiO_2$)
Wall thickness:	0.152 mm
Cells:	$62cm^{-2}$
Wash-coat	Alumina (γ-Al_2O_3) + additives
Active phase	Pt + Rh: 1.24-1.41 $g.L^{-1}$ catalyst volume,
Mass ratio Pt: Rh = 5 – 20 : 1	
Operating condition	
Temperature	570 – 1170 K
Space velocity	1- 2.105 m^3 gas m^{-3} reactor h^{-1}
Volume ratio	catalyst/cylinder = 0.8- 1.5 m^3 m^{-3}

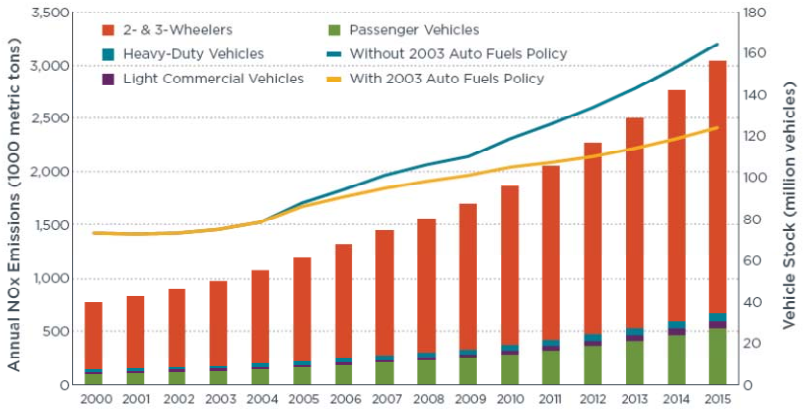

Fig. 3. Annual vehicle stock and vehicular NO_x emissions from 2000 to 2015 [21].

Particulate matter (PMs) sometimes also called diesel exhaust particles (DEP), is the particulate component of diesel exhaust which includes diesel soot and aerosols such as ash particulates. The use of a diesel engine as a power source in passenger vehicles is steadily increasing because fuel efficiency is better than its petrol counterpart. In terms of regulated emissions emitted from an internal combustion engine (i.e. carbon monoxide (CO), hydrocarbons (HC), nitrogen oxides (NO_x) and particulate matter (PMs)) emissions of CO and HC from diesel engines are significantly lower than those from gasoline engines.

However compared to gasoline engines, diesel engines produce considerably higher emissions of NO_x and PM.

Table 3. Reactions occurring on the automotive exhaust catalysts.

Process	Reaction
Oxidation	$2CO + O_2 \rightarrow 2CO_2$
	$HC + O_2 \rightarrow CO_2 + H_2O$[a]
Reduction/three-way	$2CO + 2NO \rightarrow 2CO_2 + N_2$
	$HC + NO \rightarrow CO_2 + H_2O + N_2$[a]
	$2H_2 + 2NO \rightarrow 2H_2O + N_2$
WGS	$CO + H_2O \rightarrow CO_2 + H_2$
Steam reforming	$HC + H_2O \rightarrow CO_2 + H_2$[a]

[a] Unbalanced reaction.

NO_x are not only produced from vehicle but from other sources which are listed below:

2. Origin, sources and types of nitrogen oxides (NO_x)

Origin of NO_x

Nitrogen oxide (NO_x) originates from reaction of oxygen and nitrogen at high temperature (~1600 ºC) during combustion. It includes mainly two pollutants viz. NO and NO_2. The different types of nitrogen oxides with properties and oxidation state are listed in table 4.

Sources of NO_x

The general reaction of NO_x formation is as follows

$$N_2 + O_2 \longrightarrow 2NO \qquad \Delta H^o = 180.6 KJ / mol \qquad (1)$$

It requires high activation energy. However in an internal combustion engine, because of the high temperature the reaction between nitrogen and oxygen from air to yield nitrogen oxides is thermodynamically favoured. Once formed, a part of NO reacts with air to form NO_2.

$$NO + \tfrac{1}{2}O_2 \longrightarrow NO_2 \qquad \Delta H^o = -113 KJ/mol \qquad (2)$$

Table 4. Types of Nitrogen oxides with properties

Name	Properties	Oxidation State of N
Nitrous oxide, N_2O	Colourless gas water soluble, slightly sweet odour	1
Nitric oxide, NO	Colourless, odourless gas	2
Dinitrogen dioxide, N_2O_2	Slightly water soluble	
Nitrogen trioxide, N_2O_3	Black solid, water soluble, decomposes in water, unstable at room temperature	3
Nitrogen dioxide, NO_2	Pungent, non-flammable, reddish brown gas, very water soluble, decomposes in water	4
Dinitrogen tetraoxideN_2O_4		
Nitrogen pentoxide, N_2O_5	White solid, very water soluble, decomposes in water	5

There are three types of NO_x sources.

Natural sources

Lightening oxidizes atmospheric N_2 to NO_x. Nitric oxide is produced during thunderstorms due to the extreme heat of lightning. Biomass burning, as in forest and prairie fires, oxidizes organic nitrogen producing NO_x and is caused by the splitting of nitrogen molecules.

Biogenic sources

Agricultural fertilization and the use of nitrogen fixing plants also contribute to atmospheric NO_x, by promoting nitrogen fixation by microorganisms (for example, nitrification oxidizes ammonia (NH_3) to NO_2 or NO_3.

Industrial sources

In industry NO_x formation takes place due to the combustion process. Approximately 90 to 95% of the nitrogen oxides generated in combustion processes are in the form of nitric oxide (NO). There are three primary sources of NO_x in combustion processes:thermal NO_x, fuel NO_x, prompt NO_x.

Although all of these are formed through combustion processes, they all differ slightly. Thermal NO_x formation is highly temperature dependent and is recognized as the most relevant source when combusting hydrocarbon. Fuel NO_x tends to dominate during the combustion of fuels, such as coal, which have significant nitrogen content, particularly when burned in combustors designed to minimize thermal NO_x. The contribution of prompt NO_x is normally considered negligible. Afourth source, called feed NO_x is associated with the combustion of nitrogen present in the feed material of cement rotary kilns between 300 and 800 ºC, however it is also a minor contributor [22-24].

2.1. Thermal

Thermal NO_x is produced during combustion in metallurgical furnaces, blast furnaces, plasma furnaces, kilns etc. Combustion takes place as a function of the temperature and the residence time of the nitrogen at that temperature. Formation of thermal NO_x takes place at higher temperature usually above 1600 ºC (2900 ºF), where molecular nitrogen (N_2) and oxygen (O_2) in the combustion air dissociate into their atomic states and participate in a series of reactions. Thermal NO_x contribute about 20% of the total NO_x emission in pulverised coal firing. Following are the three principal reactions producing thermal NO_x as explained by Zeldovich mechanism.

$$N_2 + O^{\bullet} \leftrightarrow NO + N^{\bullet} \qquad (3)$$

$$N^{\bullet} + O_2 \leftrightarrow NO + O^{\bullet} \qquad (4)$$

$$N^{\bullet} + {}^{\bullet}OH \leftrightarrow NO + H^{\bullet} \qquad (5)$$

All three reactions are reversible. The first step is rate limiting, and due to its high activation energy (314 KJ mol^{-1}) requires high temperatures to proceed. Reaction (5) is only significant under reducing conditions. The importance of first reaction (3 and 4) was suggested by Zeldovich. The last reaction of atomic nitrogen with the hydroxyl radical ($^{\bullet}OH$)

was added by Lavoie, Heywood and Keck to the mechanism and made a significant contribution to the formation of thermal NO_x [22].

2.2 . Fuel

Fuel NO_x is formed due to the presence of reaction of the organically bound nitrogen in the fuel with oxygen during combustion. During combustion, the nitrogen bound in the fuel is released as a free radical and ultimately forms free N_2 or NO. NO_x is a major problem in the burning of oil and coal as it can make up as much as 50% of total emissions when combusting oil and as much as 80% of total emissions when combusting coal.

2.3. Prompt

Prompt NO_x is most prevalent in rich flames. As the fuel pyrolyzes, it generates the radical which combine with available nitrogen to form nitrogen radical which promptly oxidizes at flame and form NO_x and other species. Prompt NO_x formation takes place as per the following rout

This third source is attributed to the reaction of atmospheric nitrogen (N_2) with radicals such as C, CH, and CH_2 fragments derived from fuel, where this cannot be explained by either the aforementioned thermal or fuel processes, occurring in the earliest stage of combustion. This results in the formation of fixed species of nitrogen such as NH (nitrogen monohydride), HCN (hydrogen cyanide), H_2CN (dihydrogen cyanide) and CN^- (cyano radical) which can oxidize to NO. In fuels that contain nitrogen, the incidence of prompt NO_x is especially minimal and it is generally only of interest for the most exacting emission targets.

3. Effects of NO_x on public health and environment

NO_x and volatile organic compounds react in the atmosphere in the presence of sunlight to form ground-level ozone. Ground-level ozone is a major component of smog in our cities and in many rural areas as well. Though naturally occurring ozone in the stratosphere provides a protective layer high above the earth, the ozone that we breathe at ground level has been linked to respiratory illness and other health problems, including:

- decreases in lung function, resulting in difficulty in breathing, shortness of breath, and other symptoms;

- respiratory symptoms, including bronchitis, aggravated coughing, and chest pain;
- increased incidence/severity of respiratory problems (e.g. aggravation of asthma, susceptibility to respiratory infection) resulting in more hospital admissions and emergency room visits;
- chronic inflammation and irreversible structural changes in the lungs that, with repeated exposure, can lead to premature ageing of the lungs and other respiratory illness.

NO_x chemically reacts in the atmosphere with water, oxygen and oxidants to form nitric acid (HNO_3), and nitrate particles (NO_3). The nitric acid comes to the earth by rain and causes the acid rain, which can harm forest ecosystems by directly damaging plant tissues. One of the best examples of direct damage involves the leaching of nutrients from the needles of red spruce, which reduces the ability of the trees to tolerate cold winter temperatures and has contributed to the decline of red spruce forests throughout the mountains of the eastern U.S. In other cases, acid rain can combine with other pollutants such as ozone to weaken trees and make them vulnerable to threats such as pests, which cause mortality. Acid deposition can also affect forest ecosystems indirectly by changing the chemistry of forest soils, including the leaching of plant nutrients from soils. It can also elevate levels of aluminum in soil water, which impairs the ability of trees to use soil nutrients and can be directly toxic to plant roots.

There is need to control NO_x emission by implementing the regulations which could be useful to improve the air quality and avoid the adverse effect of pollutant on human health and environment.

4. Emission legislation norms

Emission legislation norms are required to set specific limits to the amount of pollutants that can be released into the environment. Many emissions standards focus on regulating pollutants released by mobile sources (car, truck, buses etc.) and stationary sources (industry, coal mine, power plants etc.). In 1909 need to control these emissions was recognized. Emissions controlling legislative norms were accordingly introduced in the U.S. in 1970 (Clean Air Act), in Europe (European Emission norms in 1992), in Japan and in India (Bharat Stage Norms) and these have become more stringent over the years (table 5) [25-27]. Air pollution in India is increasing day by day creating problems, especially in urban areas. Many Indian cities fail consistently to meet National Ambient Air Quality Standards

(NAAQS) [21, 28]. To regulate motor vehicle emissions in India, government authority first established the Air (Prevention and Control of Pollution) Act in 1981, and Environment (Protection) Act, in 1986. The former vested powers to the individual states to regulate and enforce broad environmental standards, while the latter gave most of the same powers to the central government. The Motor Vehicles Act in 1989 fixed vehicular emission standards and authorized the central government and state governments to regulate and enforce them [4]. These idle emission regulations were soon replaced by mass emission limits for both gasoline (1991) and diesel (1992) vehicles, which were gradually tightened during the 1990's. Since the year 2000, India started adopting European emission and fuel regulations for four-wheeled light-duty and for heavy-duty vehicles. Indian emission regulations still apply to two- and three-wheeled vehicles (table 6). Despite the reduction in harmful vehicle emissions over the past decade thanks to the 2003 Auto Fuel Policy, greater and more rapid progress is urgently needed. On October 6, 2003, the National Auto Fuel Policy has been announced, which envisaged a phased program for introducing Euro 2 - 4 emission and fuel regulations by 2010 [21, 28]. The implementation schedule of EU emission standards in India is summarized in table 6 and 7. The above standards apply to all new 4-wheel vehicles sold and registered in the respective regions. In addition, The National Auto Fuel Policy introduces certain emission requirements for interstate buses with routes originating or terminating in Delhi or the other 10 cities.

Table 5. EU Emission Standards for Heavy-Duty Diesel Engines: Steady-State Testing

Stage	Date	CO	HC	NO_x	[a]PM
				$GkWh^{-1}$	
Euro I	1992, ≤ 85 kW	4.5	1.1	8.0	0.612
	1992, > 85 kW	4.5	1.1	8.0	0.36
Euro II	1996.10	4.0	1.1	7.0	0.25
	1998.10	4.0	1.1	7.0	0.15
Euro III	1999.10	1.5	0.25	2.0	0.02
	2000.10	2.1	0.66	5.0	0.10
Euro IV	2005.10	1.5	0.46	3.5	0.02
Euro V	2008.10	1.5	0.46	2.0	0.02
Euro VI	2014.05	1.5	0.13	0.40	0.01

[a] Particulate matter

Table 6. Emission norms for 2 and 3-wheelers

Vehicle	Pollutants	Year 2005	From 2010
		Bharat stage II (eq. Euro II) (gkm^{-1})	Bharat stage III (eq. Euro III) (gkm^{-1})
2-wheelers	CO	1.50	1.0
	$HC + NO_x$	1.50	1.0
3-wheelers (Petrol)	CO	2.25	1.25
	$HC + NO_x$	2.20	1.25
3-wheelers (Diesel)	CO	1.00	0.50
	$HC + NO_x$	0.85	0.50
	PM	0.10	0.50

Table 7. Emission norms for heavy duty and light duty vehicles

Vehicle	Pollutants	Year 2005	[a]Year 2010	[b]Year2010
		Bharat stage II (eq. Euro II) ($gkwh^{-1}$)	Bharat stage III (eq. Euro III) ($gkwh^{-1}$)	Bharat stage IV (eq. Euro IV) ($gkwh^{-1}$)
Buses and Trucks (Diesel)	CO	4.5	2.1	1.5
	NO_x	7	5	3.5
	HC	1.1	0.66	0.46
Light duty vehicle like car (Diesel)	CO	1.0-1.5	0.95	0.74
	NO_x+HC	0.7-1.2	0.86	0.46
	PM	0.08-0.17	0.10	0.06
Light duty vehicle like car (Petrol)	CO	2.2-5.0	2.3	1
	HC + NO_x	0.7	0.56	0.30
	PM	-	-	-

[a]Nationwide applied except Delhi and metro cities, b- Delhi and 10 major cities.

For 2-and 3-wheelers, Bharat Stage III is applicable from April 1, 2010. These emission norms are very stringent for abatement of NO_x emission from vehicle. Hence there is need of emission control strategies to reduce the air pollution.

5. Emission control strategies

A control strategy is a set of discrete and specific measures identified and implemented to achieve reductions in air pollution coming out from different sources such as stationary or mobile, as well as by the pollutant that is being targeted. The purpose of these measures is to achieve the set air quality standards. Costs and benefits are assessed in the development of the control strategy. The emission control strategies are set to control the emission of pollutants.

6. NO_x emission control from automobile engines

For the traditional stoichiometric gasoline engine, the conversion of NO_x from exhaust to N_2 is very effective by using a three-way catalyst (TWC) due to presence of less oxygen and higher CO and unburnt HC as reductant. Nevertheless, the removal of NO_x by using the TWC is ineffective for the diesel engine due to the fact that diesel engines operate with a large excess of air leading to a considerable concentration of oxygen in exhausts, which makes reduction of NO_x to N_2 difficult. The oxygen concentration in typical diesel exhausts is usually between 10 and 14% while in gasoline exhausts the oxygen concentrations is controlled to be below 1%. Accordingly, technologies like direct decomposition, NSR (NO_x storage reduction) and SCR (Selective catalytic reduction) have been developed to solve this problem [29-33].

Selective catalytic reduction (SCR) which was originally used in mobile and stationary sources like thermal power plants by using ammonia as a reducing agent called ammonia SCR, is a NO_x reduction methodology. Fundamentally, NO_x reacts catalytically with ammonia on the surfaces of a catalyst. Different precious metals (e.g. gold, silver, platinum, ruthenium, rhodium and palladium) and base metals (e.g. iron, nickel, lead, vanadium, zinc and copper) coated on a porous medium in order to increase the chemically active surface have been used as catalysts. Due to high NO_x conversion efficiencies seen in stationary applications, ammonia SCR has also been adapted in transportation for heavy-duty diesel engines. Recently, it has also been investigated in light-duty passenger vehicles.

However, there are some problems that rise with ammonia-SCR. An additional storage tank for ammonia or urea is inevitably required. Furthermore unlike the heavy-duty diesel engine which usually operates at a high and constant operating condition (i.e. engine speed and load),the light-duty diesel engine normally works in a wide range of operating conditions. These operating conditions are changed continually and suddenly. So it is difficult to control the amount of ammonia which is injected into the exhaust gas for the NO_x reduction process because this amount varies with operating conditions of the engine. As a result, there has been a worldwide effort to discover more practical technologies for the removal of NO_x emissions emitted from the light-duty diesel engine. Replacing ammonia or urea with hydrocarbons, a method that is knows as hydrocarbon SCR (HC-SCR) is the most convenient. A wide variety of hydrocarbons (e.g. oxygenated hydrocarbon, light hydrocarbon, traditional diesel fuel, biodiesel fuel and synthetic diesel fuel) have been studied in both laboratory-scale experiments and full-scale tests to discover the appropriate hydrocarbon used as the reducing agent. Moreover, several catalytic substances have been screened to determine the suitable catalyst for HC-SCR.

7. Lean-NO_x control technologies

There are three different types of lean NO_x control technologies which are Direct NO_x decomposition, Selective catalytic reduction (SCR) and NO_x storage reduction (NSR) as listed below.

7.1. Direct NO_x decomposition

In thisprocess, the NO_x gases are decomposed into nitrogen and oxygen as harmless atmospheric components by simple contactwith the catalyst surfaces. This is most desirable and challenging NO_x abatement process which is thermodynamically favorable reaction. Therefore, the direct decomposition of NO is one of the candidate reactions for the high temperature deNO_x applications. Numerous kinds of catalysts, such as supported noble metals [34-40], metal oxides [41-50] and ion exchanged zeolites [51-59] are known to show the catalytic activity for this reaction.

$$2NO \leftrightarrow N_2 + O_2 \qquad E_a = 364 \text{ kJ mol}^{-1} \qquad (11)$$

The reaction shown in eq. (11) is thermodynamically favourable at temperature below1173 K but is kinetically limited because of the high activation energy of 364 kJ mol^{-1}

in the absence of a catalyst. Below 1173 K the equilibrium reaction moves towards the right and decomposition of NO into N_2 and O_2 proceeds thermodynamically. However the binding energy of N-O is large and as such the N-O bond is not readily broken. Whereas the oxygen molecules produced by NO decomposition as well as those present in the gas phase adsorb on the catalyst surface and blocks the active sites. Hence the presence of oxygen in the gas phase inhibits the NO decomposition reaction [44].

Many researchers have reported the direct NO decomposition at different temperature using metal oxides. Conventionally Cu-ZSM-5 catalyst was used for direct NO decomposition [60]. Iwamoto et al. [59] studied the direct decomposition of NO on different zeolites such as zeolite X, Y, mordenite and ZSM-5 supports with the same copper content and observed that ZSM-5 showed higher activity as compared to other zeolites and the activity order was ZSM-5 >> zeolite Y > mordenite > zeolite X. In Cu-ZSM-5 after NO adsorption three species were detected, namely $NO^{\delta+}$, $NO^{\delta-}$, $(NO_2)^{\delta-}$. $NO^{\delta+}$ species was formed on Cu^{+1} ion whereas $NO^{\delta-}$ and $(NO_2)^{\delta-}$ were formed on Cu^{+2} ions. The anions are intermediate for decomposition which decreased with increase in the concentration of cation on catalyst surface [12]. Kustova et al. [60] improved the activity of copper exchanged zeolite by increasing its mesoporosity (Cu-ZSM-11) for direct NO decomposition reaction. When zeolite catalysts are heated above 600 ºC, de-alumination takes place due to the migration of some of the aluminum ions forming aluminum oxideon the surface of the catalyst. Such catalysts are irreversibly deactivated. For this reason, studies on direct NO decomposition using zeolite were not continued.

The rare earth metal oxides also showed higher activity for NO decomposition. Vannice et al. [61, 62] have studied the La_2O_3 and Sr promoted La_2O_3, NO decomposition activity shown by La_2O_3 may be due to the presence of basic sites and anion vacancies. On $La_2O_3$and Sr-promoted La_2O_3 irreversible uptake of NO was very significant at 300 K. The addition of Sr to La_2O_3 increased the specific activities and the TOFs. Haneda et al. [63] prepared the CeO_2 and Pr_6O_{11} which has oxygen anion vacancies and used for decomposition of NO after reducing the catalyst in H_2 at 773 K. He concluded that addition of Pt metal in rare earth oxide can improve the NO decomposition activity. Masui et al. [52] extensively studied the NO decomposition on various mixed metal oxides of rare earth and transition metal. The $(Y_{0.67}Tb_{0.30}Zr_{0.03})_2O_{3.33}$ catalyst showed highest NO decomposition activity which was as high as 67% at 900 ºC in the absence of O_2 (NO/He atmosphere) and a relatively high

conversion ratio was observed even in the presence of O_2 or CO_2. They explained that C-type cubic structure have many oxygen-deficient sites which may increase the probability of NO adsorption. It also has probability of acceleration of oxygen desorption from the surface by the redox reaction of rare earth elements compared with those obtained over conventional direct NO decomposition catalysts. Same group of scientists worked on another C-type cubic Ho_2O_3, due to its strong basicity among heavier rare earth elements as a fundamental material to develop a catalyst having a large number of basic sites. Also they substitute fraction of holmium sites with praseodymium to inhibit catalyst poisoning by O_2 and CO_2 [64]. Addition of alkali metal and alkaline earth metal also contributes to increase the activity of the rare earth oxide catalyst [44]. The basicity of catalyst can be tuned after addition of alkali and alkaline earth metal for NO decomposition and the order of activity is Ba > Cs > Na >Mg > Li and Ba > Sr > Ca > Mg [65, 66]. One of the major drawbacks of this technique is that its temperature window of working is in between 500 to 900 ºC but at low temperature catalyst become ineffective and also the presence of O_2 and CO_2 in the diesel exhaust feed can deteriorate the catalytic activity [64]. Hence up to now, none has a level of activity that would enable practical application of these techniques for the NO_x abatement.

7.2. NO_x storage reduction (NSR)

Toyota laboratories brought up this concept of NSR in the mid-1990 [67-69]. This is one of the most promising approaches which utilize the NO_x storage on barium sites to form nitrates during the lean phase and their reduction to nitrogen in a rich atmosphere. These physical and chemical processes based on the molecular level are indispensable to exploit the full potential of this technique. NO_x storage-reduction catalysts work under cyclic conditions of fuel lean and fuel rich environments. Typical NSR catalyst consist of impregnated precious metal (Pt) and alkali or alkaline earth metal or rare earth oxide on alumina support [69-71]. In NSR catalyst ceria and/or barium is added for the uptake of oxygen and nitrogen oxides. In fuel lean (high air fuel ratio) condition NO oxidation takes place to nitrogen dioxide which gets adsorbed on the surface in the form of nitrites or nitrates of barium (Fig. 4). When exhaust is switched to the rich condition (low air to fuel ratio), NO is released in the form of nitrite or nitrate sites and gets reduced to N_2 (Fig. 4) [72-75]. The possible reaction pathway is shown in Fig. 4. The experimental work is based on well-defined model catalysts of monolithic structure and of varying complexity. Platinum and rhodium are chosen as noble metal components for coating on monolith. The washcoat consists of γ-Al_2O_3 as support. Pt is

used for the oxidation of NO in lean phase of NSR. Some NSR catalyst formulations include other precious metals or mixtures of precious metals for improvement of the catalytic activity. Precious metals like palladium (Pd) or rhodium (Rh) are much less active for NO oxidation, but are much more active for NO_x reduction [72-75]. Shinjoh et al. [76] improved the activity of NSR catalyst by combining Pd/γ-Al_2O_3 as an oxidation catalyst with Pt/Rh/Ba/γ-Al_2O_3 as a NSR catalyst and Cu/ZSM-5. Pd increases the NO_x storage ability by enhancing NO_2 formation under oxidative atmosphere. The stored NO_x was reduced to NH_3 on the NSR catalyst. The generated NH_3 was adsorbed on Cu/zeolite downstream of the NSR catalyst under the reductive atmosphere and easily reacted with NO_x on the Cu/zeolite under the subsequent oxidative atmosphere (NH_3-SCR).

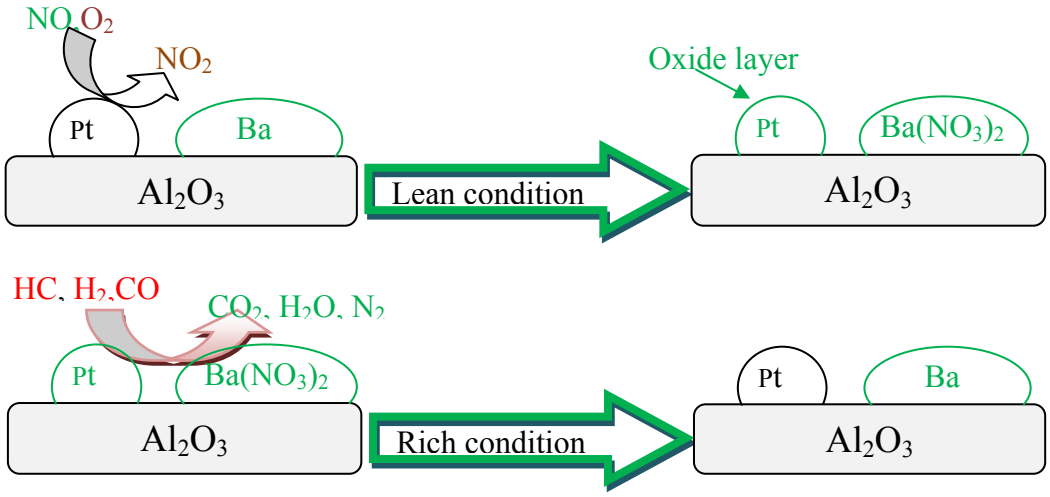

Fig. 4. NO_x storage and reduction cycle on Pt/Ba/Al_2O_3.

Although NSR technique is commercialized, it'svery high sensitivity to sulfur limits its use for fuel containing sulfur more than 10 ppm. When SO_2 reacts with Ba and Al_2O_3 it forms inactive $BaSO_3$, $BaSO_4$, $Al_2(SO_3)_3$ and $Al_2(SO_4)_3$ species which are highly stable [70, 71, 77-79]. The order of stability is BaO < $Ba(OH)_2$ < $Ba(CO)_3$ < $Ba(NO)_2$ < $Ba(NO_3)_2$ < $Ba(SO)_4$. In typical lean exhaust, sulfur is present almost exclusively in the form of SO_2, since most of the sulfur compounds are oxidized in the process of combustion. Hence the NO_x storage was inhibited. To overcome this drawback catalyst was modified with different metal/metal oxides. Some time commercial catalyst (Pt/Ba/Al_2O_3) formulations may also include: potassium, as a substitute to or in addition to Ba, TiO_2, which is reported to decrease SO_x adsorption; precious metal like Rh which favours NO_x reduction with H_2/CO/HCs and

H_2 generation via steam reforming of hydrocarbons; ZrO_2 or CeO_2–ZrO_2, which are used to promote the formation of hydrogen through steam reforming and WGS reactions [77]. Pt/CeO_2 catalyst showed improved sulfur tolerance due to the presence of oxygen deficient defect sites on ceria and presence of reactive Pt–O–Ce sites at the Pt/CeO_2 interface [80]. Hirata et al. promoted the NSR catalyst by adding TiO_2 and observed smaller particle of TiO_2 to promote the decomposition of sulfate through the interface between Al_2O_3 and TiO_2. It was also demonstrate that sulfur tolerance could be improved by addition of alkaline earth metal to Rh/ZrO_2 which improves its basicity, heat resistance and hydrogen generating performance [81]. Breen et al. [82] reported CeO_2-ZrO_2 as support instead of Al_2O_3 to improve the sulfur tolerance of $Pt/Ba/Al_2O_3$. He also concluded that lithium and strontium could form sulfate, less stable than barium. Improved sulfur tolerance and hydrothermal stability of NSR catalyst is still major challenge for better activity of catalyst.

7.3. Selective catalytic reduction of NO_x

7.3.1. With NH_3/urea as reductant

Selective catalytic reduction (SCR) of NO_x using ammonia as reductant has been used for many years in stationary diesel engine application, as well as for mobile applications. In NH_3 SCR process, NO_x reacts with ammonia, which is injected into the exhaust gas stream before SCR catalyst. SCR is the only technology capable of reducing diesel NO_x emission to levels required by future emission standard. Many transition metals have been used for SCR applications, like MoO_3, Mn, Cu, Cr and Ir supported on TiO_2, metal exchanged zeolites [83-85]. Currently, commercial SCR catalysts containing active components V_2O_5 and WO_3 supported on extruded monoliths made of TiO_2. V_2O_5 shows high performance whereas WO_3 is used as promoter [86, 87]. V_2O_5-WO_3/TiO_2 is used for stationary and mobile sources [88, 89]. This technology was first brought to the market in 2005 for heavy duty vehicles by Daimler under the trade mark BLUETEC® [90, 91]. Internal combustion engines operated with excess air such as diesel engines installed on heavy-duty vehicles uses zeolite-based washcoated monolith catalysts promoted by transition metals, such as Fe and Cu [92]. Urea has received considerable attention as a NH_3 carrier for the SCR technology due to the transportation and handling problem of ammonia [93]. For commercial applications 32.5% of urea solution (ad-blue) is used as source of ammonia [94]. Urea after hydrolysis gives ammonia as shown in eq. 12

$$CO(NH_2)_2 + H_2O \rightarrow 2NH_3 + CO_2 \quad (12)$$

Ammonia reacts selectively and stoichiometrically with nitric oxide in presence of oxygen over a catalyst with formation of the inert harmless products water and nitrogen. The reaction between ammonia and NO shown in eq. 13 is called as standard SCR [88, 94].

$$4NH_3 + 4NO + O_2 \rightarrow 4N_2 + 6H_2O \quad (13)$$

$$2NH_3 + NO + NO_2 \rightarrow 2N_2 + 3H_2O \quad (14)$$

$$8NH_3 + 6NO_2 \rightarrow 7N_2 + 12H_2O \quad (15)$$

The rate of reaction is very low hence reduction of NO_2 has been carried out by NH_3 as shown in eq. 14. NO_2 increases the rate of reaction, therefore the reaction is called as fast SCR reaction. When the exhaust feed contain maximum amount of NO_2 then it consumes excess of NH_3 as shown in eq. 15. However, vanadium is toxic and forms volatile compounds at high temperatures. Hence there is need for development of alternative catalysts, especially for mobile applications. Copper and iron exchanged zeolites are very active and promising alternatives to vanadium in SCR catalysts [94-103]. Zeolite based catalysts have the potential to operate at substantially higher temperature than base metal catalysts. Fritz et al. [106] studied the different transition metal supported on metal oxide, exchanged with zeolite and observed that Cu exchanged zeolite showed highest activity. Velasco et al. [107] compared the SCR activity of Cu exchanged with different zeolite, and concluded that Cu (II) ions are more abundant in low copper content catalysts and in BETA catalysts. The amount of CuO species was more abundant in ZSM-5 catalysts than in BETA catalysts due to the lower ionic exchange capacity of the ZSM-5 zeolite. However, CuO clusters promote NO reduction at low temperature whereas isolated Cu (II) ions maintain high NO_x conversion at high temperatures. Skarlis et al. [108] investigated the SCR activity of H- and Fe-BEA catalysts, in order to elucidate the contribution of acidic and iron sites, and also studied the kinetic modelling of it. Mihai et al. [109] suggested that acid sites dominate the decomposition of ammonium nitrate like species formed during NH_3-SCR reaction. High copper loading dominate the mechanism of ammonium nitrate complexes decomposition with the formation of nitrous oxides. Cu-exchanged zeolites with CHA-structure, like SAPO-34 and SSZ-13, have shown high activity and high hydrothermal stability for NH_3-SCR reaction [110-113].

Unfortunately catalyst used for NH_3-SCR technique possess many disadvantages like;dealumination of zeolites (hydrothermal stability) [106]. A minimum exhaust gas

temperature of about 200 ºC is required to ensure a complete decomposition and hydrolysis of urea to ammonia. When parts of the exhaust system are constantly welted by Adblue on the same spot, undesired urea crystals or polymers may form if the exhaust line temperature is lower than 300ºC. An additional disadvantage of AdBlue/Diesel Exhaust Fluid is its freezing point of -11 ºC, necessitating the use of heating of SCR systems in cold climates. SCR can exhibit inefficient NO_x reduction along with excessive ammonia slip (unreacted ammonia), unwanted oxidation of ammonia, urea/ammonia storage.

7.3.2. With hydrocarbon as reductant

Selective Catalytic Reduction (SCR) using hydrocarbons (HC) has shown a high potential in the removal of NO_x emissions from lean burn engines. It exploits hydrocarbon present in lean burn engine exhaust as shown in eq. 16. Three-way catalyst used for petrol/gasoline engine which can simultaneously convert CO, HC and NO into CO_2, H_2O and N_2 and cannot be used for diesel engine due to the presence of excess air.

$$NO + HC + O_2 \rightarrow N_2 + CO_2 + H_2O \qquad (16)$$

Diesel engine works under lean burn condition. It is beneficial for improved fuel economy and a lower emission of carbon dioxide. Hence the demand for diesel engines is continuosly increasing throughout the world. The chemical basis for NO reduction with hydrocarbons has been proposed already in the 1940's and 1950's. When unsaturated hydrocarbons (isobutene) used for NO reduction, formation of NO_2 and intermediates like nitro hydrocarbons was increased which led to the increase in N_2 formation [114].

However a boom of HC-SCR in the 1990's was related to the findings in a practical aftertreatment application, which had a wide commercial and environmental need. Therefore it is very important to develop catalyst technologies that will allow NO_x reduction in lean environments (high air to fuel ratio) for truck and passenger car applications. Researcher have tried ion exchanged zeolites like Cu, Co, Fe, Ga, various precious metal supported on alumina, transition metal supported metal oxides for this application [115-124]. However, the overall deNO_x performance of the current HC-SCR technology is not yet sufficient for commercial application, especially its low-temperature performance.

i) Zeolite based catalysts

Zeolite such as mordenite, ZSM-5, chabazite, beta zeolite, MCM 41 etc, have been studied for HC SCR of NO [125-127]. Cu exchanged ZSM-5 for the HC SCR with different hydrocarbon ranging from C_1 to C_4 and paraffine was studied by Matsumoto et al. [125], and showed that C_3 hydrocarbon gives higher NO_x conversion as compared to remaining hydrocarbon. Pt-ZSM-5 could work at lower temperature than Cu-ZSM-5, but as the temperature goes above 300 ºC poor conversion of NO into N_2 was observed [128]. Komvokis et al. [129] has studied activity of Cu-ZSM-5 with different loading of Cu on ZSM-5 for SCR of NO_x with hydrocarbon. Transition metal supported on ZSM-5 zeolite such as Cu-ZSM-5, Co-ZSM-5, Ni-ZSM-5 and Fe-ZSM-5 have been studied for HC-SCR [130, 131]. One of the major drawbacks of these catalysts is a narrow temperature window for maximum NO_x reduction. To improve the low temperature activity, Cu-ZSM-5 was modified with metal oxides or transition metals. Ceria coated Cu-ZSM-5 was used for the selective catalytic reduction (SCR) of NO with C_3H_6. CeO_2 coated Cu/ZSM-5 showed maximum NO conversion activity compared to the non-coated Cu/ZSM-5 at lower temperature under dry and wet feed conditions [129]. Cu-exchanged zeolites showed high activity in NO_x reduction, but their durability was found to be insufficient for practical application. Also their sensitivity to sulfur and water causes the lower selectivity and lower NO_x reduction [132, 133]. In another study, it was observed that Ga-ZSM-5 and In-ZSM-5 catalysts were highly active for NO reduction by CH_4. It showed that Ga-ZSM-5 was strongly inhibited by moisture, whereas In-ZSM-5 was fairly active even in the presence of 10% moisture [134].

Addition of co-cations like La, Ce, TiO_2 transition metals, noble metals or bimetallic catalysts have been used to improve the stability, sulfur tolerance, water tolerance and NO_x reduction activity of Cu/ZSM-5 [135]. The bimetallic catalysts generally have higher resistance towards metal sintering usually due to the loss of contact between metal and support. The second metal could also prevent active metal migration in the supports and improve metal dispersion. Said et al. [136] have prepared bimetallic PtCu-ZSM-5 catalyst by different methods for low temperature NO_x reduction. The bimetallic PtCu-ZSM-5 catalyst was found to offer wider temperature window than that of monometallic catalysts, Pt-ZSM-5 and Cu-ZSM-5. Abdullah et al. [137] have successfully demonstrated the high activity of Cu-ZnZSM-5 for the SCR of NO in diesel exhaust. Even though the metal exchanged/supported zeolites have been used for SCR of NO by hydrocarbon, literature survey showed that in

excess of oxygen there are major limitations for its utilization for commercial applications. These are mainly due to the limited temperature range, lower hydrothermal stability, inhibiting effect of water, and reported vulnerability to poisoning by SO_2 under realistic exhaust compositions. In conclusion, if zeolite based catalysts are to be used in automotive application their hydrothermal resistance along with their resistance to poisons such as SO_2 must be dramatically increased. Thus there is need to develop the better catalytic system for better lean-NO_x SCR by hydrocarbon, which requires both more stable supports and more active catalytic material.

ii) Platinum group metal (PGM) based catalysts

Due to the disadvantage like low sulfur tolerance and insufficient hydrothermal stability at high temperature of transition metal exchanged zeolite catalysts [138, 139], supported noble metal based catalysts attracted special attention for HC-SCR of NO_x under lean burn diesel exhaust condition due to the better low temperature activity. Particularly platinum group metals (PGM), were found to be very active for reduction of NO_x in presence of excess of O_2 especially extensive work was carried out on ruthenium and iridium. Pt/Al_2O_3 exhibits high activity at low temperatures and enhanced resistance to SO_2 and water vapour but these are active only in a narrow temperature range and exhibit low selectivity for N_2. The activity of Pt/Al_2O_3 and Pt/MWCNT (multiwall carbon nanotube) was compared by Crocker et al. for HC SCR of NO_x [140]. Pt supported on pristine MWCNTs has shown comparable NO_x reduction by propene compared to Pt/Al_2O_3.Also the MWCNT support showed higher resistance to oxidation as compared to activated carbon in a Pt/activated carbon catalyst. However, the functionalization of the MWCNT support prior to the deposition of precious metals improves both the metal dispersion and the HC-SCR performance of MWCNTs-based catalysts due to the increase in Brønsted acidity of the carrier, which in turn enhances the partial oxidation of the hydrocarbon reductant. Activity for NO_x SCR by hydrocarbon using different wt% of Pt and Rh supported on functionalized MWCNT was investigated and the 3:1 Pt–Rh alloy was shown to be catalytically more active phase which can further improve the performance of functionalized MWCNTs-supported formulations [140]. The HC-SCR activity of Pt supported on a stable de-aluminated Y zeolite showed only 20–40% NO reduction activity. NO_2 was formed under the conditions studied and it was preferentially reduced back to NO by oxidizing hydrocarbon [141]. The HC-SCR of lean NO_x at low temperatures below 200 ºC was remarkably improved using the Pt catalyst

supported on mesoporous silica (Pt/MPS) [139]. These results were achieved with a stoichiometric amount of C_6–C_{16} HCs over a wide temperature range from 170 ºC to 400 ºC ; however, pulse injection of diesel fuel into the exhaust was found to be necessary in some practical applications [139, 142]. Ohtsuka et al. [143] investigated the Pt, Pd supported on sulfated zirconia for reduction of NO_x by methane. The selective reduction of nitrogen oxides by methane on Pd–Pt supported on sulfated zirconia was due to the co-operative effect of Pd and Pt. Pd acts as the site for the reaction of NO_2 with methane, while Pt catalyzes NO oxidation to NO_2. Although platinum group metal showed low temperature activity, it would not work under excess of oxygen. Because most of the PGM metals oxides are volatile and have moderate sulfur tolerance which eventually led to metal loss, and therefore could not be used in automotive catalysts [138, 139]. Hence development of catalytic system which can withstand at high temperature and have sulfur tolerance is highly desirable.

iii) Base metal oxide catalyst

Various catalytic formulations, as discussed above, have been tested since the discovery of HC-SCR of NO_x under lean conditions. The recent deNO_x methods such as the urea-SCR are being used commercially, however it has unresolved problems that it requires storing a solution of urea and that a large portion of NO_x may be discharged in the form of nitrates and nitrites at low temperatures. In case of NO_x-storage-reduction (LNT: lean-NO_x-trap) the LNT has essential problems such as deactivation of NO_x-storage agents even by a small SO_x-content and very low activities below 200 °C. Platinum group metals are costly and showed narrow temperature window and ineffective in excess of oxygen condition, low sulfur tolerant [142]. Many metals such as Ag, Au, Fe, V, etc. supported on metal oxide like Al_2O_3, SnO_2, TiO_2, SiO_2, CeO_2 have been studied for HC-SCR of NO_x under lean burn diesel exhaust conditions [144-146]. Amongst these, Ag/Al_2O_3 was found to be the most promising catalyst for practical use since it exhibits high activity for NO reduction, high selectivity for N_2, moderate tolerance for sulfur and water vapour, especially at higher temperatures [147, 148]. Various wt% loading of Ag was loaded on alumina support have been studied. Shimizu et al. [149] have studied the activity of Ag/Al_2O_3 with various loading of Ag for HC-SCR of NO_x. He concluded that below 2 wt% Ag/Al_2O_3 highly dispersed Ag^+ ions are predominant Ag species, and they are responsible for the selective reduction of NO to N_2. At higher Ag loading, Ag_n clusters are predominant and are responsible for the non-selective hydrocarbon combustion and N_2O formation. Increasing Ag loading showed decrease in the dispersion of

Ag resulting in the formation of large Ag_2O clusters which could be reduced to Ag^0 particles by the hydrocarbons. The metallic Ag^0 particles are very active for the undesired complete oxidation of propene instead of partial oxidation required for NO reduction [150]. Hence researchers optimized the loading of Ag to ~2% for high NO_x conversion at which both a fair amount of small Ag species and large particles are formed [151-153]. The SCR reaction over Ag/Al_2O_3 catalysts is most likely dependent on two factors: the ability to reduce NO_x to N_2 and to activate (partially oxidize) the hydrocarbon as reducing agent. In practice, studies have been focused on the use of C_2-C_3 alkenes and alkanes as reductants [154]. Because these molecules are found in car exhaust gases and usually give high conversions of NO_x in the presence of excess of O_2. Oxygenated hydrocarbons, such as methanol, ethanol, propanol and aldehyde etc. are used for high NO_x conversions (95–100%) at significantly lower temperature (300 ºC) [155]. However a substantial amount of unburned total hydrocarbon (THC), hydrogen cyanide is also detected in the effluent gases besides the CO when oxygenated hydrocarbons were used as a reductant. Depending on the temperature the products range from primarily nitrogen to HCN and in terms of health dangers most of them are much less desirable than nitrogen oxide. Thus until a way is found to exclusively produce nitrogen, oxygen containing hydrocarbon species appear not to be suitable reductant with Ag/Al_2O_3 [156, 157]. The major drawback of this system is the low activity and poor sulfur tolerance at low temperatures (300-400 ºC) due to the formation of silver and aluminum sulfate [146]. Thus improvement in the low temperature activity and sulfur tolerance in the temperature range 300-400 ºC is still a major challenge for HC-SCR. The improvement in the Ag/Al_2O_3 formulation can be also realized through the addition of an element which can increase the adequate properties of the solid necessary for the SCR reaction (acidity, oxidation, stability, etc.) [158].

8. Scope and objectives of the thesis

Development of suitable catalysts for HC-SCR of NO_x is an active area of research in academic as well as industrial laboratories. Among the various catalyst compositions investigated for HC-SCR of NO_x, Ag/Al_2O_3 (2 wt% Ag) has shown promising results and is being considered as a benchmark catalyst for HC-SCR of NO_x for diesel engine exhaust. However Ag/Al_2O_3 catalyst is not efficient for practical application at lower temperature of diesel engine exhaust. Modification of either support or active component of the catalyst has been attempted for improvement of catalytic activity of Ag/Al_2O_3. Our group has

successfully modified the support previously by MgO, TiO_2, SiO_2 and improved the sulfur and water tolerance of Ag/Al_2O_3. However in present thesis second metal is added to improve the low temperature HC-SCR activity and widen the temperature window. Hence the objective of the present thesis is to improve the performance of Ag/Al_2O_3 catalyst for SCR of NO_x using hydrocarbons at lower temperature and widen the temperature window for NO_x reduction. To achieve these objectives Ag/Al_2O_3 is modified by addition of second active metal (bimetallic). By addition of Au as second metal the low temperature activity has been considerably improved as well as after ageing the low temperature activity was further increased. The effect of different pretreatments at different temperature on SCR activity of bimetallic $Ag\text{-}Au/Al_2O_3$ system was studied. The order of impregnation of Ag and Au on alumina support also played significant role in improvement of low temperature activity. The increase in Ag and Au concentration on alumina support also showed considerable increase in the low temperature activity and widening of temperature window for NO_x reduction, which showed the potential of bimetallic catalyst composition for SCR of NO_x under lean burn diesel exhaust condition. The influence of addition of Au in Ag/Al_2O_3 is studied by detailed physico-chemical characterisations techniques.

8.1. Thesis outline

This section gives the chapter wise distribution of the work done during the Ph.D. tenure.

Chapter 1: An overall perspective of the origin and types of nitrogen oxides, its effect on the public health and environment, the various emission control strategies and NO_x emission control from automobiles have been discussed in this chapter. The different lean technologies used for the abatement of NO_x have been discussed. The use of "three-way catalysts" in stoichiometric engines and their ineffectiveness in the reduction of NO_x in diesel engines which work under lean-burn condition, have been mentioned. Finally the objective of the present work undertaken with the emphasis on the selective catalytic reduction of NO with hydrocarbons as reductant under lean burn diesel exhaust condition is mentioned.

Chapter 2: This chapter describes the synthesis of $Ag\text{-}Au/Al_2O_3$ bimetallic catalyst and effect of different pretreatment on selective catalytic reduction (SCR) of NO under lean-burn diesel exhaust conditions. Catalyst was tested after different pretreatment like flow of H_2 at 250 ºC or in air at 500 ºC or in H_2 at 500 ºC for 12 h. The SCR activity was also tested after ageing

under reaction feed at 500 ºC for 12 h. The reaction feed consisted of 300 ppm NO, 300 ppm CO, 300 ppm C_3H_6, 100 ppm $C_{10}H_{22}$, 2000 ppm H_2 (when present), 10% O_2, 10% CO_2, 5% H_2O and balance He. For comparison monometallic Au/Al_2O_3 and Ag/Al_2O_3 were prepared by impregnation and urea deposition precipitation method respectively. The catalysts were characterised by different physico-chemical techniques before and after the reaction. The effect of addition of Au in Ag/Al_2O_3 system was studied with detailed characterisations.

Chapter 3: In this chapter the effect of method of catalyst preparation of Ag and Au on alumina support for SCR of NO_x under lean burn diesel exhaust condition has been studied. The bimetallic $Ag\text{-}Au/Al_2O_3$ catalysts were prepared by impregnation and co-impregnation method with 1 wt% Ag and 1 wt% Au. The activity of prepared bimetallic catalysts was compared under lean burn diesel exhaust condition. The sample with best activity was characterised in detail by various characterisation techniques.

Chapter 4: In this chapter the effect of Ag and Au concentration on alumina support for SCR of NO_x under lean burn diesel exhaust condition has been studied. The activity of $Ag\text{-}Au/Al_2O_3$ bimetallic catalyst with increasing loading of Ag and Au was studied under lean burn diesel exhaust condition. The catalyst with maximum silver loading (2 wt%) showed improved low temperature activity with widening of temperature window for NO_x reduction.

Chapter 5: This chapter presents the summary and conclusions of the thesis work.

9. References:-

[1] J. J. Berzelius, Edinburgh New Philosophical Journal, XXI, 1836, pp. 223.

[2] R. A. Van Santen, M. Neurock, *Molecular heterogeneous catalysis: a conceptual and computational approach,* Wiley-VCH, 2009.

[3] Hagen, J., Industrial Catalysis. A Practical Approach. WILEY-VCH Verlag GmbH & Co. KGaA: Weinheim, Germany, (2006) 507.

[4] G. Bansal, A. Bandivadekar. "Overview of India's vehicles Emissions Control Program". Available online at http://www.theicct.org/sites/default/files/publications/ICCT_IndiaRetrospective_2013.pdfand http://www.worldometers.info/cars/

[5] P. Brijesh, S, Sreedhara, Int. J. Auto. Technol. 14(2) (2013) 195-206.

[6] T. Ohara, H. Akimoto, J. Kurokawa, N. Horii, K. Yamaji, X. Yan, T. Hayasaka. Atmos. Chem. Phys., 7, (2007) 4419–4444.

[7] Union of concern scientists. Available online at http://www.ucsusa.org/clean_vehicles/why-clean-cars/air-pollution-and-health/cars-trucks-air-pollution.html

[8] M. Shen, L. Song, J. Wang, X. Wang, Catal. Comm. 22 (2012) 28–33.

[9] J. R. González-Velasco, J. A. Botas, R. Ferret, M. P. González-Marcos, J. L. Marc, M. A. Gutiérrez-Ortiz. Catal. Today, 59 (2000) 395–402.

[10] S. B. Kang, S. B. Nam, B. K. Cho, I. -S. Nam, C. H. Kim, S. H. Oh, Catal. Today,231(2014) 3-14.

[11] S. Yoon, S. Hu, N. Y. Kado, A. Thiruvengadam, J. F. Collins, M. Gautam, J. D. Herner, A. Ayala, Amos. Env. 83, (2014) 220–228.

[12] F. J. J. G. Janseen, R. A. van Santen, Book on "Environmental Catalysis", Catalytic science series, Vol. 1.

[13] M. Shelef, H.S. Gandhi, Ind. Eng. Chem. Prod. Res. Dev. 11 (1972) 393–396.

[14] K.C. Taylor, J.G. Larson (Eds.), , The Catalytic Chemistry of Nitrogen Oxides, Plenum Press, New York, NY, 1975, 173–189.

[15] J.C. Schlatter, K.C. Taylor, J. Catal. 49 (1977) 42–50.

[16] M. Shelef, G.W. Graham, Catal. Rev. Sci. Eng. 36 (1994) 433–457.

[17] G. Jiaxiu, S. Zhonghua, W. Dongdong, Y. Huaqiang, G. Maochu, C. Yaoqiang,Appl. Sur. Sci. 273 (2013) 527-235.

[18] S. Chauhan, J. Chem. Pharm. Res., 2(4) (2010) 602-611.

[19] V.G. Papadakis, C.A. Pliangos, I.V. Yentekakis, X.E. Verykios, C.G. Vayenas, Catal. Today, 29 (1996) 71-75.

[20] N. Peng, J. Zhou, S. Chen, X. Luo, Y. Chen, M. G.ong, J. Rare Earths,30 (2012) 342-349.

[21] Policy Summary: India's Vehicle Emissions Control Program [Online cited: http://www.theicct.org/sites/default/files/publications/ICCT_Briefing_IndiaPolicySummary_20130703.pdf

[22] Fritz, V. Pitchon, Appl. Catal. B, 13 (1997) l-25.

[23] H. Bosch, F. Janssen, Catal. Today 2 (1988) 369-379.

[24] F. Garin, Appl. Catal. A 222 (2001) 183-219.

[25] DELPHI. [Online] 2012-2013. [Cited: 2612 2013.]www.delphi.com/pdf/emissions/Delphi-Heavy-Duty-Emissions-Brochure-2012-2013.pdf.

[26] Bowles, K. Nonmethane Hydrocarbons.TermWiki. [Online] 12 01 2011. [Cited:26 12 2013.] www.ar.termwiki.com/EN:nonmethane_hydrocarbons_(NMHCs).

[27] Diesel Net. Heavy-Duty Truck and Bus Engines. [Online] [Cited: 2612 2013.] www.dieselnet.com/standards/eu/hd.php#stds.

[28] Central Pollution Control Board. National Ambient Air Quality Status 2009. January 2011. Available online at: http://cpcb.nic.in/upload/Publications/Publication_514_airqualitystatus2009.pdf

[29] M. Iwamoto, H. Yahiro, Catal. Today. 22 (1994) 5-18.

[30] B. M. Shakya, M. P. Harold, V. Balakotaiah. Chem. Eng. 237 (2014) 109-122.

[31] V. Rico-Pérez, J. M. García-Cortés, C.S. Lecea, A. Bueno-López. Chem. Eng. 104, (2013) 557-564.

[32] E. C. Corbos, M. Haneda, X. Courtois, P. Marecot, D. Duprez, H. Hamada. Appl. Catal. A, 365 (2009) 187–193.

[33] Norbert V. Heeb, Y. Zimmerli, J. Czerwinski, P. Schmid, M. Zennegg, R. Haag, C. Seiler, A. Wichser, A. Ulrich, P. Honegger, K. Zeyer, L. Emmenegger, T. Mosimann, M. Kasper, A. Mayer. Atm. Env. 45 (2011) 3203-3209.

[34] F. Garin, Appl. Catal. A, 222 (2001) 183–219.

[35] Amirnazm, J.E. Benson, M. Boudart, J. Catal. 30 (1973) 55–65.

[36] R.J. Wu, T.Y. Chou, C.T. Yeh, Appl. Catal. B, 6 (1995) 105–116

[37] M. Haneda, Y. Kintaichi, I. Nakamura, T. Fujitan, H. Hamada, J. Catal. 218 (2003)405–410.

[38] Kumar, V. Medhekar, M.P. Harold, V. Balakotaiah, Appl. Catal. B, 90(2009) 642–651.

[39] Ogata, A. Obuchi, K. Mizuno, A. Ohi, H. Ohuchi, J. Catal. 144 (1993) 452–459.

[40] R.S. da Silveria, A.M. de Oliveira, S.B.C. Pergher, V.T. da Silva, I.M. Baibich, Catal.Lett. 129 (2009) 259–265

[41] Y. Doi, M. Haneda, M. Ozawa, J. Mol. Catal. A, 383 (2014) 70–76.

[42] S. Tsujimoto, C. Nishimura, T. Masui, N. Imanaka,Catal. Comm. 43 (2014) 84–87.

[43] M. Iwamoto, H. Hamada, Catal. Today 10 (1991) 57–71.

[44] N. Imanaka, T. Masui, Appl. Catal. A, 431–432 (2012) 1–8.

[45] G.K. Boreskov, Discuss. Faraday Soc. 41 (1966) 263–276

[46] W. Hong, S. Iwamoto, M. Inoue, Catal. Today 164 (2011) 489–494.

[47] E.R.S. Winter, J. Catal. 22 (1971) 158–170.

[48] S. Tsujimoto, K. Yasuda, T. Masui, N. Imanaka, Catal. Sci. Technol., 3 (2013) 1928-1936.

[49] H. Falsig, T. Bligaard, C. H. Christensen, J. K. Nørskov, Pure Appl. Chem., 79 (2011) 1895–1903.

[50] H. Falsig, J. Shen, T. S. Khan, W. Guo, G. Jones, S. Dahl, T. Bligaard, DOI 10.1007/s11244-013-0164-5 (2013).

[51] M. Iwamoto, H. Furukawa, Y. Mine, F. Uemura, S. Mikuriya, S. Kagawa, Chem.Commun. 12 (1986) 1272–1273.

[52] T. Masui, S. Uejima, S. Tsujimoto, N. Imanaka, Mater. Sci. Applications, 3 (2012) 733-738.

[53] Ganemi, E. Björnbom, B.Demirel, J. Paul, Micro. Meso. Meter.38(2) (2000) 287–300.

[54] Pulido, P. Nachtigall, ChemCatChem 1 (2009) 449–453.

[55] K. Marina, Rasmussen, S. Birk, Kustov, Arkadii, Christensen, Claus H. Appl. Catal. B, 67 (1) (2006) 60-67.

[56] P. J. Smeets, M. H. Groothaert, Teeffelen, R.M. van, H. Leeman, E. J. M. Hensen, R. A. Schoonheydt,*J. Catal., 245*(2) (2007) 358-368.

[57] Z. Schay, L. Guczi, Catal. Today, 17 (1993) 175-180.

[58] Y. Li , W. Keith. Hall, *J. Phys. Chem.,* 94 (16) (1990) 6145–6148.

[59] M. Iwamoto, H. Furukawa, S. Kagawa, Stud. Surf. Sci. Catal. 28 (1986) 943.

[60] M.Yu. Kustova, S.B. Rasmussen, A. L. Kustov, C. H. Christensen. Appl.Catal. B, 67 (2006) 60–67.

[61] Klingenberg, M. A. Vannice, Appl. Catal. B, 21 (1999) 19-33.

[62] S. J. Huang, A.B. Walters, M.A. Vannice, Appl. Catal. B, 17 (1998) 183-193.

[63] M. Haneda, Y. Kintaichi, H. Hamada, Phys. Chem. 4(13) (2002) 3146-3151.

[64] S. Tsujimoto, C. Nishimura, T. Masui, N. Imanaka, Catal. Commun. 43 (2014) 84–87.

[65] G. Tsuboi, M. Haneda, Y. Nagao, Y. Kintaichi, H. Hamada, J. Jpn. Petrol. Inst. 48 (2005) 53–59.

[66] W.J. Hong, S. Iwamoto, M. Inoue, Catal. Today 164 (2011) 489–494.

[67] N. Miyoshi, S. Matsumoto, K. Katoh, T. Tanaka, J. Harada, N. Takahashi, K. Yokota, M. Sugiura, K. Kasahara, SAE Tech. Pap. Ser. 1995, 950809.

[68] S. Matsumoto, Catal. Today, 29 (1996) 43–45.

[69] N. Takahashi, H. Shinjoh, T. Iijima, T. Suzuki, K. Yamazaki, K. Yokota, H. Suzuki, N. Miyoshi, S. Matsumoto, T. Tanizawa, T. Tanaka, S. Tateishi, K. Kasahara, Catal. Today, 27 (1996) 63–69.

[70] L. Lietti, P. Forzatti, I. Nova, .E. Tronconi, J. Catal. 204 (2001) 175–191.

[71] M. Takeuchi, S. Matsumoto, Top. Catal. 28 (2004) 1–4.

[72] H. Ohtsuka, T. Tabata, Appl. Catal. B, 29 (2001) 177.

[73] W. S. Epling, L. E. Campbell, A. Yezerets, N. W. Currier, J. E. Parks. Catal. Review. 46 (2) (2004) 163–245.

[74] H. Ohtsuka, Appl. Catal. B, 33 (2001) 325-333.

[75] Amberntsson, E. Fridell, M. Skoglundh, Appl. Catal. B, 46 (2003) 429-439.

[76] H. Shinjoh, N. Takahashi, K. Yokota,Top. Catal. 42–43, (2007) 215-219.

[77] S. Matsumoto, Catal. Technol., 4 (2000) 102-109.

[78] S. Matsumoto, Y. Ikeda, H. Suzuki, M. Ogai, N. Miyoshi. Appl. Catal B, 25 (2000) 115-124.

[79] H. Mahzoul, L. Limousy, J. Brilhac, P. Gilot, J. Anal. Appl. Pyrolysis 56 (2000) 179-193.

[80] Z. Say, E. I. Vovk, V. I. Bukhtiyarov, E. Ozensoy, Top. Catal 56 (2013) 950–957.

[81] H. Hirata, I. Hachisuka, Y. Ikeda, S. Tsuji, S. Matsumoto, Top. Catal. 16/17 (2001) 1–4.

[82] J. B. Breen, M. Marell, C. Pistarino, J. R. H. Ross, Catal. lett. 80 (2002) 3-4.

[83] L. J. Alemany, L. Lietti, N. Ferlazzo, P. Forzatti, G. Busca, E. Giamello, F. Bregani, J. Catal. 155 (1) (1995) 117-130.

[84] L. Li, F. Zhang, N. Guan, M. Richter, R. Fricke, Catal. Comm. 8 (3) (2007) 583-588.

[85] P. Gabrielsson, Top. Catal. (28) (2004) 1–4.

[86] O. Krocher, M. Elsener, Appl. Catal. B, 75 (2008) 215–227.

[87] N. Y. Topsoe, J. Dumesic, H. Topsoe, J. Catal. 151 (1995) 241-252.

[88] L. J. Pinoy, L. H. Hosten, Catal. Today, 17 (1993) 151-158.

[89] Grossale, I. Nova, E. Tronconi, Catal. Today, 136 (2008) 18–27.

[90] Nova, M. Colombo, E. Tronconi,Oil and Gas Sci. Tech. Rev. 66 (4) (2011) 681-691.

[91] U. Torre, B. Ayo, R. Juan, G. Velasco, Chem. Eng. J. 207-208 (2012) 10-17.

[92] P. Forzatti, I. Nova, E. Tronconi, *Ind. Eng. Chem. Res.,* 49 (21) (2010) 10386–10391.

[93] J. H. Baik, S. D. Yim, I. -S. Nam, Y. S. Mok, J. H. Lee, B. K. Cho, S. H. Oh, Top. Catal. 30-31 (2004) 1–4.

[94] S. Wiesche, Appl.Therm. Eng.(11-12), (2007) 1790–1798.

[95] Kieffer, J. Lavy, E. Jeudy, N. Bats, G. Delahay, Top. Catal. 56 (2013) 40–44.

[96] H. Sjövall, L. Olsson, E. Fridell, R.J. Blint, Appl. Catal. B, 64 (2006) 180–188.

[97] S. Brandenberger, O. Krocher, A. Tissler, R. Althoff, Catal. Rev. Sci. Eng., 50 (2008) 492–531.

[98] K. R. Tolonen, T. Maunula, M. Lomma, M. Huuhtanen, R.L. Keiski Catal. Today, 100 (2005) 217–222.

[99] S. Kieger, G. Delahay, B. Coq, B. Neveu, J. Catal., 183 (1999) 267–280.

[100] J.H. Park, H.J. Park, J.H. Baik, I.S. Nam, C.H. Shin, J.H. Lee, B.K. Cho, S.H. Oh, J. Catal., 240 (2006) 47–57.

[101] J.A. Sullivan, J. Cunningham, M.A. Morris, K. Keneavey, Appl. Catal. B, 7 (1995) 137–151.

[102] H. Sjövall, E. Fridell, R. Blint, L. Olsson Top.Catal., 42–43 (2007) 113–117.

[103] Grossale, I. Nova, E. Tronconi, D. Chatterjee, M. Weibel, J. Catal. 256 (2008) 312–322.

[104] O. Krocher, M. Devadas, M. Elsener, A. Wokaun, N. Soger, M. Pfeifer, Y. Demel, L. Mussmann, Appl. Catal. B, 66 (2006) 208–216.

[105] Grossale, I. Nova, E. Tronconi, Catal.Lett., 130 (2009) 525–531.

[106] Fritz, V. Pitchon, Appl. Catal. B, 13 (1997) 1-25.

[107] B. Ayo, U. Torre, M. Gómez, A. López, J. Velasco, Appl. Catal. B, 147 (2014) 420–428.

[108] S. A. Skarlis, D. Berthout, A. Nicolle, C. Dujardin, P. Granger, Appl. Catal. B, 148–149 (2014) 446–465.

[109] O. Mihai, C. R. Widyastuti, S. Andonova, K. Kamasamudram, J. Li, S. Y. Joshi, N. W. Currier, A. Yezerets, L. Olsson, J. Catal. 311 (2014) 170–181.

[110] W. Fickel, E. D'Addio, J. A. Lauterbach, R. F. Lobo, Appl. Catal. B, 102 (2011) 441–448.

[111] J. Xue, X. Wang, G. Qi, J. Wang, M. Shen, W. Li, J. Catal. 297 (2013) 56–64.

[112] J.H. Kwak, R.G. Tonkyn, D.H. Kim, J. Szanyi, C.H.F. Peden, J. Catal. 275 (2010)187–190.

[113] J. Szanyi, J.H. Kwak, H. Zhu, C.H.F. Peden, Phys. Chem. Chem. Phys. 15 (2013)2368–2380.

[114] R. Smits, Y. Iwasawa, Appl. Catal. B, 6 (1995) L201.

[115] H. Bosch, F.J.J.G. Janssen, Catal. Today, 2 (1988) 369.

[116] M. Iwamoto, H. Yahiro, S. Shundo, Y. Yu, N. Mizuno, Appl. Catal., 69 (1991) L15.

[117] S. Sato, Y. Yu, H. Yahiro, N. Mizuno, M. Iwamoto, Appl. Catal., 70 (1991) Ll.

[118] H. Yahiro, H. Hirabayashi, H. K. Shin, N. Mizuno M. Iwamoto, Trans. Mater. Res. Sot. Jpn., 18A (1994) 409.

[119] H. K. Shin, H. Hirabayashi, H. Yahiro, M. Watanabe, M. Iwamoto, Catal. Today, 26 (1995) 13.

[120] Y. Li, J. N. Armor, Appl. Catal. B, 3 (1993) Ll.

[121] Witzel, G.A. Sill, W. K. Hall, J. Catal., 149 (1994) 229.

[122] R. Burch, P.J. Millington A.P. Walker, Appl. Catal. B, 4 (1994) 65.

[123] T. E. Hoost, K. Otto, K. A. Laframboise, J. Catal., 155 (1995) 303.

[124] K. A. Bethke, D. Alt, M. C. Kung, Catal. Lett., 25 (1994) 37.

[125] S. Matsumoto, K. Yokota, H. Doi, M. Kimura, K. Sekizawa, S. Kasahara, Catal. Today, 22 (1994) 127-146.

[126] P. G. Blakeman, E. M. Burkholder, H. Chen, J. E. Collier, Joseph M. Fedeyko, H. Jobson, R. R. Rajaram, Catal. Today,231(2014) 56-63.

[127] M. Karthik, H. Bai, Appl. Catal. B, 144 (2014) 809–815.

[128] W. Held, A. Ko¨nig, T. Richter, L. Puppe, SAE Trans., Section 4 No. 900 496 (1990) 209.

[129] V. G. Komvokis, E. F. Iliopoulou, I. A. Vasalos, K. S. Triantafyllidis, C. L. Marshall, Appl. Catal. A, 325 (2007) 345–352.

[130] P. J. Ramirez, G. Cortes, J.M.I. Gomez, F. Kapteijn, J.A. Moulijn, and S.M.C. Lecea, React. Kinet. Catal. Lett., 69 (2) 2000 385-392.

[131] M., Saaid, A.R. Mohamed, and S. Bhatia, React. Kinet. Catal. Lett., 75(2) 2002359-365.

[132] G. Centi, S. Perathoner, Appl. Catal. A 132 (1995) 179.

[133] M. N. Kim, I. -S. Nam, Y. Y. Kim, 1st World Congr. Environ. Catalysis, Pisa, Italy, 1–5 May 1995, p. 251.

[134] E. Kikuchi, K. Yogo, Catal. Today, 22 (1994) 73-86.

[135] Z. R. Ismagilov, R. A. Shkrabina, L. T. Tsykoza, V. A. Sazonov, S. A. Yashnik, V. V. Kuznetsov, N. V. Shikina, H. J. Veringa. Top. Catal. (16) (2001) 307-310.

[136] M. Saaid, A. R. Mohamed, S. Bhatia,J. Mol. Catal. A, 189 (2002) 241–250.

[137] Z. Abdullah, H. Abdullah, S. Bhatia, B. Salamatinia, N. Razali, IIUM Engineering Journal, 11(1) 2010 106-122.

[138] T, Komatsu, K. Tomokuni, I. Yamada, Catal. Today, 116 (2006) 244–249.

[139] T. Komatsu, K. Tomokuni, M. Konishi, T. Shirai, The Open Catal. J., 3 (2010) 24-29.
[140] E. S. Jimenez, V. M. Koci, M. Crocker, K. Wilson, Appl. Catal. B, 102 (2011) 1–8.
[141] M. D. Amiridis, K. L. Roberts, C. J. Pereira, Appl. Catal. B, 14 (1997) 203–209.
[142] Y. Zhang, R. W. Cattrall, I. D. McKelvie, S. D. Kolev, Gold Bull. 44 (2011) 145–153.
[143] H. Ohtsuka, T. Tabata, Appl. Catal. B, 29 (2001) 177–183.
[144] R. Burch, Catal. Rev. 46 (2004) 271–333.
[145] D. Worch, W. Suprun, R. Gläser, Catal. Today, 176 (2011) 309–313
[146] P. Miquel, P. Granger, N. Jagtap, S. Umbarkar, M. Dongare, C. Dujardin, J. Mol.Catal. A, 322 (2010) 90–97.
[147] P. S. Kim, M. K. Kim, B. K. Cho, I. –S. Nam, S. H. Oh, J. Catal. 301 (2013) 65–76.
[148] C. Stere, W. Adress, R. Burch, S. Chansai, A. Goguet, W. G. Graham, F. de Rosa, V. Palma, C. Hardacre, ACS Catal., 2014.
[149] Shimizu, J. Shibata, H. Yoshida, A. Satsuma, T. Hattori, Appl. Catal. B, 30 (2001) 151–162.
[150] T. Chaieb, L. Delannoy, C. Louis, C. Thomas, Appl. Catal. B, 142– 143 (2013) 780–784.
[151] S. Klacar, H. Gronbeck, Catal. Sci. Technol. 2012.
[152] H. Kannisto, K. Arve, T. Pingel, A. Hellman, H. Harelind, K. Eranen, E. Olsson, M. Skoglundh, D. Y. Murzin, Catal. Sci. Technol., 3 (2013) 644-653.
[153] A. Bethke, H. Kung, J. Catal. 172 (1997) 93–102.
[154] H. Kannisto, H. Ingelsten, M. Skoglundh, J. Mol. Catal.A, 302 (2009) 86–96.
[155] H. He, X. Zhang, Q. Wu, C. Zhang, Y. Yu, Catal. Surv. Asia 12 (2008) 38–55.
[156] E. Seker, J. Cavataio, E. Gulari, P. Lorpongpaiboon, S. Osuwan, Appl. Catal. A 183 (1999) 121.
[157] C. Zhang, H. He, S. Shuai, J. Wang, Env. Pollution, 147 (2007) 415-421.
[158] C. Petitto, H. P. Mutin, G. Delahay, Appl. Catal. B, 134– 135 (2013) 258– 264.

Chapter 2: Ag-Au/Al_2O_3 Bimetallic catalysts for improved low temperature HC-SCR of NO_x for lean burn engine exhaust: Influence of thermal activation pretreatment

Abstract:-Bimetallic Ag-Au/Al_2O_3 catalyst with 1% Au and 1% Ag loading on in house prepared high surface area alumina (450 m^2/g) was synthesized by successive impregnation method. For comparison the monometallic catalysts were also prepared by loading 1% Ag or 1% Au on the same high surface area alumina. The catalysts were characterised by various physico-chemical techniques and tested for SCR activity under lean burn engine exhaust condition. Ag-Au/Al_2O_3 catalyst prepared by successive impregnation method showed considerably higher NO reduction (100%) to N_2 compared to 1% Au/Al_2O_3 (70%) whereas the activity was comparable with that of 1% Ag/Al_2O_3 (96%).The effect of various pretreatments on SCR activity of Ag-Au/Al_2O_3 was studied and pretreatment at 250 ºC in flow of hydrogen was found to give the best results with 100% NO conversion to N_2 at 353 ºC. Further ageing of the catalyst under reaction feed at 500 ºC resulted in considerable increase in low temperature activity of bimetallic catalyst with ~40% NO conversion at 222 ºC. Even though the SCR activity of pretreated Ag-Au/Al_2O_3 and Ag/Al_2O_3 were comparable, after ageing the Ag-Au/Al_2O_3 showed significantly higher NO conversion (95%) compared to Ag/Al_2O_3 (83%) and Au/Al_2O_3 (70%). The formation of H_2 and CO due to steam reforming of higher hydrocarbon (decane) was evidenced at the temperature of highest deNO_x activity. Detailed investigation of the textural properties of the pretreated and aged catalysts showed presence of well dispersed metallic Au and $Ag_n^{\delta+}$ clusters after pretreatment in hydrogen at 250 ºC.

1. Introduction

The selective catalytic reduction (SCR) of NO_x using hydrocarbon (HC-SCR) is considered as the most promising alternative technology for removal of NO_x from automobile engine exhaust, operating under lean condition to overcome the drawbacks associated with other deNO_x technologies such as urea SCR and lean NO_x trap (LNT). Development of suitable catalysts for HC-SCR of NO_x is an active area of research in academic as well as industrial laboratories. Among the various catalyst compositions investigated for HC-SCR of NO_x, Ag/Al_2O_3 (2 wt% Ag) has shown promising results and is being considered as a potential catalyst for HC-SCR of NO_x for diesel engine exhaust. However Ag/Al_2O_3 catalyst is not efficient for practical application at lower temperature of diesel engine exhaust. The improvement in low temperature deNO_x activity of Ag/Al_2O_3 catalyst is being investigated by varying the catalyst composition and the method of preparation [1-5].

Supported gold catalysts have also been investigated for HC-SCR of NO_x [6, 7]. Ueda et al. [8] and Haruta et al. [9] have carried out a study of gold supported on various metal oxides for HC-SCR of NO_x and among the screened catalysts Au/Al_2O_3 showed higher NO_x conversion to N_2 in presence of moisture and oxygen [8, 9]. Previous investigations of HC-SCR on Au/Al_2O_3 were performed in the presence of alkanes, alkenes [8–11] or CO as reductant [12, 13]. Ilieva et al. [12, 13] have recently reported reduction of NO_x by CO with 100% selectivity to N_2 at 200 ºC over gold supported on ceria-alumina mixed support. However, the catalytic activity of Au/Al_2O_3 was lower than Ag/Al_2O_3 catalyst for SCR of NO_x using hydrocarbons under lean burn conditions.

To improve the catalytic activity of Ag/Al_2O_3, the modification of either support or active component of the catalyst has been attempted before [14-17]. There have been previous attempts on the use of bimetallic catalyst for enlarging the temperature windows of maximum SCR activity. He et al. [18] modified Ag/Al_2O_3 with Pd which showed higher SCR activity compared to Ag/Al_2O_3 in temperature range of 300 to 450 ºC. The catalytic activity has been related to the formation of more enolic species on $Ag\text{-}Pd/Al_2O_3$ compared to Ag/Al_2O_3. Arve et al. [14] reported the SCR activity of bimetallic nano gold and silver with varying silver and gold loading on alumina and titania. Bimetallic catalysts showed only 30% NO conversion at 500 ºC which was lower compared to Au/Al_2O_3 (~45%). Recently we have reported the SCR activity of Au/Al_2O_3 (1 wt% Au) prepared by deposition precipitation method. However the catalytic activity of Au/Al_2O_3 was found to be lower than in-house

prepared Ag/Al_2O_3 (2 wt% Ag) catalyst [19]. The gold based catalysts exhibited good resistance to thermal ageing which could certainly be adapted to bimetallic formulations. As a general trend, a complex surface chemistry takes place both on gold and silver based catalysts which involve the metal and the support [20]. It was previously found that the extent of metal/support interface and optimal ratio of electrophilic to metallic Au or Ag species govern the overall performances in terms of activity and selectivity toward N_2 production [20-22].

Hence to further improve the low and high temperature activity of Ag/Al_2O_3 catalyst system, we have prepared 1% Ag-1% Au/Al_2O_3 catalysts by successive impregnation method and tested for SCR of NO_x. The effect of different pretreatments on SCR activity of the bimetallic catalysts has been investigated in order to optimize the surface properties regarding the above-mentioned parameters which influence the catalytic activity. Catalytic properties are compared to extended bulk and surface characterisation using various physico-chemical techniques for subsequent comparisons.

2. Experimental

2.1. Catalysts preparation

Chemicals and Reagents: $AgNO_3$ (99.8 wt%, Thomas Baker) and $HAuCl_4$ (49 wt% Au, LOBA Chemie) were used without further purification.

Alumina (γ-Al_2O_3) support was prepared by sol gel method by dissolving 248.96 g aluminium tri-sec-butoxide (97%, Aldrich) in 300 g isopropanol followed by dropwise addition of isopropanol solution (50 mL) of NH_4OH (5 mL, 25%) with constant stirring till formation of the semitransparent gel. Gel was dried in air for 12 h, and calcined at 500 ºC for 4 h and further used as support for preparation of all the catalysts in present work.

1 wt% Au/Al_2O_3 catalyst was prepared by deposition precipitation method using urea. A slurry of γ-alumina (9.9 g) in water (700 mL) was heated at 80 ºC with dropwise addition of gold (III) chloride solution (0.204 g $HAuCl_4$ in 10 mL H_2O) with constant stirring. Urea solution (250 mL 10 M aqueous solution) was added dropwise to the above solution. The obtained sample was aged for 12 h, then filtered and washed with water till complete removal of chlorides and dried at 80 ºC for 12 h. Finally solid was calcined at 500 ºC for 6 h and labeled as AuAl.

Wet impregnation method was used to prepare 1 wt% Ag/Al_2O_3 by adding silver nitrate (0.157 g $AgNO_3$ in 20 mL H_2O) solution to the slurry (700 mL H_2O) of γ-Al_2O_3 (9.9 g) prepared by sol gel method. The catalyst was dried at 80 ºC for 12 h followed by calcination at 500 ºC for 6 h and labeled as AgAl.

Bimetallic catalyst $1Ag\text{-}1Au/Al_2O_3$ was prepared by successive impregnation method. Initially 1 wt% Au/Al_2O_3 was prepared by deposition-precipitation method using urea as mentioned previously (except calcination step). This 1 wt% Au/Al_2O_3 catalyst (dried at 80 ºC for 12h) was further impregnated with $AgNO_3$ (0.157 g in 20 mL H_2O) solution to get bimetallic 1% Ag-1% Au/Al_2O_3 catalyst. The catalyst was dried at 80 ºC for 12 h and then calcined at 500 ºC for 6 h and labeled as AgAuAl.

2.2. Catalyst characterisations

2.2.1. Powder X-ray diffraction studies

The powder X-ray diffraction data was collected on a Philips (X pert) equipped with a Ni filtered Cu Kα radiation (λ = 1.5406 Å, 40 kV, 30 mA). The data was collected in the 2θ range 10-80º with a step size of 0.02º and scan rate of 4º min^{-1}.

2.2.2. Nitrogen adsorption studies

The BET surface area of the calcined samples was determined by N_2 sorption at 77 K using NOVA 1200 (Quanta Chrome) equipment. Prior to N_2 adsorption, the material was evacuated at 300 ºC under vacuum. The specific surface area, S_{BET}, was determined according to the BET equation.

2.2.3. UV-vis diffuse reflectance studies (UV–vis DRS)

UV–vis DRS spectra were recorded with a UV–vis spectrophotometer PerkinElmer, Lambda 650 with integrating sphere assembly in the diffuse reflectance mode between 200 and 800 nm at a step of 0.2 nm with a slit width of 1 nm. $BaSO_4$ was used as a reference sample to confirm the baseline spectrum.

2.2.4. X-ray photoelectron spectroscopy study (XPS)

X-ray photoelectron spectroscopy (XPS) was used for the characterisation of surface of pretreated and aged catalysts. XPS experiments were performed using a V. G. Microtech (UK) Unit ESCA 3000 spectrometer equipped with a Mg Kα X-ray source (hν = 1253.6 eV) and a hemispherical electron analyzer. The X-ray source was operated at 150 W. The residual pressure in the ion-pumped analysis chamber was maintained below 1 x 10^{-9} Torr during data acquisition. Binding energy (B.E.) values were referenced to the binding energy of the Al 2p core level (74.6 eV).

2.2.5. Energy dispersive X-ray spectroscopy (EDS)

The dispersion of metal on the catalyst surface was measured using EDS elemental mapping images taken by Quanta FEI 200 3D equipped with tungsten filament as source of electron.

2.2.6. Transmission electron microscopy (TEM)

TEM experiment was performed with Tecnai FEI G2 microscope, using an accelerating voltage of 300 kV. For TEM analysis, the sample was previously ultrasonically dispersed in isopropanol solvent and then drop of the suspension was deposited on a carbon coated Cu grid of 200 mesh.

2.3. Catalytic activity

The selective catalytic reduction (SCR) of NO_x under realistic synthetic exhaust condition corresponding to lean engine was carried out at atmospheric pressure in quartz tubular down flow reactor (inner diameter 20 mm). Catalyst powder (360 mg) diluted with commercial silicon carbide (2 g) was placed in the reactor and a thermocouple was inserted in the center of the catalyst bed to measure the temperature. Typical reaction feed used for SCR activity was 300 ppm NO, 300 ppm CO, 300 ppm C_3H_6, 2000 ppm H_2, 100 ppm $C_{10}H_{22}$, 10% CO_2, 10% O_2, 5% H_2O, He balance. The total flow rate of the gas mixture was 300 mL min^{-1} to obtain a gas hourly space velocity of 50,000 $mL.g^{-1}.h^{-1}$. The flow rate was monitored by mass flow controller.

Fig. 1b and 1c represent the schematic diagram and photograph of DeNOx set up. Fig. 1c illustrates the typical experimental procedure implemented for the catalytic measurements.

Initially (step I) the catalyst was pretreated under different oxidative or reductive atmosphere for 12 h. The different pretreatment conditions used were (i) at 250 ºC in hydrogen flow (ii) at 500 ºC in hydrogen flow or (iii) at 500 ºC in air flow. After pretreatment the catalyst was cooled to 80 ºC and the reaction feed was passed on catalyst surface with increasing the temperature from 80 ºC to 500 ºC with heating rate of 2 ºC min^{-1} (step II). The reaction feed was stabilized on the catalyst at 500 ºC for 12 h for catalyst ageing (step III). Later the catalyst was cooled to 80 ºC and in the last stage (step IV) the catalytic activity was monitored under reaction feed with increasing the temperature from 80 to 500 ºC with heating rate of 2 ºC min^{-1}.

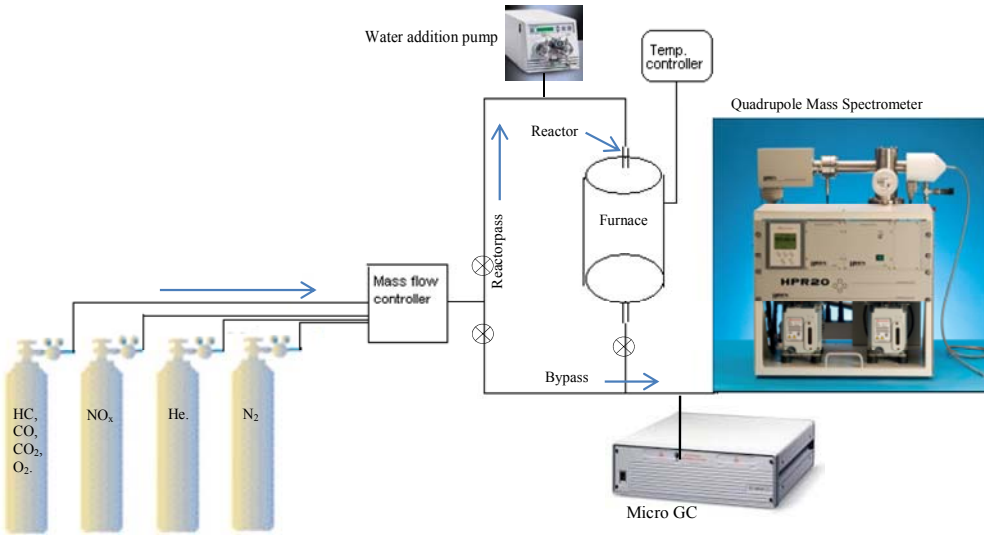

Fig. 1a. Schematic diagram of DeNOx set up

Fig. 1b. Photograph of DeNOx set up

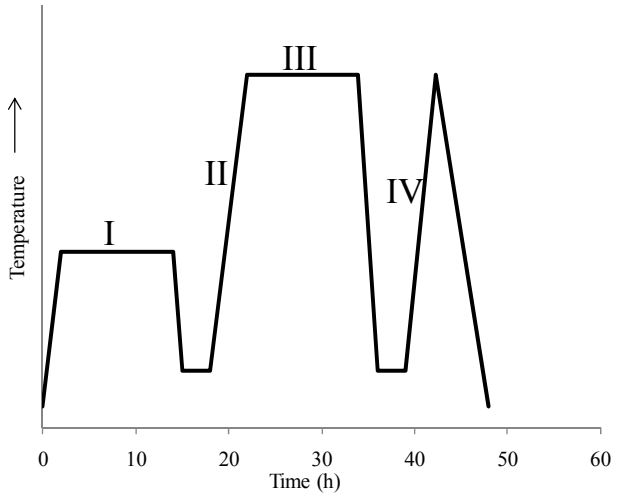

Fig. 1c. Typical protocol for catalyst testing

The concentrations of the inlet and outlet gases were simultaneously monitored using Micro GC (Varian, CP 4900) and NO_x analyzer (Environment SA MIR 9000). The micro GC has two columns to detect different gases: molecular sieves (MS 5A) with TCD detector for H_2, N_2, O_2, NO, CO and Porapak Q for H_2, CO_2, N_2O, C_3H_6 and H_2O.

The NO conversion was calculated from outlet molar flow rates of N_2 + N_2O formation (F_{N_2}, F_{N_2O}) and inlet molar flow rate of NO ($F_{0,\,NO}$) using the following Eq. (1):

$$\%NO\ Conv. = 100 \times \frac{2 \times \left(F_{N_2} + F_{N_2O}\right)}{F_{0,\,NO}} \qquad (1)$$

N_2 selectivity was calculated using following Eq. (2) :

$$S_{N_2} = 100 \times \frac{F_{N_2}}{F_{N_2} + F_{N_2O}} \qquad (2)$$

3. Result and discussion

3.1. Catalytic activity

The catalytic activity of monometallic Ag/Al_2O_3 (AgAl) and Au/Al_2O_3 (AuAl) catalysts was compared with bimetallic $Ag\text{-}Au/Al_2O_3$ (AgAuAl) catalyst during the selective

catalytic reduction (SCR) of NO by hydrocarbons. The influence of various thermal pretreatments using bimetallic Ag-Au/Al_2O_3 catalyst (AgAuAl) was investigated. The selectivity for N_2 and N_2O formation as well as the involvement of different reductants during the temperature-programmed reaction was carefully examined.

3.1.1. Catalytic activity of monometallic and bimetallic catalysts

SCR activity of bimetallic AgAuAl catalyst was compared with monometallic AuAl and AgAl catalysts. The NO to N_2 conversion curves of catalysts treated in H_2 at 250 ºC (step I) are presented in Fig. 2A. Both monometallic AuAl and bimetallic AgAuAl catalysts showed 100% selectivity for N_2 over a complete temperature range whereas AgAl catalyst showed less than 100% selectivity for N_2 up to 275 ºC with corresponding N_2O formation.

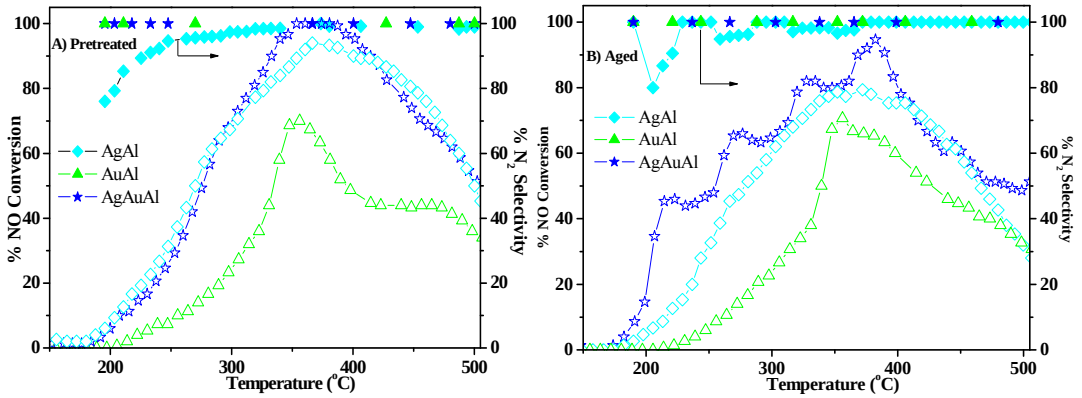

Fig. 2. %NO conversion (open symbols) and N_2 selectivity (filled symbols) of catalysts A) pretreated at 250 ºC in H_2 and B) aged. Reaction feed: 300 ppm NO, 300 ppm CO, 300 ppm C_3H_6, 2000 ppm H_2, 100 ppm $C_{10}H_{22}$, 10% CO_2, 10% O_2, 5% H_2O, He balance, GHSV= 50,000 $mL.g^{-1}.h^{-1}$.

A typical volcano-type profile was obtained for NO conversion on AgAl catalyst which was previously ascribed to the involvement of NO_2 as intermediate [20]. The spill-over of NO_2 from the metal to activated hydrocarbon onto the support was proposed by Burch et al. [23]. The volcano-type curve can be explained by kinetically limited reaction at low temperature (NO conversion to NO_2) whereas thermodynamic unfavoured NO_2 formation at high temperature. The decrease in the NO conversion at higher temperature can also be attributed to unselective oxidation of hydrocarbon contributing to the volcano type curve of

NOx reduction. At low temperature, the AgAl catalyst showed highest NO conversion whereas AgAuAl catalyst presented marginally lower conversion and AuAl catalyst showed significantly lower NO conversion. The SCR activity of pretreated AgAuAl and AgAl catalysts around 350 ºC was comparable with maximum NO conversion of 100% and 96% respectively. The maximum NO conversion for AuAl catalyst was considerably lower (70%) than that of AgAuAl and AgAl catalysts. Above 400 ºC, AgAuAl and AgAl catalysts exhibited similar conversion curves with decreasing NO conversion with increase in temperature. The three catalysts were then aged overnight under reaction feed before a second temperature-programmed reaction (step IV - Fig. 1) was carried out. Clearly the catalytic activity (Fig. 2B) was altered after ageing procedure. AgAuAl catalyst had shown improved low temperature activity compared to pretreated catalysts under H_2 at 250 °C. However there was no improvement in low temperature activity for AuAl and AgAl catalysts. After ageing AgAuAl catalyst has shown better low temperature activity (222 ºC) with 40% NO conversion compared to AgAl (14%) and AuAl (~2%) catalysts. Higher maximum NO conversion (95%) was obtained on AgAuAl catalyst compared to AgAl catalyst (78%) and AuAl catalyst (70%). There was marginal increase in temperature corresponding to maximum NO conversion after ageing in case of AgAuAl and AgAl catalysts. A decrease in high temperature activity (above 400 ºC) was evidenced for AgAuAl and AgAl catalysts. A reverse tendency was observed for AuAl with increase in high temperature activity after ageing which is in agreement with the previous report [21]. Arve et al. reported lower NO conversion on bimetallic Au-Ag/Al_2O_3 catalyst compared to monometallic Au/Al_2O_3 catalyst (45% NO to N_2 conversion at 500 ºC) [14]. This difference can be assigned to the presence of hydrogen in the reaction mixture in present study.

3.1.2. Effect of different pretreatments on SCR activity of AgAuAl

The effect of different pretreatments on SCR activity of AgAuAl catalyst is shown in Fig. 3A. AgAuAl catalyst was pretreated under three different conditions; at 250 ºC in presence of hydrogen, at 500 ºC in presence of hydrogen or at 500 ºC in presence of air. Complete selectivity for N_2 was obtained using AgAuAl catalyst over the entire range of temperature irrespective of the thermal pretreatment. The activation of NO initiated around 200 ºC and the catalysts showed almost similar NO conversion profiles up to 300 ºC. AgAuAl catalyst pretreated at 250 ºC in presence of hydrogen showed maximum activity with 100% NO conversion at 353 ºC. Catalyst pretreated at 500 ºC in hydrogen showed 86%

NO conversion at 372 ºC whereas the same catalyst after pretreatment in air at 500 ºC showed only 70% NO conversion at 375 ºC. Above 400 ºC, the NO conversion decreased for catalyst pretreated under different conditions. However the catalyst pretreated under H_2 at 250 ºC exhibited highest NO conversion compared to other pretreated catalysts. To our knowledge effect of different pretreatments on SCR activity of NO_x in lean condition for bimetallic Ag-Au based catalysts has not been reported in the literature. Nam et al. [24] underlined the effect of pretreatment in presence of O_2 and $H_2 + O_2$ on reducibility of silver species in Ag/Al_2O_3. The reducibility of Ag species was improved when pretreated in flow of $H_2 + O_2$ compared to only O_2. The reduction of Ag initiated at room temperature with H_2 consumption maxima at 150 ºC when pretreated in $H_2 + O_2$ whereas the catalyst pretreated in only O_2 showed reduction initiation temperature at 100 ºC with H_2 consumption maxima at 350 ºC. On the other hand the pretreatment can affect surface composition of bimetallic AgAuAl catalyst as suggested by catalytic measurements.

The stability of the catalytic performances depending on initial activation procedure was investigated by ageing the catalyst at 500 ºC under reaction conditions for 12 h (Fig. 1 step III). The NO conversion measured on aged catalysts is presented in Fig. 3B. It should be noted that the selectivity for N_2 is not altered with 100% N_2 selectivity in the whole temperature range studied even after ageing irrespective of the thermal pretreatment. The aged catalysts showed higher activity at low temperature whereas the maximum NO conversion level decreased around 350 ºC for all catalysts. The aged catalyst pretreated in hydrogen at 250 ºC showed almost 40% NO conversion at 222 ºC whereas aged catalyst pretreated in hydrogen and air at 500 ºC showed ~24% and ~2% NO conversion respectively. The catalysts pretreated in hydrogen at 250 and 500 ºC showed almost similar maximum conversion (90%) at 353 ºC whereas catalyst pretreated in air showed only 62% NO conversion at 372 ºC. The catalyst pretreated in H_2 at 250 ºC showed significant enhancement in SCR activity after ageing as compared to other pretreatments. The comparison of the temperature corresponding to 50% NO conversion (T_{50}) also emphasized the best catalytic performances of the catalyst pretreated under hydrogen at 250 ºC with the lowest T_{50} (250 ºC) whereas highest T_{50} (336 ºC) was obtained for the catalyst pretreated at 500 ºC under air.

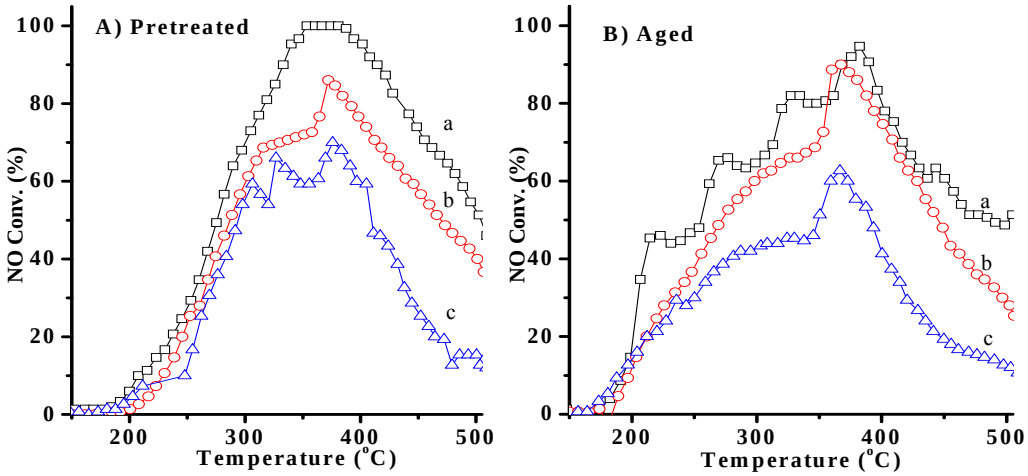

Fig. 3. SCR activity of AgAuAl catalyst A) after different pretreatments a) 250 ºC in H_2, b) 500 ºC in H_2, c) 500 ºC in air. B) aged. Reaction feed:- 300 ppm NO, 300 ppm CO, 300 ppm C_3H_6, 2000 ppm H_2, 100 ppm $C_{10}H_{22}$, 10% CO_2, 10% O_2, 5% H_2O, He balance, GHSV=50,000 $mL.g^{-1}.h^{-1}$.

The catalyst pretreated at 500 ºC under H_2 showed intermediate T_{50} at 276 ºC. In addition the experiments were carried out under steady state conditions (not presented) and the results showed similar NO conversion profiles. As a general trend, it seems obvious that a pre-reductive thermal treatment prior to SCR reaction has a beneficial effect. However, it depends on the reduction temperature, a moderate pre-reduction temperature seems more appropriate due to possible thermal sintering at high temperature (500 ºC).

Interestingly, ageing overnight at 500 ºC under reaction conditions has two opposite effects related to slightly lower maximum NO conversion and a significant broadening of the operating window with a significant rate enhancement in NO conversion at low temperature. All those observations reflect significant surface reconstructions during reaction which may depend on the nature of the pre-activation thermal treatment. Indeed, the equilibration of the oxidation state of gold and silver can be of capital importance.

3.1.3. Correlation of NO_x reduction activity with CO, H_2 and C_3H_6 evolution

In our previous work, the role of hydrogen in activation of NO in the presence of decane, propene and CO were reported on AuAl catalyst [19, 21]. The concentration of

different reactants like H_2, CO and propene were monitored during temperature programmed reaction on AgAuAl, AgAl and AuAl catalysts (Fig. 4-6 respectively). In case of AgAuAl catalyst pretreated at 250 ºC in H_2 (Fig. 4) a continuous decrease in hydrogen concentration with corresponding increase in NO conversion was observed from 180 ºC without considerable change in CO and C_3H_6 concentration upto 230 ºC indicating low temperature hydrogen SCR of NO_x.

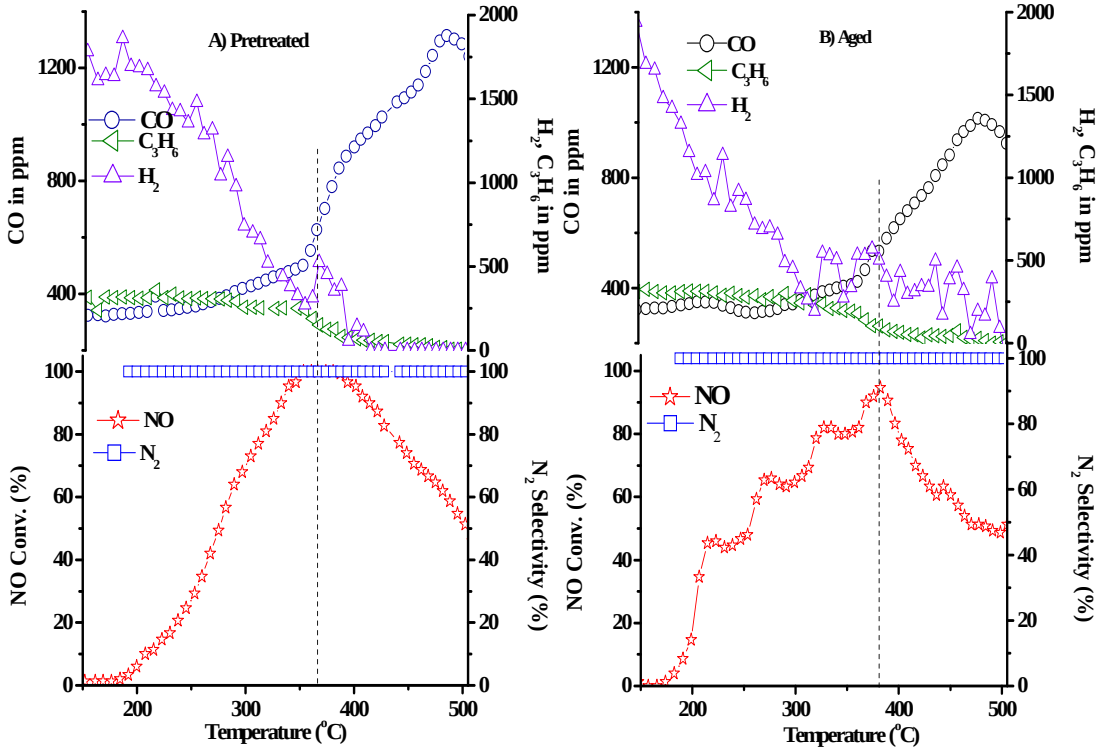

Fig. 4. Evolution of CO, H_2, C_3H_6 and NO_x conversion during HC-SCR of AgAuAl A) pretreated in H_2 at 250 ºC and B) aged. Reaction feed: 300 ppm NO, 300 ppm CO, 300 ppm C_3H_6, 2000 ppm H_2, 100 ppm $C_{10}H_{22}$, 10% CO_2, 10% O_2, 5% H_2O, He balance, GHSV=50,000 $mL.g^{-1}.h^{-1}$.

From 230 to 353 ºC, marginal increase in CO concentration could be related to activation of decane. A significant formation of hydrogen and CO at 353 ºC may be due to the steam reforming of higher hydrocarbon (decane) in the feed [20], whereas decrease in C_3H_6 concentration may be due to propene SCR of NO_x. Concentration of H_2 decreased after 380 ºC whereas CO concentration increased continuously and reached 1300 ppm at 500 ºC which correspond to the partial oxidation/ reforming of decane (100 ppm) to CO and initial CO content in the feed. However the amount of CO generated does not match with increase in hydrogen concentration when steam reforming of decane is considered. Hydrogen is known to be better reductant compared to CO and C_3H_6 in SCR reaction and is known to help in lowering the temperature of SCR activity [1, 19]. The hydrogen generated during steam reforming of decane on AgAuAl catalyst was consumed during SCR activity and equivalent amount of hydrogen was not observed in the analysis. Pretreated and aged AgAuAl catalyst showed 100% selectivity for N_2 over complete temperature range.

Lee et al. [25] have studied the fuel reforming assisted SCR of NO_x using Ag/Al_2O_3 catalyst where higher hydrocarbon was used for catalytic partial oxidation (CPOx) for generation of CO/H_2 using separate commercial diesel fuel cracking (DFC) catalyst. The study has shown very poor NO_x and hydrocarbon conversion upto 350 ºC with the individual hydrocarbons in absence of DFC catalyst whereas in presence of DFC considerable improvement in low temperature (< 300 ºC) SCR activity was observed. DFC catalyst generates hydrogen *in situ* by partial oxidation of decane which acts as an additional reductant with improved SCR activity below 300 ºC [25]. In the present case reforming and SCR activity are observed on the same AgAuAl catalyst and no separate catalyst was required for reforming of the higher hydrocarbon (decane) resulting in improved low temperature SCR activity. However this catalyst was not efficient for the selective reduction of NO_x by CO leading to release of unreacted and formed CO at high temperature.

Interestingly in the case of AgAuAl catalyst aged overnight under reaction feed (Step III – Fig. 1), low temperature H_2-SCR appeared to be more prominent (nearly 40% NO conversion at 222 ºC) as seen in Fig. 4B. The concentration of H_2 at 222 ºC was significantly lower for aged catalyst (862 ppm) compared to the freshly pretreated catalyst (1547 ppm) which is in agreement with higher NO conversion after ageing. This indicates the broadening of temperature window for NO conversion after ageing.

Similar trend was observed for evolution of other reductants on aged catalysts compared to the pretreated catalyst. The concentration of H_2 and propene remain unchanged after ageing except CO. At 500 ºC the CO concentration was 967 ppm which could reflect incomplete reforming of decane after ageing. Marginal decrease in both NO conversion and extent of steam reforming indicated slight deactivation of the catalyst during ageing procedure.

Similar features were observed for monometallic AgAl catalyst and are reported in Fig. 5. The formation of H_2/CO with AgAl catalyst pretreated in H_2 at 250 ºC was observed at temperature of maximum NO conversion though it started at lower temperature (from 250 ºC). It should be mentioned that the selectivity was not complete to N_2 at low temperature. N_2 selectivity was lower with corresponding formation of N_2O. Maximum NO conversion of 96% was obtained at 375 ºC for the catalyst after reduction at 250 ºC (Fig. 4A). At higher temperature CO concentration increased upto 1073 ppm at 500 ºC, indicating lower efficiency of AgAl for CO SCR of NO_x.

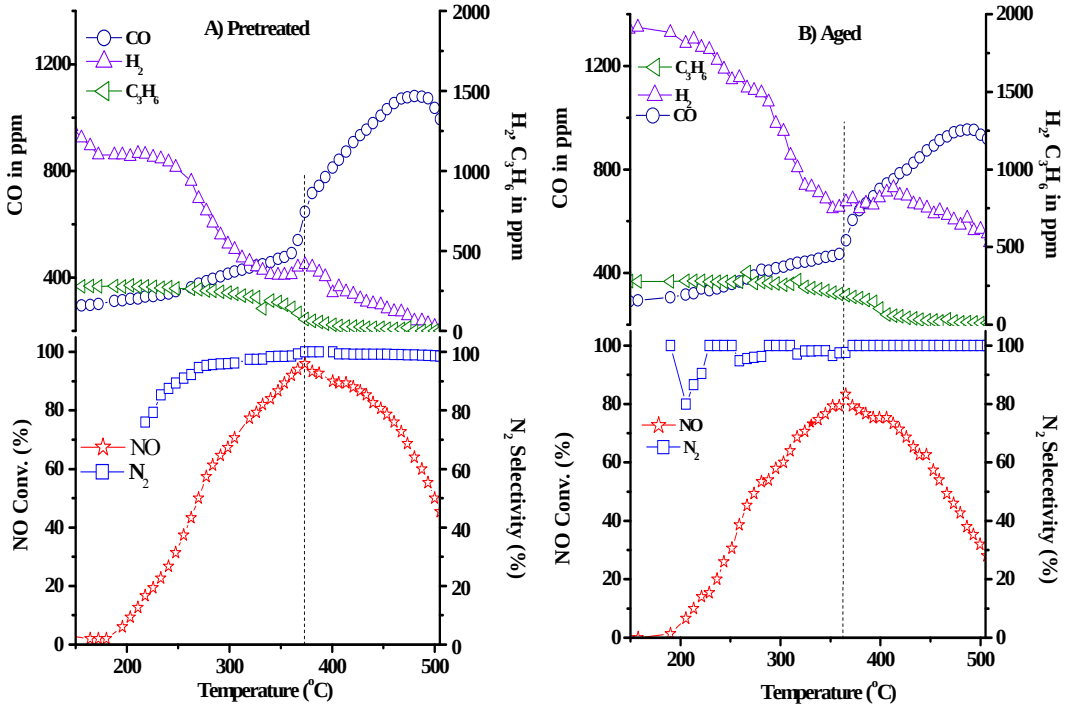

Fig. 5. Evolution of CO, H_2, C_3H_6concentration and NO_x conversion during HC-SCR of AgAl a) pretreated in H_2 at 250 °C and B) aged catalysts. Reaction feed: 300 ppm NO, 300 ppm CO, 300 ppm C_3H_6, 2000 ppm H_2, 100 ppm $C_{10}H_{22}$, 10% CO_2, 10% O_2, 5% H_2O, He balance, GHSV=50,000 $mL.g^{-1}.h^{-1}$.

When the same catalyst was aged under reaction feed at 500 ºC (Fig. 5B), the maximum conversion decreased to 83%. However there was no change in the NO conversion profile at lower temperature up to 350 ºC. At 500 ºC the CO concentration was 873 ppm for aged catalyst which could reflect lower extent of decane reforming after ageing procedure. Decrease in NO conversion and CO formation again point out at slight deactivation of the catalyst during ageing procedure. Also presence of CO at high temperature in pretreated and aged catalyst indicated that CO was not activated on silver. On the other hand the formation of CO at high temperature on AgAuAl catalyst can be attributed to the presence of silver.

However in case of AuAl catalyst (Fig. 6) the two major differences were observed. The formation of H_2 through steam reforming at the maximum NO conversion was not evidenced on monometallic AuAl catalyst as it was previously observed in the case of AgAl and AgAuAl catalysts. Then the formation of small amount of CO may be due to partial oxidation of hydrocarbon.

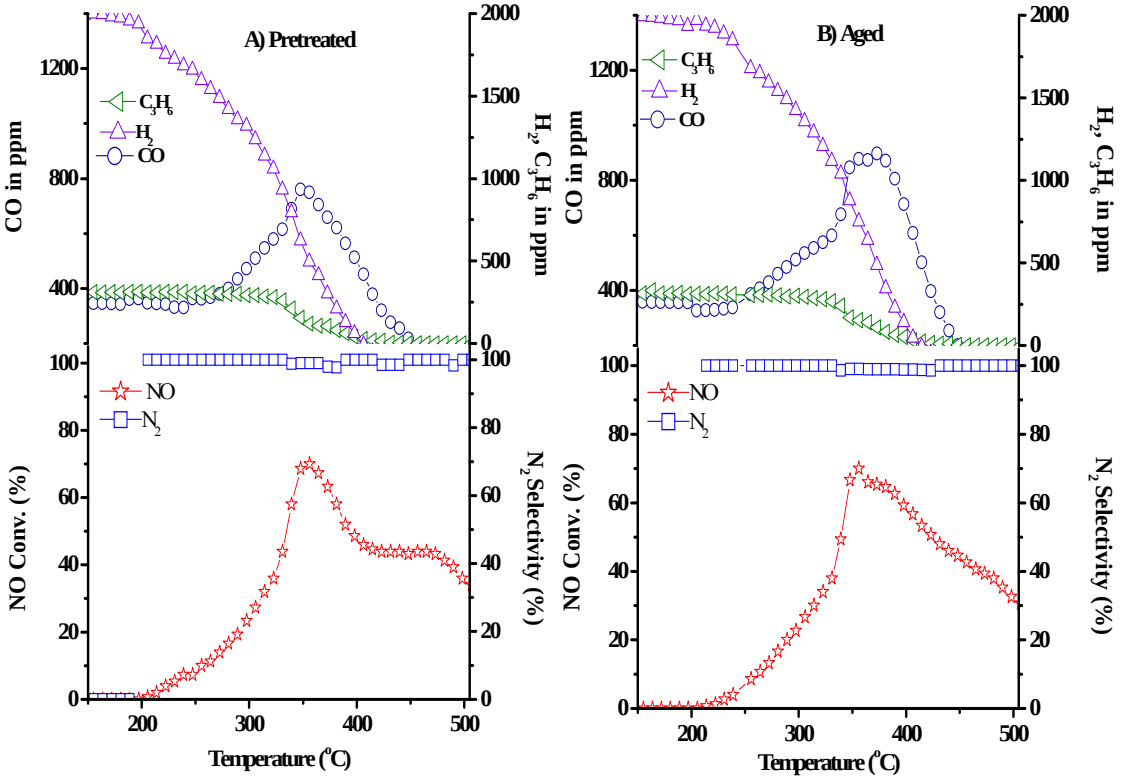

Fig. 6. Evolution of CO, H_2, C_3H_6 concentration and NO_x conversion during HC-SCR of AuAl (A) pretreated in H_2 at 250 ºC and (B) aged catalyst. Reaction feed:- 300 ppm NO, 300 ppm CO, 300 ppm C_3H_6, 2000 ppm H_2, 100 ppm $C_{10}H_{22}$, 10% CO_2, 10% O_2, 5% H_2O, He balance, GHSV=50,000 $mL.g^{-1}.h^{-1}$.

At high temperature the successive oxidation of decane to CO and CO to CO_2 or the selective catalytic reduction of NO_x by CO could be suggested. The CO concentration was only around 90 ppm at 500 ºC underlining the fact that AuAl catalyst was more efficient to activate CO at high temperature. It is also interesting to note that there was no deactivation of AuAl after ageing unlike AgAl or AgAuAl. The maximum NO conversion (70%) as well as temperature of maximum activity (350 ºC) was unaltered after ageing. In fact there was improvement in high temperature activity after ageing. At 400 ºC NO conversion increased from 49% to 59% after ageing. The increase in CO formation (750 to 878 ppm at 356 ºC) due to the increase in partial oxidation of hydrocarbon could be suggested for improvement in activity of AuAl after ageing. When catalytic performances of bimetallic AgAuAl catalyst was compared with monometallic AgAl and AuAl catalysts, the participation of both gold and silver was evidenced from the concentration profile of the reductants. Complete selectivity for N_2 at lower temperature could be attributed to presence of gold whereas presence of silver could be involved in the steam reforming at higher temperature (>230 °C). In case of monometallic catalyst a slight deactivation was observed after aging (NO conversion decreased from 100 to 83% in case of AgAl catalyst).

However no such deactivation due to ageing was evident in case of bimetallic AgAuAl catalyst, in fact there was improvement in low temperature activity (40% NO conversion at 222 °C). This suggests slight modifications of Au and/or Ag nanoparticles during the ageing procedure resulting in formation of more catalytically active Ag and Au species which led to increase in catalytic activity. Moreover the increase in NO conversion at low temperature with complete selectivity for N_2 suggested that gold could be responsible for improved silver dispersion after ageing in case of bimetallic AgAuAl catalyst. Generally the diesel engine exhaust temperature does not exceed 500 ºC. However during regeneration of diesel particulate filter (DPF) the temperature may exceed 500 ºC. Hence AgAuAl catalyst was aged at 650 ºC instead of 500 ºC in reaction feed for 12 h to test the catalyst stability at high temperature. The SCR activity of AgAuAl catalyst after ageing at 500 or 650 ºC was similar with respect to NO conversion and N_2 selectivity confirming the high temperature stability of the AgAuAl catalyst.

3.2. Catalyst characterisation

Effect of various pretreatments and ageing on the dispersion of metals on alumina surface as well as formation of different metallic species on the surface was studied by detailed bulk and surface characterisation of the pretreated and aged catalysts.

3.2.1. Specific surface area and powder X-ray diffraction analysis

The alumina support prepared by sol-gel method using aluminum tri-sec-butoxide as precursor showed very high specific surface area (450 m^2g^{-1}) (table 1) compared to conventionally prepared alumina by calcination of boehmite (237 m^2g^{-1}) [15]. The slow hydrolysis of aluminum tri-sec-butoxide led to the formation of semi transparent gel which after drying and calcination gave very high surface area. The specific surface area of the catalyst decreased after deposition of 1 wt% Au (AuAl), 1 wt% Ag (AgAl) or both 1 wt% Au and 1 wt% Ag (AgAuAl). Surprisingly the specific surface area of AgAuAl (224 m^2g^{-1}) was higher compared to AuAl (210 m^2g^{-1}), though in AgAuAl silver nitrate is impregnated on AuAl. Agglomeration of Au during calcination could be prevented due to the presence of Ag in AgAuAl catalyst leading to slightly higher specific surface area of final calcined catalyst compared to AuAl. The lower surface area of AuAl could be due to the agglomeration of Au during calcinations which is otherwise prevented in bimetallic AgAuAl. Table 1 shows elemental analysis of Ag and Au in AgAuAl, AgAl and AuAl catalysts pretreated in H_2 at 250 ºC which is in agreement with the preparation. EDS results of AgAuAl indicated more availability of silver compared to gold on the catalyst surface. Arve et al. [14] have reported that bimetallic Ag-Au/Al_2O_3 catalyst with less amount of Au on the surface compared to Ag shows better NO conversion to N_2.

Table1. Specific surface area and elemental analysis of Al_2O_3, AgAuAl, AgAl and AuAl catalysts

Sr. No.	Catalysts	Surface area (m^2g^{-1})	Element wt%	
			Ag	Au
1	γ-Al_2O_3	450	-	-
2	AgAuAl	224	1.04	0.80
3	AgAl	239	0.90	-
4	AuAl	210	-	0.96

The XRD patterns of the catalysts pretreated in H_2 at 250 ºC (Fig. 7A) and after ageing overnight in the reaction feed at 500 ºC (Fig. 7B) were recorded to study the effect of thermal treatment on the structure of the catalyst. The XRD pattern of Ag_2O was also recorded for comparison. The broad XRD peaks (Fig. 7A-a) observed at 2θ 32.2, 38.01, 46.02 and 66.7º confirmed formation of γ-Al_2O_3 (JCPDS, 29-0063). The broad and low intensity peaks indicated a low crystallinity and high surface area material in agreement with the BET measurements. The XRD pattern of AgAl catalyst showed peaks (Fig. 7A-c) at 2θ 38.2, 44.2, 64.4º corresponding to metallic silver (JCPDS, 04-0783). Metallic gold crystallites were detected on AuAl catalyst with characteristic XRD peaks (Fig. 7A-b) at 2θ 38.18, 44.39, 64.57º (JCPDS, 04-784). However peaks of metallic Ag and Au could not be easily differentiated in case of AgAuAl catalyst due to high dispersion of metals as well as overlapping peaks of Ag and Au at 2θ 38.2, 44.2, 64.4º with peaks of γ-Al_2O_3 due to the small difference in d-spacing. In case of AgAuAl (Fig. 7A-d) due to presence of metallic Ag and Au the peak at 44.4 and 64.5º appeared as shoulder with broadening of alumina peak at 46.02 and 66.7º respectively. The XRD patterns of all the catalysts after ageing in reaction feed at 500 ºC are given in Fig. 7B. After ageing monometallic catalysts (AgAl and AuAl catalysts) showed similar characteristics as that of pretreated. In case of bimetallic AgAuAl catalyst (Fig. 7B-d) the broadening of the peaks was observed after ageing with significant decrease in peak intensity. The broadening suggested a better dispersion of silver and gold particles on alumina support with formation of smaller metallic particles.

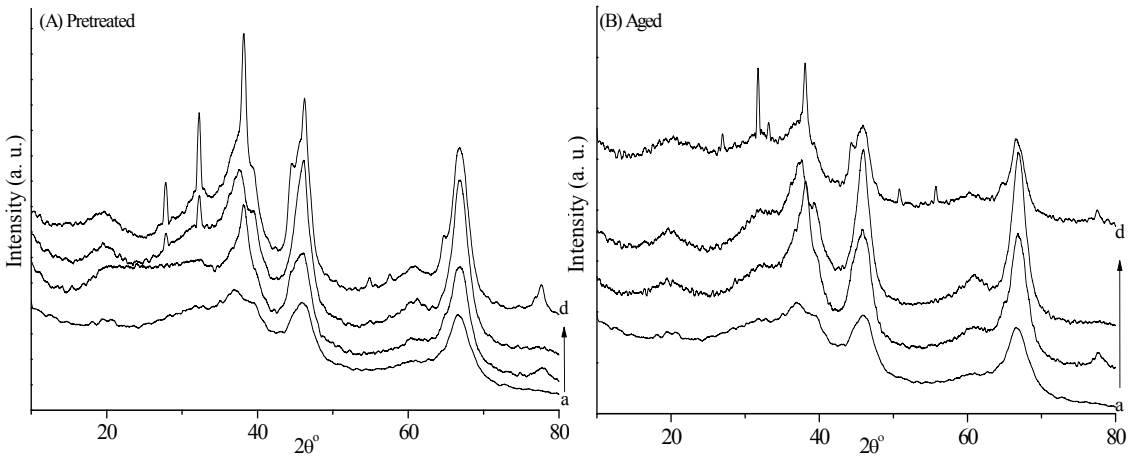

Fig. 7. XRD patterns of (A) Pretreated in H_2 at 250 ºC and (B) Aged a) Al_2O_3 b) AuAl c) AgAl d) AgAuAl.

3.2.2. UV-vis diffuse reflectance spectroscopy study (UV-vis DRS)

A UV-vis diffuse reflectance spectrum of AgAuAl catalyst after various pretreatments is shown in Fig. 8. For clarity in distinguishing the peaks for different species of active component, UV spectrum of Al_2O_3 was subtracted from UV of all the catalyst samples. AgAuAl catalyst after pretreatment in H_2 at 250 ºC (Fig. 8a) showed bands at 450 nm and 525 nm corresponding to the metallic silver and gold respectively. The presence of $Ag_n^{\delta+}$ clusters was evidenced with the band at 275 nm [16, 19, 24-31]. The pretreatment in presence of H_2 at 500 ºC (Fig. 8b) has led to change of the UV-vis spectra with the decrease of contributions at 550 nm and 275 nm. Decrease in intensity of band at 275 nm suggested the decrease in concentration of $Ag_n^{\delta+}$ species due to more intense reduction of Ag^+. Also band at 490 nm corresponding to the AgAu alloy was observed, indicates that high temperature pretreatment under H_2 (500 ºC) led to the formation of alloy, which was not observed after reduction at 250 ºC. A shift was observed in metallic silver (450 nm) and gold (525 nm) bands when AgAuAl catalyst was pretreated in presence of air at 500 ºC (Fig. 8c). Clearly the nature of Ag and Au particles was significantly modified by the pretreatment. The intensity of $Ag_n^{\delta+}$ band was maximum when AgAuAl catalyst was pretreated in H_2 at 250 ºC indicating formation of more $Ag_n^{\delta+}$ clusters compared to other pretreatments.

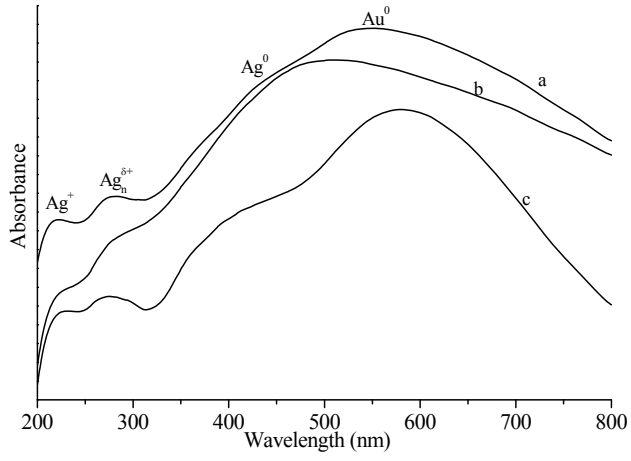

Fig. 8. UV-vis DRS spectra of AgAuAl catalyst pretreated in a) 250 ºC in H_2, b) 500 ºC in H_2, c) 500 ºC in air.

The comparison of UV-vis spectra of AgAuAl, AgAl and AuAl catalysts after pretreating in presence of H_2 at 250 ºC is presented in Fig. 9A. The intensity of band at 275 nm was significantly higher for AgAuAl catalyst compared to AgAl catalyst, indicating higher concentration of $Ag_n^{\delta+}$ species. AgAl catalyst also showed the presence of Ag^+ at 230 nm. The metallic silver was observed at 450 nm in AgAl as well as AgAuAl catalysts. The large metallic Ag clusters are reported to lead to the formation of N_2O at low temperature in HC-SCR using Ag/Al_2O_3 catalyst [32]. Hence in present case also the formation of N_2O at low temperature (below 250 ºC) on AgAl catalyst (Fig. 5A) can be attributed to larger silver particles whereas in case of AgAuAl catalyst no N_2O formation was observed. Arve et al. have also reported 100% selectivity for N_2 using bimetallic Ag-Au system [14]. Both AuAl and AgAuAl catalysts showed presence of metallic gold at 554 and 550 nm respectively [19, 26, 28-31]. There was no AuAg alloy formation observed in UV (band at 460-490 nm) after reduction at 250 ºC.

The effect of ageing in reaction feed at 500 ºC was studied by UV-vis DRS for all the catalysts after pretreating in presence of H_2 at 250 ºC (Fig. 9 B). The intensity of $Ag_n^{\delta+}$ species (275 nm) increased considerably on aged AgAuAl catalyst compared to pretreated catalyst. At the same time the band corresponding to the metallic silver (450 nm) disappeared. There was no change in band position of Au^o (550 nm) after ageing indicating no agglomeration of gold particles due to ageing at 500 ºC.

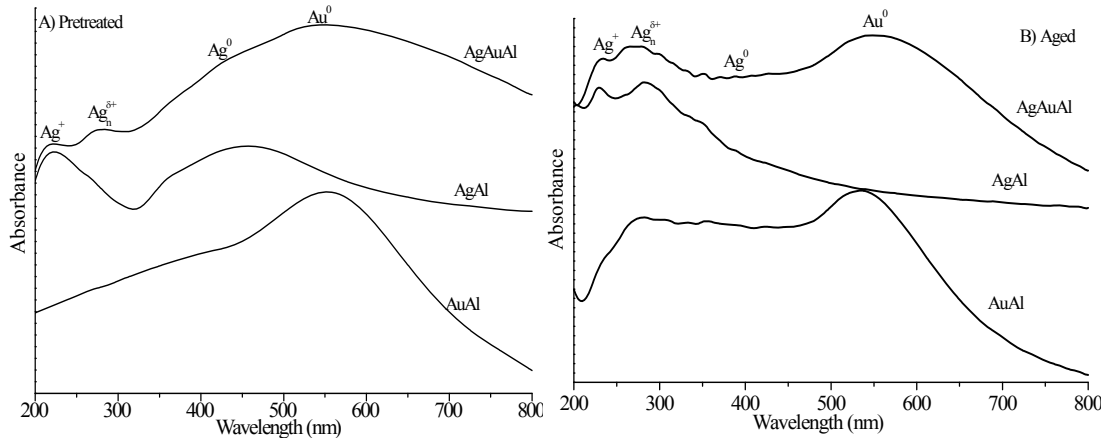

Fig. 9. UV-vis DRS spectra of AgAuAl, AgAl and AuAl (A) pretreated in H_2 at 250 ºC and (B) aged catalysts.

The band related to $Ag_n^{\delta+}$ species developed in case of aged AgAl catalyst at the expense of the band corresponding to the metallic silver which confirmed the oxidation of metallic silver to $Ag_n^{\delta+}$ (through Ag^+) during ageing procedure. The Ag^+ species may get converted to $Ag_n^{\delta+}$ clusters in presence of H_2 and O_2 [24]. AuAl catalyst showed shift in peak maxima for metallic gold to lower wavelength (554 to 534 nm) after ageing which suggested an improved dispersion of Au particles with corresponding decrease in particle size.

Increase in the relative concentration of $Ag_n^{\delta+}$ species in AgAuAl catalyst after ageing could be due to the presence of H_2, O_2 and hydrocarbon in the reaction feed [33]. H_2 and O_2 can adsorb dissociatively to form -OH species. A transfer of charge from Ag to OH was proposed in the literature on Ag-OH (Ag^+) accompanied with back donation from OH to Ag, in this case former is greater than later leading to the formation of $Ag_n^{\delta+}$ from Ag^+ [27, 24]. Similarly also in AgAl, $Ag_n^{\delta+}$ formation take place may be proposed from Ag^0 via Ag^+. Partially charged metallic silver and metallic gold were clearly observed in UV-vis DRS analysis and could influence the SCR of NO_x [4-5, 14-15, 18, 19, 26, 22].

3.2.3. X-ray photoelectron spectroscopy studies (XPS)

Fig. 10 shows the comparison of XPS data for pretreated and aged AgAuAl catalyst plotted on the common scale of intensity. Table 2 summarizes the binding energy as well as surface concentration of Ag and Au on AgAuAl catalyst. The catalyst reduced at 250 ºC showed considerably lower intensity of silver species compared to aged catalyst on the surface (Fig. 10). XPS data clearly revealed increased intensity of silver species on aged catalyst compared to pretreated AgAuAl catalyst.

Table 2. Binding energy of Ag and Au in AgAuAl catalyst.

Catalyst		**Binding energy (eV.)**		**%Surface atomic composition (relative accuracy ± 20%)**	
		$Au4f_{7/2}$	$Ag3d_{5/2}$	Au (%)	Ag (%)
AgAuAl	Fresh	84.0	368.2	<0.1	0.14
	Aged	83.7	367.9	<0.1	0.27

The BE for Ag^+ was observed at 367.15 eV in pretreated AgAuAl catalyst which remained almost unchanged after ageing, however the BE for Ag^0 was observed at 368.6 eV which shifted to 368.5 eV after ageing. The ratio of Ag^0/Ag^+ was calculated to be 3.95 for pretreated AgAuAl catalyst which changed to 2.25 after ageing clearly indicating decrease in Ag^0 species due to ageing which is in well agreement with UV results where the peak corresponding to Ag^0 at 450 nm diminished after ageing. The UV spectrum of the sample after subtraction of alumina also shows formation of more $Ag_n^{\delta+}$ species after ageing.

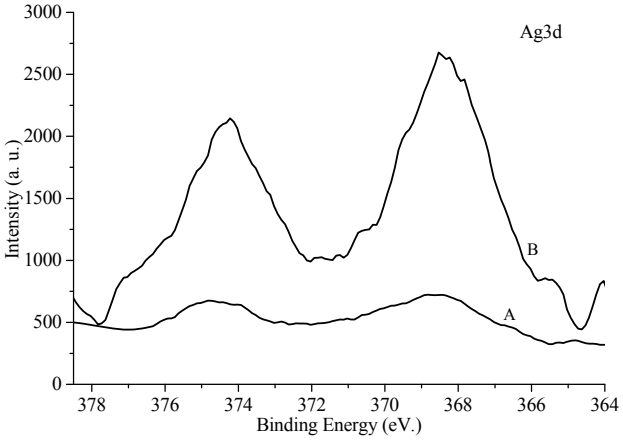

Fig. 10. Comparison of XPS spectra of AgAuAl catalyst after (A) pretreatment in H_2 at 250 °C and (B) ageing.

The surface silver concentration calculated from XPS was found to be 0.14 for catalyst pretreated in H_2 at 250 ºC which increased to 0.27 after ageing in reaction feed at 500 ºC confirming increased surface concentration of silver species after ageing. Hence the XPS and UV-vis data is in agreement with catalytic activity data. This indicated a reorganization of the silver species on the surface due to ageing which generated an increase in the number of silver species available on the surface. This has led to the improved catalytic activity of AgAuAl catalyst after ageing. Nam et al. [34] have reported that increase in concentration of various silver species on the surface led to improved low temperature SCR activity in Ag/Al_2O_3 catalyst. The XPS data has been deconvoluted in Fig. 11. AgAuAl catalyst reduced at 250 ºC (Fig. 11A) showed peaks at 368.8 and 367.1 eV, corresponding to Ag^0 and Ag^+ species respectively [35].

The Ag $3d_{5/2}$ photopeaks shifted to lower binding energy after ageing (Fig. 11B) from 368.8 eV to 368.5 eV. The initial binding energy value of Ag $3d_{5/2}$ photopeak at 368.8 eV

indicated partial oxidation of silver species. This shift may be attributed to the formation of higher number of $Ag_n^{\delta+}$ species which is in agreement with UV results as shown in Fig. 9 [22]. However there was no detectable shift observed for the peak at 367.1 eV for Ag^+ after ageing. Sato et al. [16] have reported $Ag_n^{\delta+}$ cluster to be responsible for the formation of isocynate species which are key intermediate in NO_x reduction reaction.

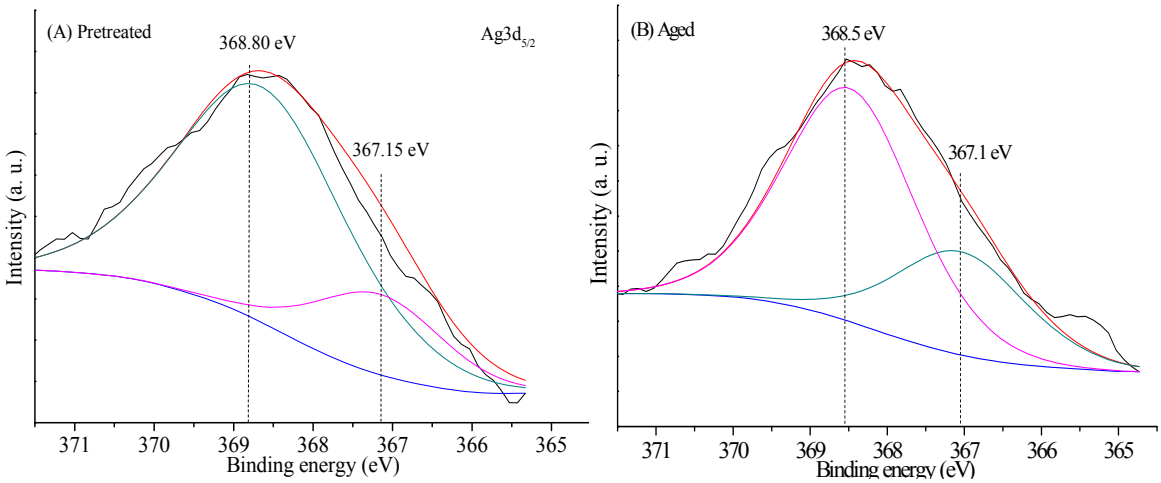

Fig. 11. Deconvoluted Ag $3d_{5/2}$ photopeak of AgAuAl catalyst (A) pretreated at 250 ºC in H_2 and (B) aged.

3.2.4. Energy dispersive X-ray spectroscopy (EDS) analysis

The metal dispersion after pretreatment and ageing was studied by elemental mapping of catalysts in 7.5 x 7.5 μm^2 area (Fig. 12). Energy dispersive X-ray spectroscopic analysis of AgAuAl catalyst indicated higher density of silver spots than gold. This difference was much higher than the ratio between Ag and Au molecular weight ratio on AgAuAl catalyst reduced at 250 ºC in hydrogen. This suggested more availability of silver nanoparticle compared to gold on the catalyst surface. Arve et al. [14] have reported that bimetallic Ag-Au/Al_2O_3 catalyst with less amount of Au on the surface compared to Ag shows better NO conversion to N_2.

The ageing of monometallic AgAl and AuAl catalyst led to opposite behavior. The density of Au spots decreased marginally whereas the density of Ag spots decreased significantly. This behavior was in agreement with the evolution of the catalytic performances after ageing.

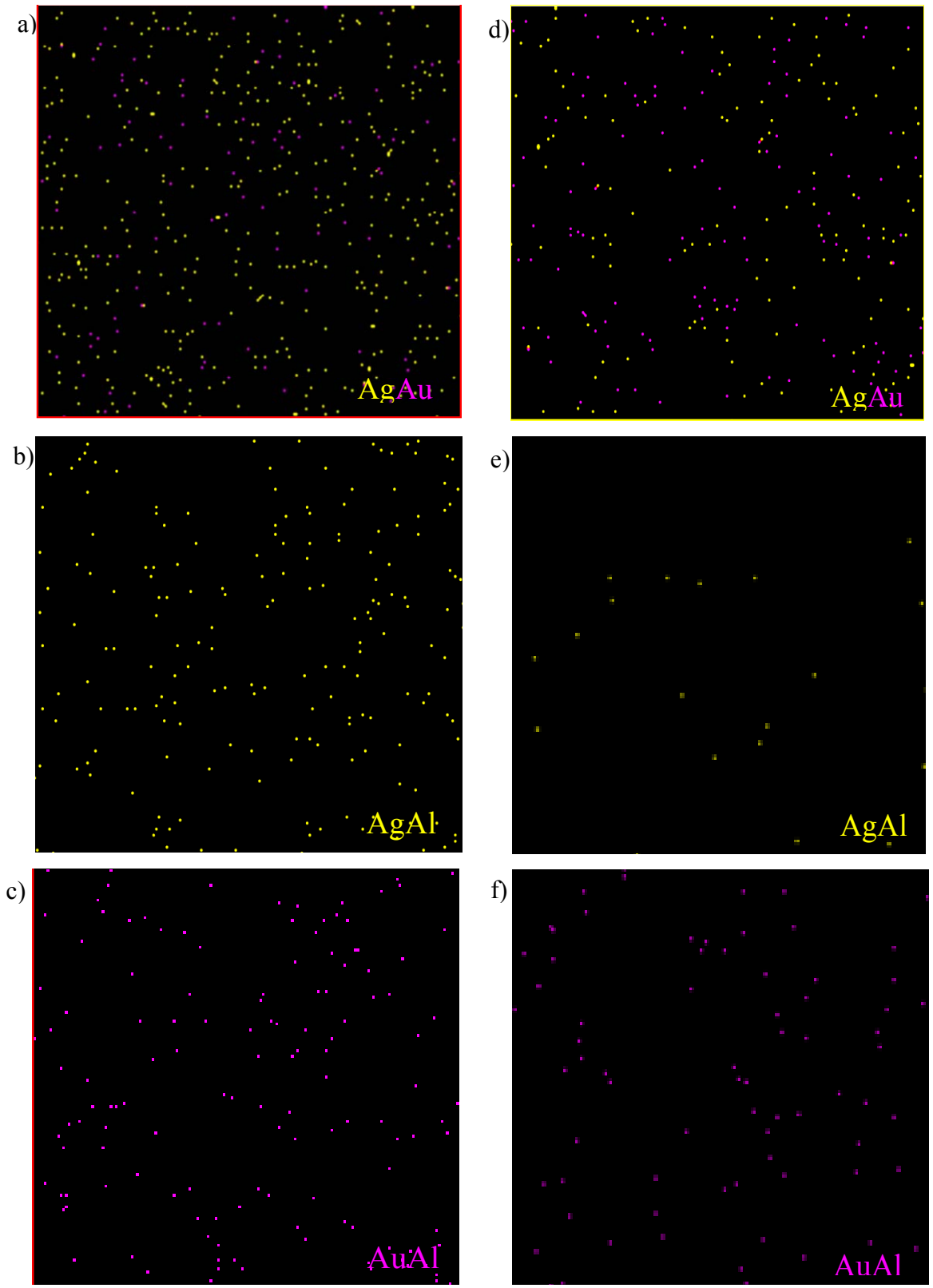

Fig.12. Elemental mapping images of catalysts after pretreatment at 250 ºC in H_2:a) AgAuAl b) AgAl c) AuAl and after ageing:d) AgAuAl e) AgAl f) AuAl.

Bimetallic AgAuAl catalyst showed improved dispersion of silver and gold particles compared to freshly pretreated catalysts. The ageing of AgAuAl catalyst gave rise to a slight decrease of spots related to Ag and Au. The decrease in Ag and Au spot in elemental mapping images having area 7.5×7.5 micron area indicates the maximum dispersion of Ag and Au on catalyst surface. The stabilization of silver particles in the presence of gold was then suggested according to EDS analysis. As elemental mapping by EDS analysis gives only metal dispersion and not particle size of the elements, further TEM analysis was carried out to determine the particle size of Ag and Au before and after ageing.

3.2.5. Transmission electron microscopy analysis (TEM)

TEM images and particle size distribution of pretreated and aged AgAuAl catalyst is presented in Fig. 13 and 14 respectively. AgAuAl catalyst after pretreatment in H_2 at 250 ºC showed presence of well dispersed silver and gold particles on alumina surface. The larger particles (>20 nm) were found to be of silver whereas smaller particles (<10 nm) were found to be of gold as analysed by spot EDS analysis (Fig. 13 inset). Haruta et al. [9] have shown that Au/Al_2O_3 prepared by deposition precipitation method gives Au particles of 4-5 nm whereas wet impregnation method leads to Au particles of 32 nm.

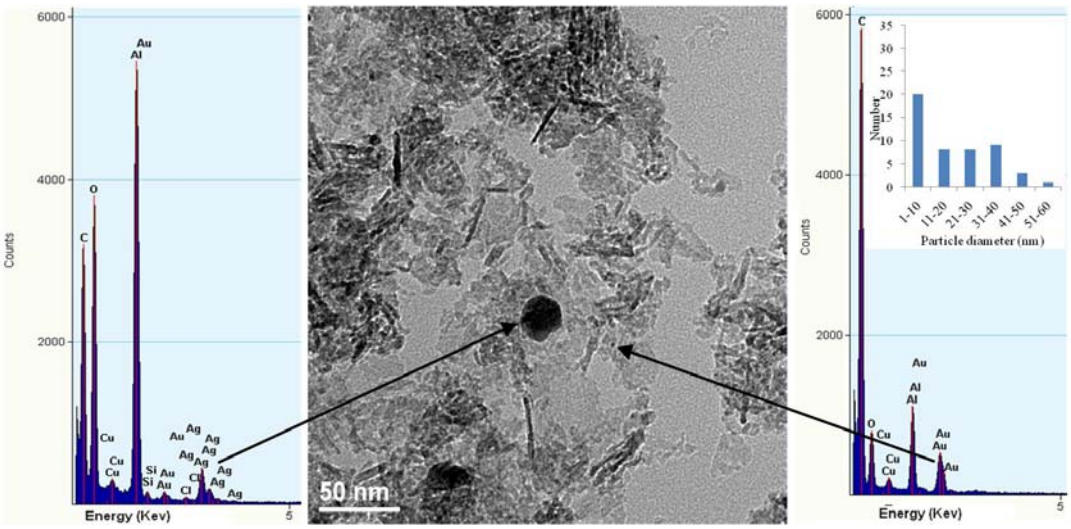

Fig. 13. TEM image, spot EDS and particle size distribution (inset) of AgAuAl catalyst pretreated in H_2 at 250 ºC.

After ageing the particle size distribution showed gold particles to be in the range of 1-10 nm. However the particle size of silver after ageing was found to be smaller than that of

pre-treated catalyst. The TEM images of AgAuAl catalyst showed well dispersed silver and gold nanoparticles with uniform distribution on the surface which is in well agreement with the XRD and EDS results. Bukhtiyarov et al. [36] demonstrated that silver particles greater than 30 nm forms nucleophilic oxygen. Thompson et al. [37] have reported nucleophilic oxygen to be responsible for the mild oxidation of hydrocarbon. Hence in present study it can be proposed that adsorbed nucleophilic oxygen on silver species can partially oxidize decane to assist further reforming reaction which in turn improves the SCR activity.

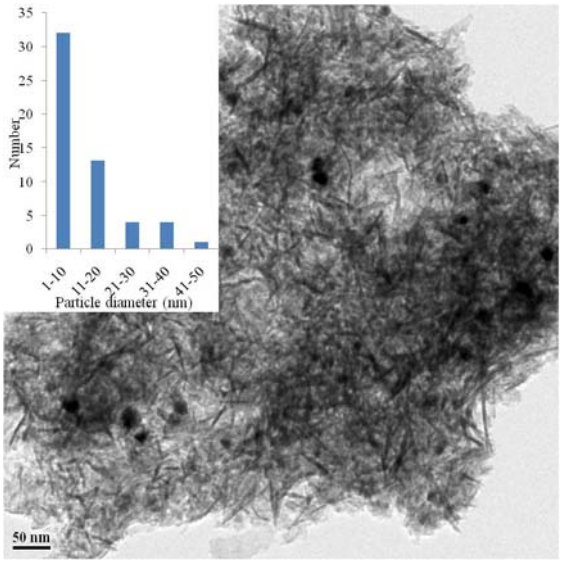

Fig. 14. TEM image and particle size distribution of AgAuAl catalyst aged in reaction feed.

The characterisation data can be correlated to the improved SCR activity of bimetallic AgAuAl catalyst compared to corresponding monometallic AgAl and AuAl catalysts. The high specific surface area of alumina support (450 m^2g^{-1}) prepared by sol gel method can favor high dispersion of active metals on the surface especially for gold nanoparticles. UV-vis characterisation of AuAl catalyst showed a shift in peak maxima for metallic gold to lower wavelength (554 to 534 nm) after ageing suggesting an improved dispersion of Au particle with corresponding decrease in particle size. This could be responsible for enhanced NO conversion at higher temperature after ageing on AuAl catalyst. Gold particles of 1 to 20 nm are reported to be active for NO_x reduction [9, 20].

On AgAuAl catalyst, several characterisations especially UV-vis confirm the formation of Ag^+ and $Ag_n^{\delta+}$ species which are known for high NO conversion. $Ag_n^{\delta+}$ is

proposed to be responsible for high SCR activity at low temperature whereas well dispersed Au particles are known for high temperature activity. The maximum number of $Ag_n^{\delta+}$ clusters were observed in AgAuAl catalyst when it was pretreated at 250 ºC in presence of H_2, resulting in higher activity compared to other pretreatments at 500 ºC in air and H_2. UV-vis spectroscopy also underlined the higher intensity of band at 275 nm for AgAuAl catalyst compared to AgAl, indicating higher concentration of $Ag_n^{\delta+}$ species which is in agreement with the higher SCR activity observed as shown in Fig. 3B. AgAuAl and AgAl showed increase in low temperature activity after ageing under reaction feed which could be due to the maximum dispersion of $Ag_n^{\delta+}$ species supporting the UV and EDAX data. The slight decreases in activity with concomitant decrease in formation of CO indicate the increased oxidative nature of surface Ag species. Whereas AuAl catalyst showed increase in CO concentration after ageing above 350 ºC indicating increase in partial oxidation of hydrocarbon which could be due to the change in redox properties of gold. The increase in intensity of XPS peaks (Fig. 10) for silver species as well as increase in $Ag_n^{\delta+}$ related contribution (UV) after ageing could be related to the high activity of AgAuAl catalyst after ageing. The significant improved metal dispersion in case of AgAuAl, AgAl and AuAl catalysts after ageing as evidenced from EDS and TEM analysis. It could also be related to improved low temperature activity in case of AgAuAl and AgAl catalysts whereas improved high temperature activity in case of AuAl. Hence in present case AgAuAl catalyst with lower gold content compared to silver on surface could be optimal for optimizing the catalytic activity for hydrocarbon SCR.

4. Conclusion

Bimetallic catalyst Ag-Au supported on high surface area alumina prepared by successive impregnation method has shown high SCR activity when pretreated in hydrogen at 250 ºC. The performance of bimetallic catalyst was better when AgAuAl catalyst was pretreated at 250 ºC in H_2 compared to pretreatment at 500 ºC in H_2 or air. The SCR activity further improved (94% NO conversion at 382 ºC) after ageing at 500 ºC in reaction feed. The SCR activity of bimetallic AgAuAl catalyst was higher compared to corresponding AuAl and AgAl catalysts after ageing. The higher activity of bimetallic AgAuAl catalyst for NO reduction after ageing has been correlated to the formation of well dispersed $Ag_n^{\delta+}$ clusters and small metallic gold particles on alumina support as confirmed by various characterisation technique. Detailed characterisation revealed modification of the catalyst surface by

improved silver dispersion and hence metal support interaction after ageing which led to enhanced low temperature activity of bimetallic catalyst. Improved activity of AgAuAl catalyst can also be attributed to steam reforming reaction which was confirmed by formation of CO at the temperature of highest activity.

5. References

[1] R. Burch, J. P. Breen, F.C. Meunier, Appl. Catal. B. 39 (2002) 283–303.

[2] S. Matsumoto, K. Katoh, T. Tanaka, J. Harada, N. Takahashi, K. Yokota, M. Sugiura, K. Kasahara, SAE Technica Paper 950809 (1995).

[3] M. Takeuchi, S. Matsumoto, Top. Catal. 28 (2004) 151–156.

[4] W. Held, A. Konig, T. Richter, L. Pupper, SAE Paper 900496, (1990).

[5] S. Chansai, R. Burch, C. Hardacre, J. Breen, F. Meunier. J. Catal. 281 (2011) 98–105.

[6] E. Seker, E. Gulari, Appl. Catal. A. 232 (2002) 203–217.

[7] C. Gluhoi, S. D. Lin, B. E. Nieuwenhuys, Catal. Today. 90 (2004) 175–181.

[8] A. Ueda, M. Haruta, Appl. Catal. B. 18 (1998) 115–121.

[9] A. Ueda, T. Oshima, M. Haruta, Appl. Catal. B. 12 (1997) 81-93.

[10] A. Ueda, M. Haruta, Gold Bull. 32 (1999) 3–11.

[11] L. Q. Nguyen, C. Salim, H. Hinode, Appl. Catal. A. 347 (2008) 94–99.

[12] L. Ilieva, G. Pantaleo, I. Ivanov, A. M. Venezia, D. Andreeva, Appl. Catal. B. 65 (2006) 101–109.

[13] L. Ilieva, G. Pantaleo, J. W. Sobczak, I. Ivanov, A. M. Venezia, D. X. Reeva, Appl. Catal. B. 76 (2007) 107–114.

[14] K. Arve, A. Simakova, L. Capek, K. Eranen, D. Yu. Murzin. Top. Catal. 52 (2009) 1762-1765.

[15] N. Jagtap, S. B. Umbarkar, P. Miquel, P. Granger, M. K. Dongare, Appl. Catal. B. 90 (2009) 416–425.

[16] K. Sato, J. Adam, T. Yoshinari, Y. Kintaichi, M. Haneda, H. Hamada. Appl. Catal. B. 44 (2003) 67–78.

[17] P. M. More, N. Jagtap, A. B. Kulal, M. K. Dongare, S. B. Umbarkar. Appl. Catal. B. 144 (2014) 408– 415.

[18] H. He, Y. Yu, Catal. Today. 100 (2005) 37–47.

[19] P. Miquel, P. Granger, N. Jagtap, S. Umbarkar, M. Dongare, C. Dujardin. J. Mol. Catal. A. 322 (2010) 90–97.

[20] P.M. More, D.L. Nguyen, M.K. Dongare, S.B. Umbarkar, N. Nuns, J.-S. Girardon, C. Dujardin, C. Lancelot, A.-S. Mamede, P. Granger, Appl. Catal. B. 162 (2015) 11–20.

[21] D. L. Nguyen, S. Umbarkar, M. K. Dongare, C. Lancelot, J. S. Girardon, C. Dujardin, P. Granger. Top. Catal. 56 (2013) 157 – 164.

[22] V. I. Parvulescu, B. Cojocaru, R. Richards, V. Parvulescu, Z. Li, C. Cadigan, P. Granger, P. Miquel, C. Hardacre. J. Catal. 272 (2010) 92–100.

[23] R. Burch, T. C. Watling, J. Catal. 169 (1997) 45–54.

[24] P. S. Kim, M. K. Kim, B. K. Cho, I.–S.Nam, Se H. Oh. J. Catal. 301 (2013) 65–76.

[25] J. Lee, S. Song, K. Min Chun. Ind. Eng. Chem. Res. 49 (2010)3553–3560.

[26] J. P. Breen, R. Burch, Top. Catal. 39 (2006) 53-58.

[27] Z. Qu, M. Cheng, C. Shi, X. Bao. J. Catal. A. 239 (2005) 22–31.

[28] E. Seker, J. Cavataio, E. Gulari, P. Lorpongpaiboonb, S. Osuwan, Appl. Catal. A. 183 (1999) 121-134.

[29] V. Abdelsayed, K. M. Saoud, M. Samy El-Shall, J. Nanopart. Res. 8 (2006) 519-531.

[30] D. Y. Yoon, J. H. Park, H. C. Kang, P. S. Kim, I. –S. Nam, G. K. Yeob, J. Ki Kil, M. S. Cha, Appl. Catal. B. 101 (2011) 275-282.

[31] P. Sazama, L. Capek, H. Drobná, Z. Sobalík, J. Dedecek, K. Arve, B. Wichterlová, J. Catal. 232 (2005) 302–317.

[32] K. A. Bethke, H. H. Kung, J. Catal. 172 (1997) 93-102.

[33] A. Satsuma, J. Shibata, A. Wada, Y. Shinozaki, and T. Hattori, Stud. Surf. Sci. Catal. 145 (2003) 235-238.

[34] P. S. Kim, M. K. Kim, B. K. Cho, I. –S. Nam, J. Catal. 292 (2012) 44–52.

[35] A. Q. Wang, J. H. Liu, S.D. Lin, T. S. Lin, C.Y. Mou. J. Catal. 233 (2005) 186–197.

[36] V. I. Bukhtiyarov, V.V. Kaichev. J. Mol. Catal. A. 158 (2000) 167–172.

[37] D. Thompson, B. K. Hodnett. Top. Catal. 50 (2008) 116–123.

Chapter 3: Rational preparation of Ag and Au bimetallic catalysts for the hydrocarbon-SCR of NO_x: Sequential deposition vs. co-precipitation method

Abstract: - This study emphasizes the importance of the preparation method for bimetallic Au–Ag catalysts supported on alumina in the selective catalytic reduction of NO_x by hydrocarbons with gas feed compositions representative of diesel fuelled engine exhaust. An optimal balance between oxidative and reductive surface properties was obtained when Au and Ag were successively introduced. Significant re-dispersion processes was observed after ageing at 500 ºC leading to a gain in activity at low temperature and ascribed to a better interaction between Au and Ag species. Co-impregnation of Ag and Au led to a preferential formation of intermetallic Au–Ag particles which were detrimental to the catalytic performances. Ageing at 500 ºC led to a significant particle sintering and a strengthening of the metallic character.

1.Introduction

Commercial Lean-NO_x Trap (LNT) [1] and urea-Selective Catalytic Reduction (SCR) technologies are widespread for diesel engine exhaust aftertreatment of NO_x [2] but still suffer from significant drawbacks due to the implementation of complex architectures including urea injection systems and the use of precious metal catalysts to pre-oxidize NO, activate the fast SCR process or store NO_x on LNT systems. Strong kinetic and thermodynamic limitations are generally associated with both technologies which lead to narrower operating windows. Further optimization of complex dosage strategies for urea injection [3] is an important to avoid deactivation phenomena [4]. Tentative developments combining both technologies [5] as well as optimizing dual-layer (SCR + LNT) systems [6] are promising but not mature enough to envision rapid commercial applications. In this context, the selective reduction of NO_x using unburnt hydrocarbons still remains an attractive solution because the use of platinum group metal (PGM) based catalysts in this technology is not a pre-requisite. Indeed, gold and silver can be considered as potential substitutes for PGM in end-of-pipe technologies for diesel engines enhancing significantly the selective conversion of NO_x to nitrogen in a wider operating window [7–11]. Earlier investigations, reported broad and high conversion ranges at moderate temperature on Ag/Al_2O_3 [12, 13] whereas gold seems to be more active at higher temperature [7]. Previous attempts led to significant rate enhancement at low temperature when gold interacts with Mn_2O_3 [14].

In most cases, a bi-functional catalysis involving metallic and oxidic sites to oxidize NO to NO_2 and to activate the SCR reaction respectively which is currently envisioned. Hence, one of the objectives of this study was to combine both Au and Ag to promote synergistic effects for obtaining a complete selective conversion of NO to N_2 at lower temperatures and a broader operating window compared to single Ag and Au based catalysts. In a recent paper, Hamill et al. showed that the combination of gold and palladium leads to a strong synergistic effect compared to the catalytic properties of the individual metals [15]. Alloying gold with PGM can be useful for exhaust gas treatment systems running at high temperature for limiting the detrimental effects due to particle sintering especially under wet atmosphere. Indeed, noble metals exhibiting higher melting points can slower gold particle sintering when they are alloyed [16,17]. Different types of interactions can exist when Au interacts with metallic substrates, such as Ag especially with oxidic silver species which can act as spacer preventing the aggregation of gold particles [18]. As a matter of fact, the

optimization of bimetallic Ag–Au catalysts is not an easy task and usually needs a better understanding of the physical origin of synergy currently ascribed to geometric or electronic effects due to the highest electronegativity of gold among the transition metals. Based on these considerations, the methodology selected for the preparation of bimetallic Au–Ag catalysts (impregnation, co-impregnation, and thermal treatment) may drastically affect their catalytic properties.

By way of illustration, high activity and stability in CO oxidation for Au–Ag/TiO_2 catalyst prepared by sequential deposition precipitation was ascribed to a compromise between metal particle size and the bimetallic character of the particles [19, 20]. However, some discrepancies sometimes arise. It is particularly true for the low temperature CO oxidation performed on Au-Ag alloy formed during one pot synthesis of the bimetallic catalyst for which 20–30 nm large particles exhibit an exceptionally high activity for CO conversion to CO_2 [21]. Such a result differs from previous statements demonstrating that nano sized gold particles below 5 nm are generally intrinsically more active. Based on these previous observations, in this study we have compared two different methods for the preparation of bimetallic Au–Ag supported on alumina for the selective catalytic reduction of NO_x in lean burn conditions which can originate different types of interactions between Au and Ag segregated on alumina or alloyed in bimetallic particles. It was found that co-impregnation and two-step deposition routes lead to drastic changes in their catalytic performances. Such differences have been tentatively rationalized on the basis of extensive bulk and surface characterisations.

2. Experimental

2.1. Catalyst synthesis

2.1.1. Sequential deposition method

Initially 1 wt% Au/Al_2O_3 was prepared by deposition-precipitation method using urea. $HAuCl_4$ solution was dropwise added to a slurry of alumina in water at 80 ºC with constant stirring. Urea solution was added dropwise to the above solution in order to promote the precipitation of $Au(OH)_3$ on the surface of alumina. The solid thus obtained was filtered and abundantly washed with water to remove chloride until the lack of silver chloride precipitation after addition of aqueous solution of $AgNO_3$ in the filtrate. The solids were

subsequently dried at 80 ºC for 12 h. Afterwards, the gold loaded catalyst (Au/Al_2O_3) was impregnated with an aqueous $AgNO_3$ solution with adjusted concentration in order to get 1 wt% Ag in $Ag\text{-}Au/Al_2O_3$ catalyst. Finally the catalyst was dried at 80 ºC followed by calcination at 500 ºC for 6h and labeled as AgAuAl. For $Au–Ag/Al_2O_3$, the starting material was 1 wt% Ag/Al_2O_3 prepared by impregnation on alumina by an aqueous $AgNO_3$ solution according to the same experimental conditions. After drying at 80 ºC for 12 h, gold was added via the above mentioned deposition precipitation method. The obtained sample was filtered and washed with water till complete removal of chloride. Catalyst was dried at 80 ºC for 12 h followed by calcinations in air at 500 ºC for 6 h and labeled as AuAgAl.

2.1.2. Co-impregnation

$Au–Ag/Al_2O_3$ was prepared by simultaneous co-impregnation method by adding of aqueous solutions of $HAuCl_4$ and $AgNO_3$ to a slurry of alumina in water maintained at a constant temperature of 80 ºC with constant stirring. The slurry was dried at 80 ºC for 12 h and calcined at 500 ºC for 6 h and labelled as Au–Ag/Al.

2.2. Physicochemical characterisation

2.2.1. Bulk characterisation

X-ray powder diffraction patterns were collected on a Philips (X pert) diffractometer equipped with a Ni filtered Cu Kα radiation (λ = 1.5406 Å, 40 kV, 30 mA). The data were collected in the 2θ range 30–90º with a step of 0.02º and scan rate of 4º min^{-1}. UV–visible DRS spectra were recorded with a UV–visible spectrophotometer (PerkinElmer, Lambda 650) in the diffuse reflectance mode between 200 and 800 nm at a step of 0.2 nm with a slit width of 1 nm. $BaSO_4$ was used as reference sample. TEM measurements were performed with Tecnai FEI G2 microscope, using an accelerating voltage of 200 kV and a LaB 6 mono-crystal. For TEM analysis, all samples were deposited on a carbon coated 200 mesh Cu grid. Gold and silver were analysed by inductively coupled plasma atomic emission spectroscopy (ICP-AES) at the chemical analysis centre of the CNRS. Elemental analysis data are collected in table 1. It was found that chlorine content was lower than 2000 ppm in all calcined samples.

Table 1. Elemental composition and textural properties of bimetallic Ag-Au catalysts supported on alumina

Catalyst	Preparation Method		Bulk Composition (wt%)		Textural Properties (N_2 physisorption)		
			Ag	Au	SSA (m^2g^{-1})	d_p (nm)	V_p (cm^3g^{-1})
Al_2O_3					450	6.1	1.30
AgAuAl	Successive Impregnation	Pretreated	1.04	0.60	224	7.8	0.52
		Aged			216	7.8	0.52
AuAgAl	Successive Impregnation	Pretreated	1.01	0.80	281	3.6	0.34
		Aged			229	4.4	0.35
Au-Ag/Al	Co-impregnation	Pretreated	0.98	0.90	224	8.0	0.61
		Aged			207	9.1	0.56

2.2.2. Surface characterisation

The specific surface area of the calcined samples was determined by N_2 sorption at −196 ºC using NOVA 1200 (Quanta Chrome) equipment. Prior to N_2 physisorption, the sample was out gassed at 300 ºC under vacuum. The specific surface area, S_{BET}, was calculated according to the BET equation and the pore size distribution from the nitrogen adsorption isotherm by using the BJH (Barrett–Joyner–Halenda) method. XPS experiments were performed on an AXIS Ultra DLD Kratos spectrometer equipped with a monochromatized aluminium source for excitation (150 W). The analyzer was operated in a constant pass energy mode (E_{pass} = 40 eV). The Al 2p (74.6 eV) binding energy (BE) from Al_2O_3 was used as internal reference. Peak area was estimated after subtracting the background according to the procedure suggested by Shirley [22].

Time-of-flight secondary ion mass spectrometry (ToF-SIMS) and low energy ion scattering (LEIS) were utilized for analyzing the composition of the outermost surface of materials under ultra-high-vacuum (UHV) conditions. Practically, primary Bi^{3+} ion doses (25

keV and 0.25 μA current) are pulsed at the surface of the catalysts during the ToF-SIMS measurements (TOFSIMS V, ION TOF GmbH). Low Energy Ion Scattering measurements were performed on a Qtac 100 spectrometer (ION TOF GmbH) as earlier described [23]. LEIS measurements were performed with 3 keV $^4He^+$ scattering. A sputter yield of 0.1 atoms per He-ion was assumed with a primary beam intensity of a 4 nA. According to these operating conditions ~3.0×10^{13} cm^{-2} atoms were sputtered from the sample surface during the analysis.

2.3. Catalytic measurements

Temperature-programmed reaction (TPR) experiments were performed in a fixed bed flow reactor by using 300 mg of catalyst exposed to a gas mixture composed of 300 ppm NO, 300 ppm CO, 300 ppm C_3H_6, 2000 ppm H_2, 100 ppm $C_{10}H_{22}$, 10% O_2, 10% CO_2, 5% H_2O and He balance. The total flow rate was adjusted to 300 mL min^{-1} in order to get a gaseous hourly space velocity of 50,000 $mL.g^{-1}.h^{-1}$. The flow rate was monitored by mass flow controller. Reactants and products were analysed online by using a CP 4900 Varian micro-GC with TCD detector which allowed the separation and the quantification of CO, H_2, nitrogen, propene and N_2O. Specific MIR 9000 NO_x analyzer supplied by Environment SA were utilized for measuring the specific response of NO and NO_2.

Prior to reaction, the catalyst samples were pre-reduced in pure H_2 at 250 ºC. After a first TPR-1 with a heating rate dT/dt = 2 ºC min^{-1}, in the above-mentioned specific operating conditions the catalyst samples were kept in isothermal conditions at 500 ºC overnight under reaction feed. After cooling down at 80 ºC, a second TPR-2 was performed in similar experimental conditions. The NO conversion was calculated from outlet molar flow rates of N_2 and N_2O, respectively F_{N_2}, F_{N_2O} and inlet molar flow rate of NO ($F_{NO,0}$) according to Eq. (1). The selectivity towards nitrogen formation S_{N_2} was given by Eq. (2).

$$X_{NO} = \frac{2 \times \left(F_{N_2} + F_{N_2O}\right)}{F_{NO,0}} \qquad (1)$$

$$S_{N_2} = \frac{F_{N_2}}{F_{N_2} + F_{N_2O}} \qquad (2)$$

3. Results and discussion.

The influence of the preparation method (sequential deposition vs. co-impregnation) for the elaboration of supported bimetallic gold–silver catalysts will be discussed based on the comparison of their catalytic properties and changes in structural and surface properties on fresh and aged catalysts after reaction at 500 ºC. As 2 wt% Ag/Al_2O_3 [13] and 2 wt% Au/Al_2O_3 [7] have shown promising activity for HC-SCR, we kept constant the metal loading on all bimetallic catalysts i.e. 2 wt%. Consequently, 1 wt% Ag and 1 wt% Au were loaded on alumina. First, it has been shown that different types of interactions between Au and Ag can be created according to the preparation route which drastically influences their performance and can led to different surface reconstruction under reaction conditions.

3.1. Catalytic properties of bimetallic Ag–Au catalysts in the hydrocarbon-SCR of NO_x

3.1.1. Au–Ag/Al_2O_3 catalyst prepared by co-impregnation.

Prior to catalytic measurements, all samples were pre-reduced in pure H_2 at 250 ºC. Temperature-programmed NO conversion curves of Au-Ag/Al are collected in Fig. 1(A) showing a poor activity with maximum NO conversion lower than 23% in the whole temperature range on the pre-reduced sample. Only nitrogen is produced with no significant gaseous N_2O and NO_2 formation. As seen the concentration of H_2 gradually decreases above 200 ºC with a complete conversion at 450 ºC. Regarding propene, the concentration remains unchanged up to ~350 ºC then a discontinuity appears coinciding with a parallel conversion of NO and formation of CO. These results agree with previous observations on gold [7] and silver based catalysts [24] showing that the direct reduction of NO by hydrogen should not occur. The extra formation of CO has been previously explained by the involvement of reforming and/or partial oxidation of decane [7, 12]. In the presence of water, the residual concentration of H_2 and CO is also governed by the water–gas-shift reaction.

While we cannot exclude that NO can be partly reduced by propene, it was found that decane plays a crucial role. Indeed, the absence of decane in the feed induces a quasi-complete suppression of NO conversion especially at low temperature [7, 12]. TPR-2 experiments illustrated in Fig. 1(B) do not reveal significant improvement in NO conversion. On the contrary, NO conversion in the low temperature range attenuates. The most prominent observation is related to the lack of extra CO production likely due a significant rate

enhancement of CO, H_2 and propene oxidation into CO_2 and H_2O suggesting that the balance between the reductive and oxidative properties of the catalyst have been modified after exposure to the reaction mixture overnight at 500 ºC.

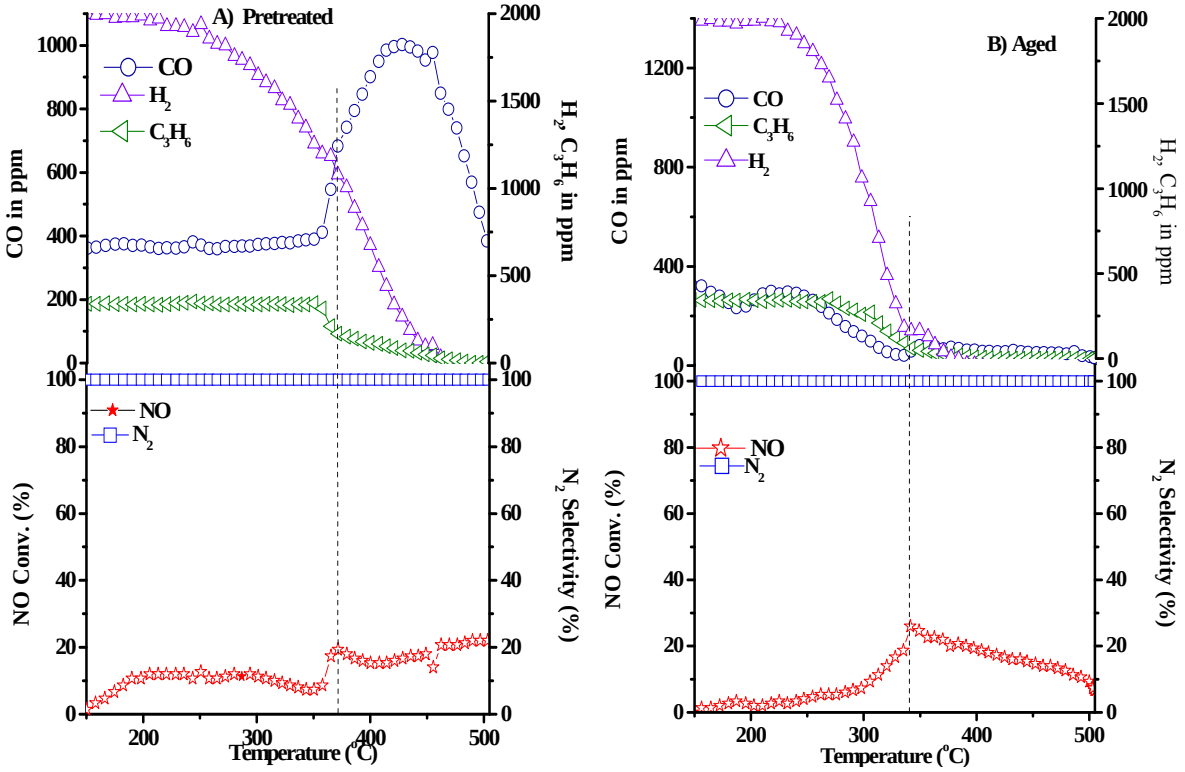

Fig. 1. Comparison of NO_x SCR performances on co-impregnated Au–Ag/Al sample prereduced (pretreated) in H_2 at 250 ºC from TPR-1 experiment (a) and on aged sample after exposure overnight in reaction conditions at 500 ºC from TPR-2 (b). Reaction feed: 300 ppm NO, 300 ppm CO, 300 ppm C_3H_6, 2000 ppm H_2, 100 ppm $C_{10}H_{22}$, 10% O_2, 10% CO_2, 5% H_2O, He balance. GHSV: 50,000 $mL.g^{-1}.h^{-1}$.

3.1.2. Au–Ag/Al_2O_3 catalysts prepared by sequential deposition

Two different samples were prepared starting from Au/Al_2O_3 prepared by deposition-precipitation then impregnated with aqueous solution of silver nitrate (AgAuAl) or impregnated Ag/Al_2O_3 sample where gold was subsequently incorporated by deposition–precipitation (AuAgAl). Similarly, both were pre-reduced in H_2 at 250 ºC. Their catalytic performances are presented in Fig. 2 and 3. As seen, significant improvements are observed in NO conversion compared to co-precipitated samples. A typical volcano type NO conversion curve is observed which highlights the role of NO_2 as key intermediate in the

overall process of the selective reduction of NO_x. This behaviour has been initially described over noble metals [25] and silver based catalysts [26].

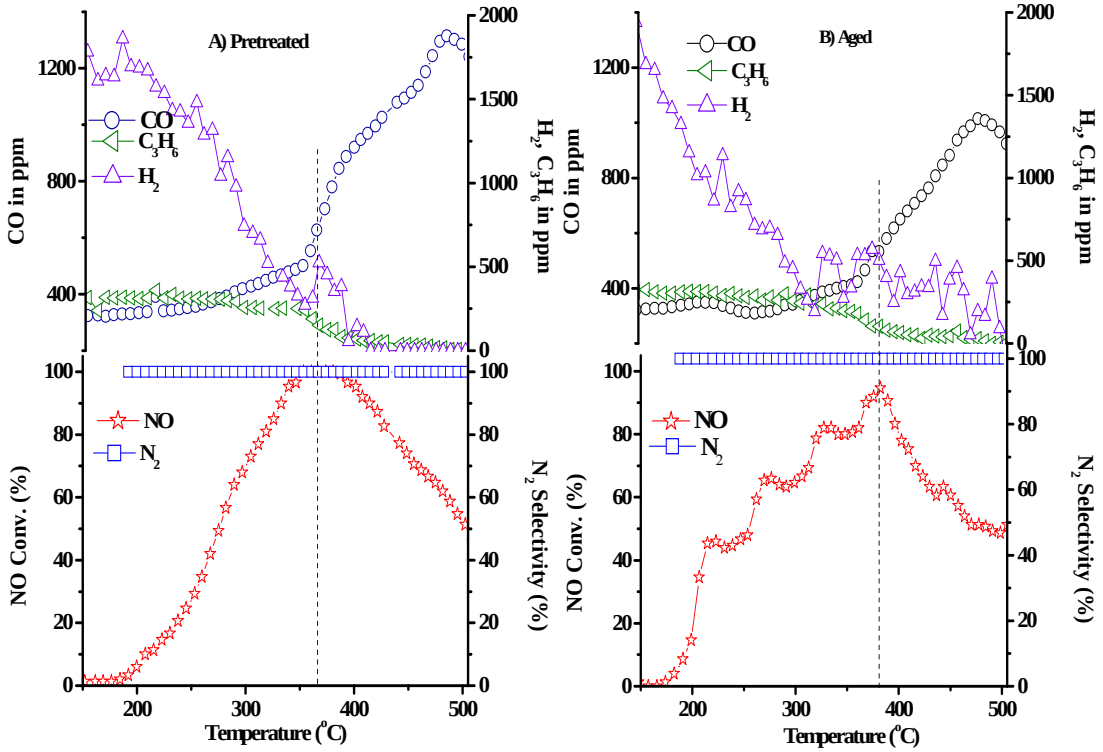

Fig. 2. Comparison of NO_x SCR performances on AgAuAl sample prereduced (pretreated) in H_2 at 250 ºC from TPR-1 experiment (a) and on aged sample after exposure overnight in reaction conditions at 500 ºC from TPR-2 (b). Reaction feed: 300 ppm NO, 300 ppm CO, 300 ppm C_3H_6, 2000 ppm H_2, 100 ppm $C_{10}H_{22}$, 10% O_2, 10% CO_2, 5% H_2O, He balance. GHSV: 50,000 $mL.g^{-1}.h^{-1}$.

NO dissociation on the metallic particles is not a major route in the overall reduction process under lean conditions (in an excess of oxygen). Burch et al. [25] proposed that it can go through spill-over of NO_2 from the metal to the support to react with C_xH_y ad-species stored on the support. Hence, this typical volcano-type curve at high temperature as explained in previous chapter. As seen on the pre-reduced sample from TPR-1, a quasi-complete NO conversion to nitrogen is achieved on AgAuAl in the range 180–420 ºC (Fig. 2A).

On the aged catalyst, TPR-2 in Fig. 2B reveals a slightly lower maximum conversion of 95%. More importantly, a broadening of the operating window with significant

enhancement in NO conversion to N_2 at low temperature is observed. Interestingly, it is remarkable that the conversion profiles for CO, propene and H_2 remain quasi unchanged compared to previous observations on the co-precipitated sample.

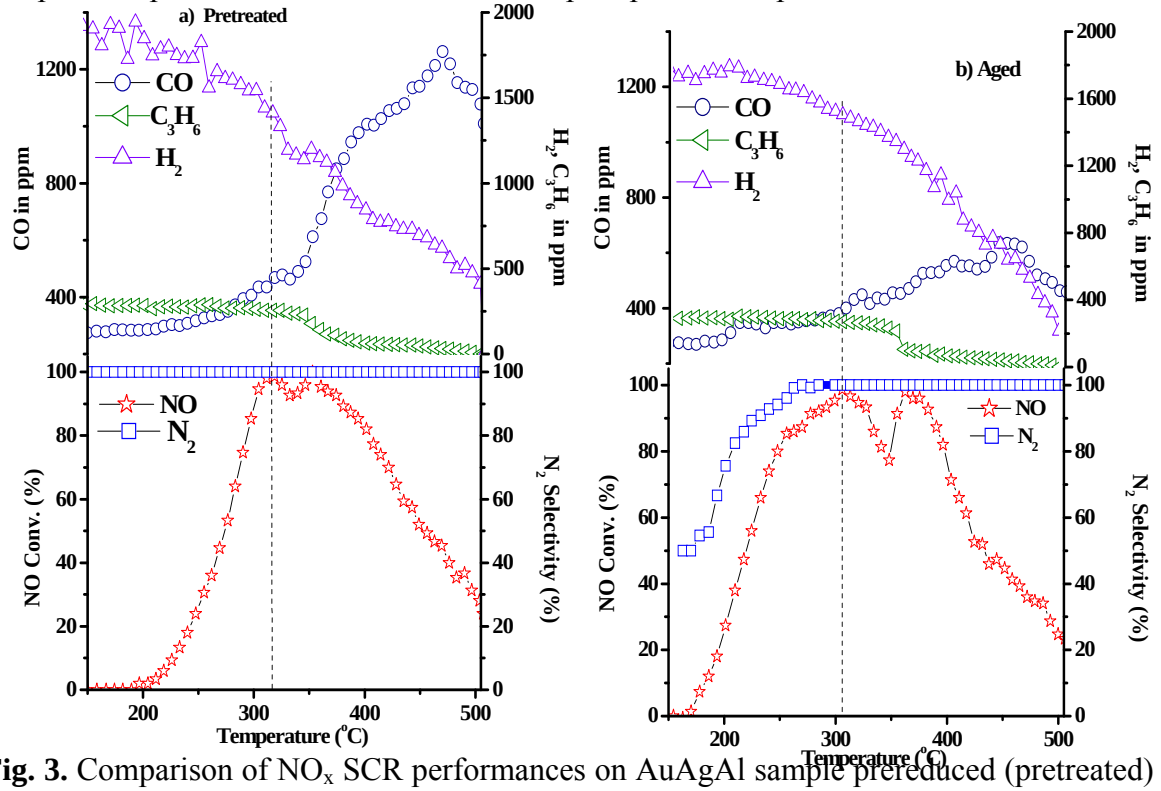

Fig. 3. Comparison of NO_x SCR performances on AuAgAl sample prereduced (pretreated) in H_2 at 250 ºC from TPR-1 experiment (a) and on aged sample after exposure overnight in reaction conditions at 500 ºC from TPR-2 (b). Reaction feed: 300 ppm NO, 300 ppm CO, 300 ppm C_3H_6, 2000 ppm H_2, 100 ppm $C_{10}H_{22}$, 10% O_2, 10% CO_2, 5% H_2O, He balance. GHSV: 50,000 $mL.g^{-1}.h^{-1}$.

Hence, after exposure overnight at 500 ºC under reaction mixture, AgAuAl remains stable preserving a good compromise between its oxidative and reductive properties. This is also true for AuAgAl with a more extensive conversion of NO at low temperature with 100% selectivity for nitrogen(Fig. 3). After exposure overnight at 500 ºC, TPR-2 reveals the same tendency as previously described with a broadening of the operating window and a slight detrimental effect on the selectivity behaviour highlighted by a significant formation of N_2O below 230 ºC (Fig. 3B).

3.2. Comparative bulk and surface properties of freshly pretreated and aged supported Au–Ag/Al_2O_3 catalysts

3.2.1. Characterisation of different types of interactions between gold and silver according to the preparation protocol

XRD patterns recorded on bimetallic Au–Ag/Al_2O_3 are collected in Fig. 4. Similar lines appear in all diffractograms at 2θ 38.2º, 44.5º, 77.5º ascribed to the (1 1 1), (2 0 0) and (2 2 0) planes characteristic of Ag, Au and Au–Ag solid solution in agreement with earlier investigations [27–29].

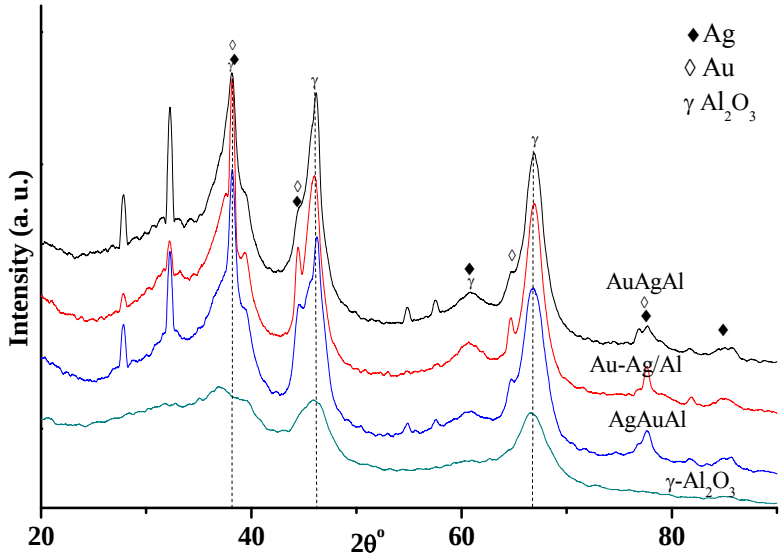

Fig. 4. XRD pattern of bimetallic catalysts.

UV–visible spectroscopic measurements provide different spectral features on samples prepared by sequential deposition and co-impregnation. Preliminary experiments collected in Fig. 5 on single Au/Al_2O_3 catalysts revealed the characteristic excitation of surface plasmon resonance of metallic gold particles at 550 nm [30, 31]. For Ag/Al_2O_3, absorption bands arise at 222, 257, 292 and 346 nm previously ascribed to a $4d^{10} \rightarrow 4d^9s^1$ transition characteristic of highly dispersed Ag^+ ions and small $Ag_n^{\delta+}$ clusters, respectively [32].

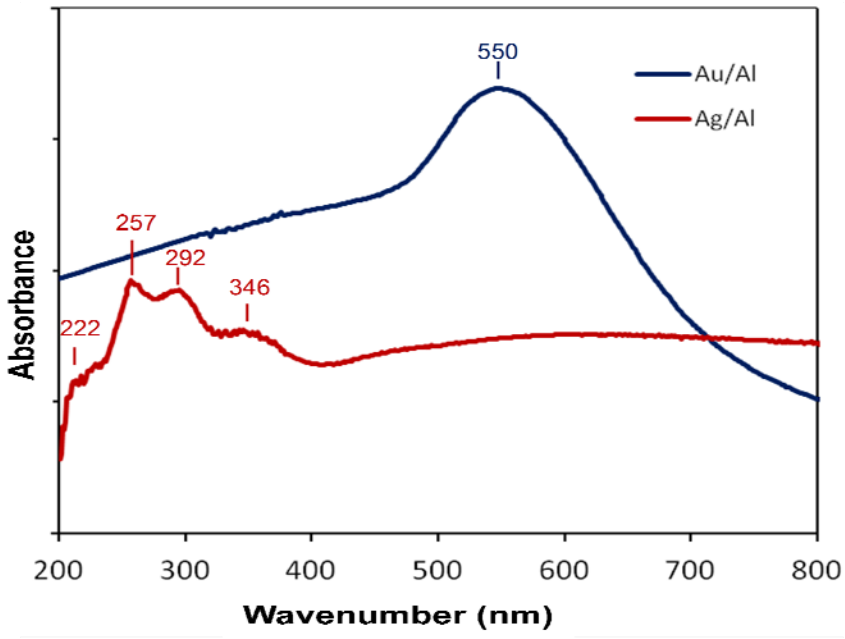

Fig. 5. UV–visible DRS spectra recorded on freshly-prepared (a) Au/Al_2O_3 (Au/Al) and (b) Ag/Al_2O_3 (Ag/Al).

Fig. 6 shows UV–visible spectra recorded on bimetallic Au–Ag samples. As shown, significant shifts are distinguishable on the 550 nm absorption band previously ascribed to gold nanoparticles compared to the reference monometallic gold catalyst. Parallel, to these observations, spectra recorded on bimetallic samples prepared by sequential deposition are mainly characterised by UV–visible bands previously ascribed to Ag^+ ions and/or small $Ag_n^{\delta+}$. No significant contribution in the range 300–450 nm related to the excitation of large metallic Ag particles is discernible as reported elsewhere on bimetallic Au/Ag composite film [33]. Based on these observations, the characterisation of Ag^+ and/or $Ag_n^{\delta+}$ species as well as gold metallic species on AuAgAl would suggest a preferential segregation of Au and Ag rather than the formation of alloyed Au–Ag particles. On the contrary, the presence of only one contribution on Au–Ag/Al displaying a red shift (522 nm) compared to single gold catalyst has been earlier discussed and tentatively assigned to the formation of alloyed and/or intermetallic Au–Al particles [28]. Hence, based on those observations, it can be suggested that segregated cationic and metallic Au and Ag species would coexist in the samples prepared by sequential deposition while only single or intermetallic Au–Ag particles would predominate on the co-precipitated sample.

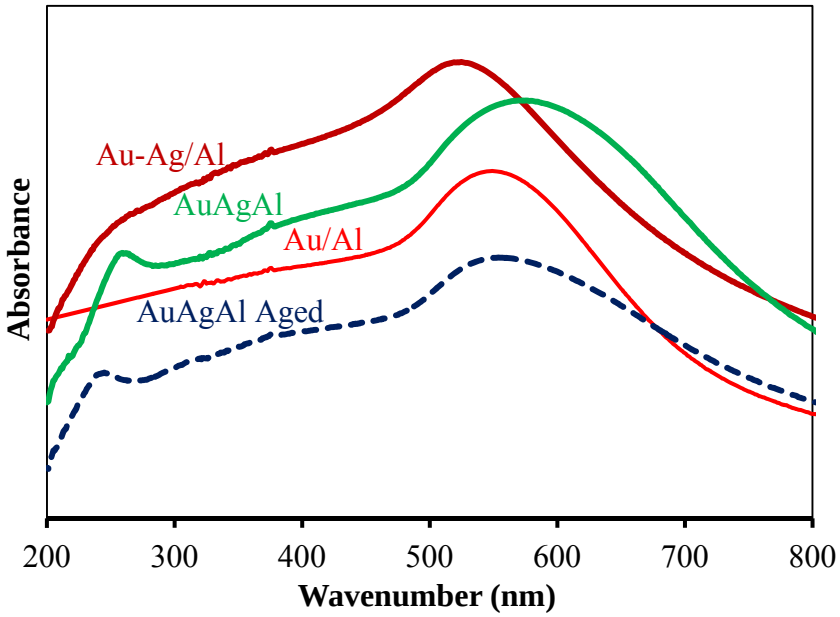

Fig. 6. UV–visible DRS spectra recorded on freshly-prepared bimetallic Au–Ag catalysts supported on alumina prepared by co-impregnation Au–Ag/Al, sequential deposition AuAgAl and on aged AuAgAl.

Surface analysis combining XPS, LEIS and ToF-SIMS analysis provides more arguments which converge to the preferential segregation of Au and Ag and/or weakly interacting Ag and Au on AuAgAl and AgAuAl whereas bimetallic particles would preferentially form on Au–Ag/Al. XPS spectral features are summarized in table 2. Particular attention was paid to the characteristic Au $4f_{7/2}$ and Ag $3d_{5/2}$ photopeaks of gold and silver, respectively. B.E. values in table 2 are consistent with gold in metallic state [28, 33]. For silver, B.E. values mostly reflect the presence of metallic species but no decisive conclusions can be drawn regarding the presence of cationic Ag species. In fact, more precise information regarding the oxidation state of silver would be obtained by examining the peak kinetic energy of the Auger MNN transition line recognized as more sensitive to the chemical environment than the corresponding XPS Ag 3d photopeak [34, 35].

Table 2. Surface analysis of fresh and used bimetallic Au-Ag/Al_2O_3 catalysts after TPR-2 experiments.

Catalyst		Bulk composition		B.E. values (eV) [a]		Surface composition		
		Ag (wt%)	Au (wt%)	Au 4f $_{7/2}$ [a]	Ag 3d $_{5/2}$	Au (%)[b]	Ag (%)[b]	Au/Ag [b]
Au-Ag/Al	Fresh	0.98	0.90	84.0	368.2	0.37	0.68	0.54
	Aged[d]			83.7	3687.9	0.30	0.80	0.38
AgAuAl	Fresh	1.04	0.60	84.3	368.3	0.01	0.14	0.071
	Aged[d]			84.3	368.6	n. m.	0.27	n. m.
AuAgAl	Fresh	1.01	0.80	84.1	368.5	0.01	0.21	0.048
	Aged[d]			84.0	368.4	0.01	0.24	0.041

[a] Binding Energy expressed in eV (accuracy ± 0.1 eV)
[b] surface atomic composition (relative accuracy ± 20%)
[d] pre-reduced in pure H_2 at 250 ºC and exposed overnight at 500 ºC to 300 ppm NO, 300 ppm CO, 300 ppm propene, 100 ppm decane, 0.2 % H_2, 5% H_2O, 10% CO_2, 10% O_2.

Semi-quantitative analysis reveals a sharp silver enrichment on samples prepared by sequential deposition whereas the surface composition doesn't differ from the bulk one for the co-precipitated catalyst taking into account the relative accuracy. Tof-SIMS is a useful technique to analyze the outermost layer of catalysts. Practically, primary Bi^{3+} ions were pulsed at the surface of the samples representing 10^{12} ion doses per cm^2. This corresponds approximately to one primary ion for 1000 surface atoms which makes this technique non destructive. After bombardment, secondary ions are emitted and can be analyzed with different polarities leading to the detection of cationic or ionic fragments which can reflect the local chemical environment of surface atoms. The different fragments *i* analyzed with their relative abundance corresponding to the intensity I_i of the fragment *i* to the global intensity of all fragments $I_i/\Sigma I_i$ are collected in table 3. As seen the presence of trace amount of chlorine is detected preferentially bonded to silver. Particularly attention was paid to specific fragments combining Ag and Au since they would evidence the presence of alloyed particles.

Table 3. Relative abundance of positive and negative fragments analysed from Tof-SIMS analysis of bimetallic Au–Ag/Al_2O_3 catalysts prepared by sequential deposition AuAgAl and co-impregnation Au–Ag/Al.

Fragment	Au-Ag/Al (%)		AuAgAl (%)	
	Pretreated	Aged	Pretreated	Aged
$AgAuCl^-$	0.11	0.13	-	-
$AgAu^-$	0.03	0.03	-	-
$AgAu_2^-$	0.04	0.03	-	-
Au^-	0.15	0.16	0.12	0.10
Au_2^-	0.02	0.01	-	-
Au_3^-	0.04	0.03	-	-
$AgCl_2^-$	-	-	1.75	0.12
$Ag_2Cl_3^-$	-	-	1.66	0.13
$Ag_3Cl_4^-$	-	-	0.52	-
Ag^+	3.09	4.47	1.61	1.92
Ag_2^+	0.24	0.33	-	0.31
Ag_2Cl^+	-	--	0.86	0.20
Ag_3^+	0.62	0.59	-	0.22
$Ag_3O_2^+$	0.22	0.27	-	0.21
$Ag_3Cl_2^+$	-	-	0.54	0.65
Ag_2Au^+	0.13	0.12	-	-
$Ag_4Cl_3^+$	-	-	0.08	-
Ag_5^+	0.08	0.04	-	0.09

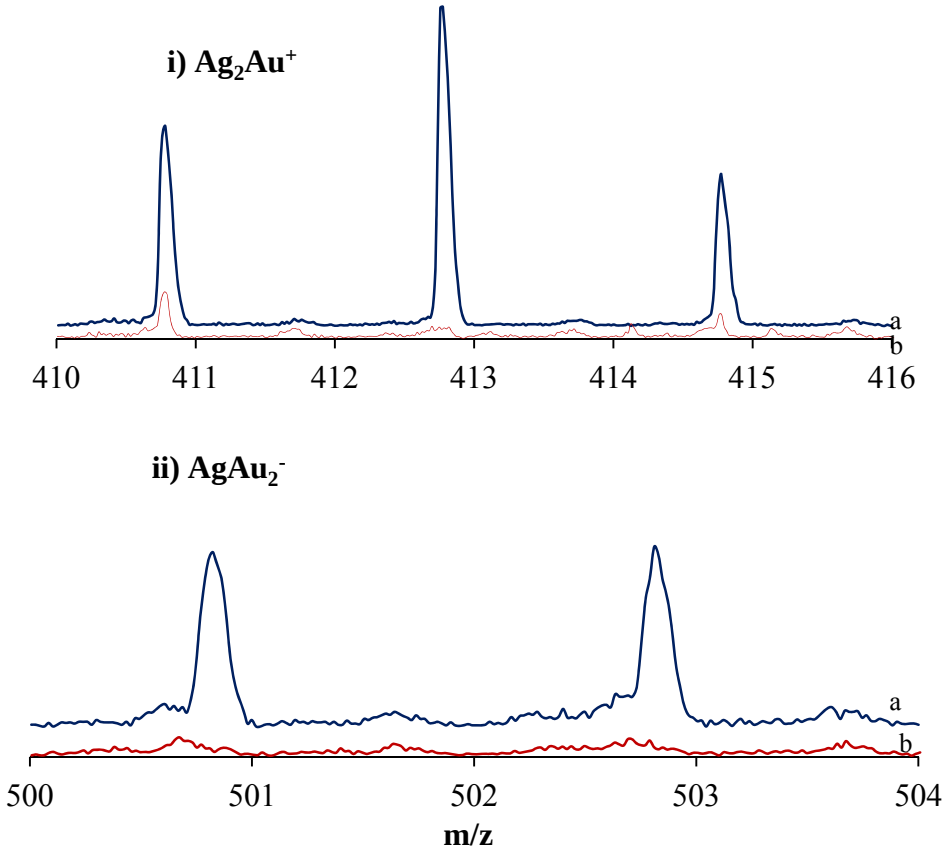

Fig. 7. ToF-SIMS analysis of freshly-prepared Au–Ag/Al_2O_3 prepared by co-impregnation (a) and sequential deposition (b) relative abundance of m/z signal corresponding to Ag_2Au^+ and $AgAu_2^-$ in positive and negative polarization.

Interestingly, Fig. 7 underlines that the most abundant Ag_2Au^+ is only detected on bimetallic Au-Ag/Al (Ag-Au/Al_2O_3) prepared by co-impregnation whereas the lack of observation of this fragment suggests the absence of significant formation of bimetallic particles on AuAgAl samples prepared by successive impregnation.

More quantitative information can be obtained from Low Energy Ion Spectroscopy which is an analytical tool that provides information on the atomic composition of the outer surface. LEIS analysis was performed at room temperature in static conditions. One spectrum corresponds to less than 1% monolayer sputtered using primary 3 keV $^4He^+$ beam with a scattering angle of 90º and an impact spot of approximately 0.25 mm^2.

Fig. 8 shows a typical LEIS spectrum on the co-impregnated Au-Ag/Al catalyst corresponding to a depth analyzed of 1.5 monolayers. As exemplified four peak are clearly

distinguishable at 1192 eV, 1726 eV, 2588 eV and 2748 eV corresponding to ions backscattered by O, Al, Ag and Au. Fig. 9is focused on the peak related to Ag and Au on co-impregnated Au-Ag/Al and AuAgAl obtained from successive impregnation recorded under conditions mentioned above.

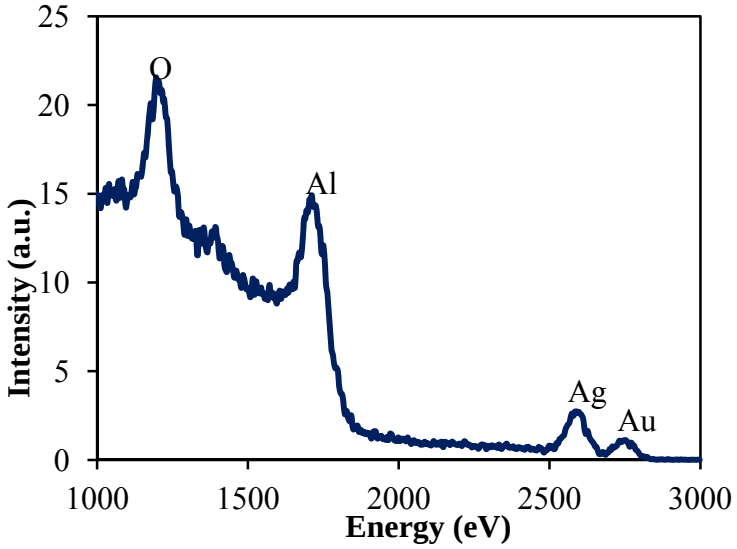

Fig. 8. LEIS spectrum performed with 3 keV $^{4}He^{+}$ scattering on co-impregnated Au–Ag/Al sample.

Regarding the LEIS spectra of fresh samples in Fig. 9(a) and (b), one can observe the same trends with a surface silver enriched Au-Ag/Al catalyst. Semi-quantitative analysis show atomic Al/O ratio ~ 0.55 slightly lower compared to the theoretical value for Al_2O_3 but acceptable taking the margin of error into account. The surface coverage of Au (0.33) and Ag (1.13) led to an atomic Au/Ag ratio ~ 0.29, lower than that obtained from XPS (Au/Ag = 0.54) analyzing on a depth corresponding to approximately 10 monolayers. Further comparisons with the bulk composition from elemental analysis (Au/Ag = 0.42) do not highlight significant divergences.

All those observations seem to support a preferential formation of alloyed Au-Ag particles in Au-Ag/Al catalyst in agreement with UV-visible and Tof-SIMS analysis emphasizing the fact that gold and silver would be quasi-homogeneous distributed from the core to the surface of those bimetallic particles. On the other hand, a different configuration characterise AuAgAl and AgAuAl which exhibit a sharp surface Ag enriched surface compared to the bulk composition.

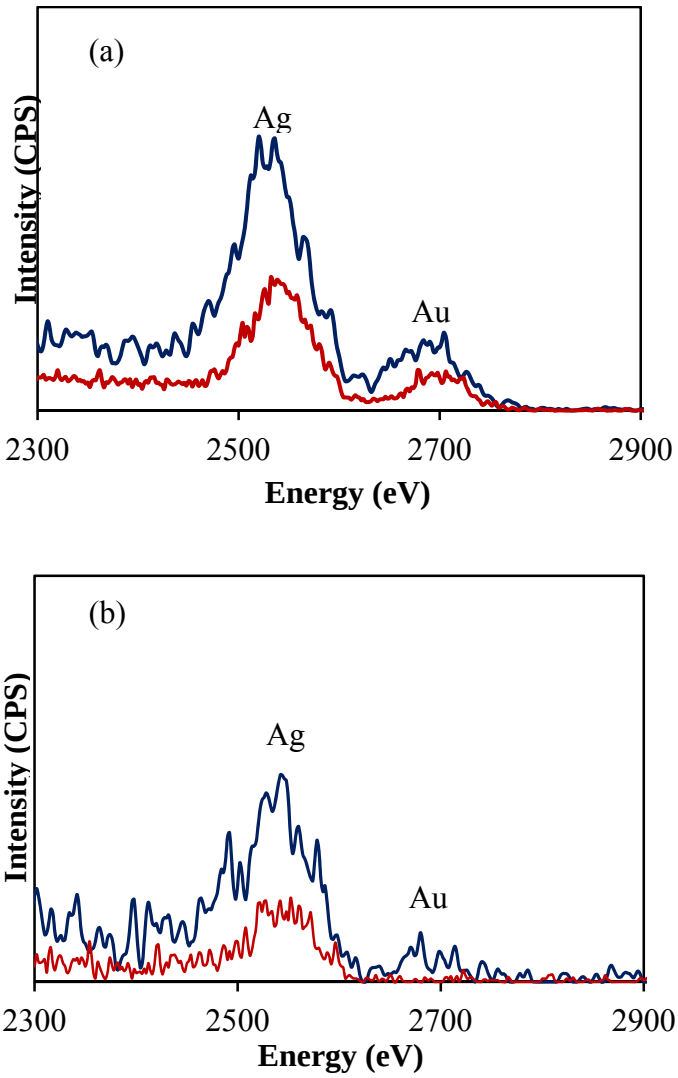

Fig. 9. LEIS spectrum performed with 3 keV $^{4}He^{+}$ scattering on pretreated (blue) and aged samples (red) after ageing overnight at 500 ºC: (a) Au–Ag/Al and (b) AuAgAl.

3.2.2. Evolution of the structural and surface properties in the course of the reaction

Textural parameters collected in table 1 do not reveal significant changes in textural properties on aged samples irrespective of the preparation method for gold and silver deposition. The hysteresis is characteristic of mesoporous materials. No significant change on pore size distribution, pore volume and specific surface area seems to occur on aged catalysts which emphasize the relative thermal stability of those solids in our operating condition (500 ºC in wet atmosphere 10% H_2O).

Now regarding the stability of nanosized gold and silver particle after reaction at 500 ºC significant surface reconstruction occurred altering differently the bimetallic catalysts.

TEM images and particle size distribution are reported in Fig. 10 on pre-reduced AgAuAl, AuAgAl and co-impregnated Au-Ag/Al. One can observe the presence of small and large particles of silver and gold of different sizes ranging from 1 to 70 nm but with different distribution according to the preparation methods. Hence successive impregnation leads to the segregation of smaller particles with diameter size in the range 1-10 nm, co-existing with larger ones up to 50 nm, compared to the co-impregnated sample. EDS analysis showed that large particles are essentially composed of Ag whereas smaller gold particles segregate at the surface (results not shown). Such tendency seems more accentuated on AuAgAl for which small particles in the range 1-10 nm predominantly form. For the co-impregnated sample, larger particles segregate with particle size in the range 11-30 nm.

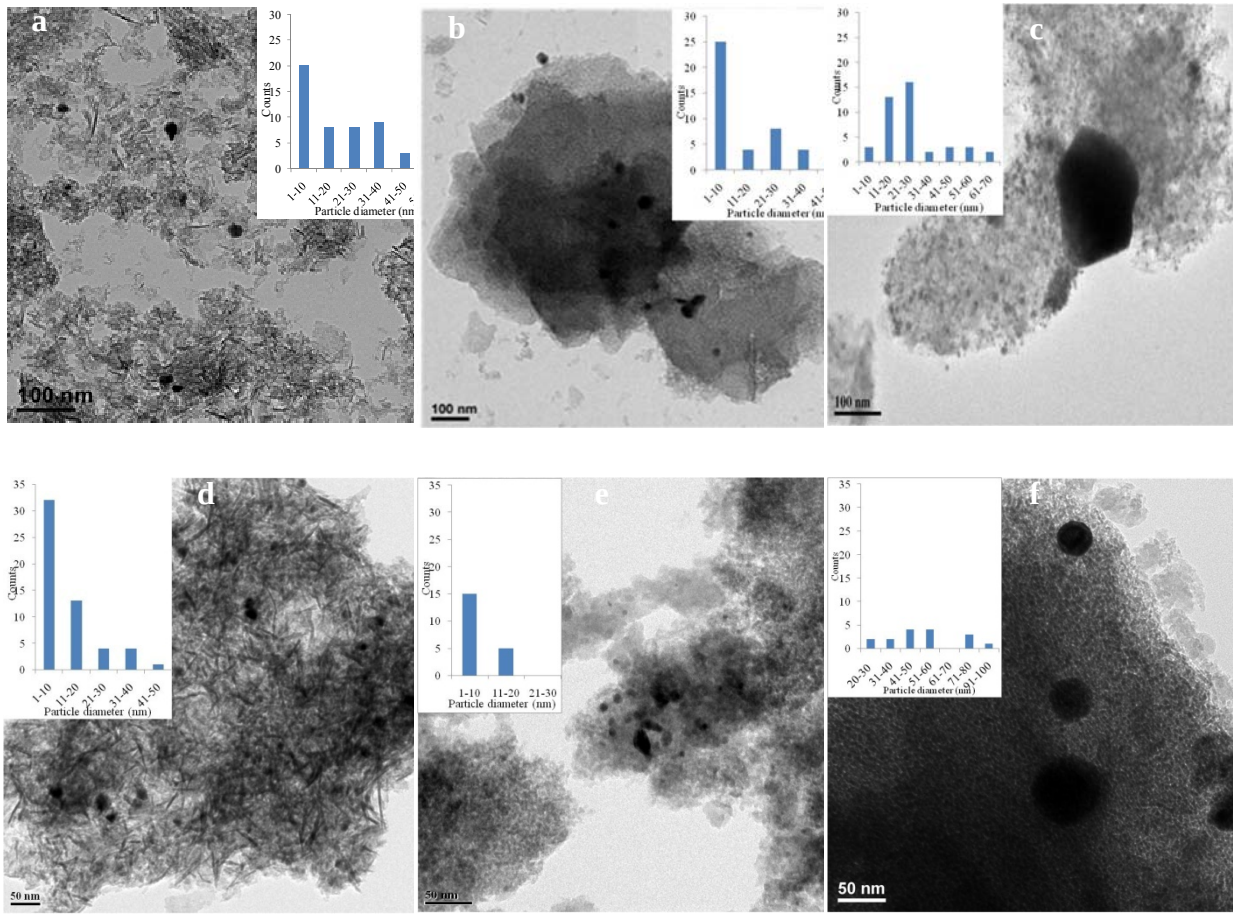

Fig. 10. TEM images and particle size distribution of pretreated catalysts: AgAuAl (a) and AuAgAl (b), Au–Ag/Al (c) and aged catalysts AgAuAl (d), AuAgAl (e), Au–Ag/Al (f).

It is obvious that particle sintering is more accentuated on this sample since most of the particles having size diameter in the range 1-30 nm are converted into larger ones exhibiting diameter up to 100 nm. This seems in relative good agreement with the trends observed on the B.E. values for the Au $4f_{7/2}$ and Ag $3d_{5/2}$ core levels since lower values recorded on the aged samples reflects a greater metallic character. Interestingly, the reverse tendency seems to occur on AgAuAl with the occurrence of re-dispersion processes based on the observation that Au and Ag particles are mostly distributed in the range 1-20 nm. Such a tendency is also verified on the AuAgAl sample even if this re-dispersion seems less pronounced considering the lower number of particle taken into account for this sample.

UV-visible spectroscopy do not reveal drastic changes in spectral features except the shift of low wavelength contribution to lower value (Fig. 6) which could suggest silver cluster re-dispersion to isolated Ag^+ species. As a matter of fact, Tof-SIMS analysis likely provides information which seems consistent with this later observation. Indeed, the examination of table 3 showed that the relative intensity of the different fragments coming from the Tof-SIMS analysis of the aged AuAgAl remains unchanged except when Ag is combined with chlorine.

In that case, the relative abundance of $AgCl_2^-$, $Ag_2Cl_3^-$ and Ag_2Cl^+ sharply decrease. Tof-SIMS is sensitive to trace amount of chlorine coming from the precursor salt of gold ($HAuCl_4$) aged during the deposition step. The lowest solubility of AgCl likely originates the formation of large crystallites of AgCl. In our operating conditions, the Deacon reaction taking place above 400 ºC under lean atmosphere (with an excess of oxygen) can promote the removal of chlorine. Based on these above-mentioned considerations, Eq. (3) can be envisioned as the starting process for further re-dispersion of silver species.

$$4AgCl_{(s)} + O_{2(g)} = 2Cl_{2(g)} + 2Ag_2O_{(s)} \qquad (3)$$

3.3. Catalytic properties vs. surface properties : How to optimise via a rational method?.

The selective reduction of NO_x under lean conditions involves complex chemical processes at the surface of silver and gold catalysts. It seems obvious that sometimes no consensus can be found regarding the effective role of hydrogen and oxygen depending on the feed gas composition and the nature of intermediates and key elementary steps is still under debate [32, 33]. Indeed, the presence or absence of heavy hydrocarbons representative of the exhaust gas composition of diesel engines, may also drastically modify the nature of

reactions taking place at the catalyst surface. This exhaust also modify the nature of intermediates and/or the structural properties of the surface with equilibration of the oxidation states of silver and gold, which likely governs the oxidative/reductive properties of the catalyst. Arve et al. [32] found a correlation between the complete oxidation of CO and unburned hydrocarbons (such as hexadecane) to CO_2 and H_2O and a simultaneous increase in the rate of NO conversion to N_2. However, those authors also reported that the rate of the kinetically important steps in HC-SCR partly depends on the chemical nature of the reducing agent (acyclic vs. cyclic hydrocarbons).

More recently, different observations have been reported on single gold and silver catalysts supported on alumina associated to an extra production of CO and H_2 [7, 20-21, 23] due to the involvement of reforming and/or partial oxidation of decane. Parallel to that observation, a significant rate enhancement in NO conversion was observed. Up to now, such rate enhancement is not clearly understood and may reflect the bi-functional character of silver and gold based catalysts related to a two-step process involving the intermediate formation of NO_2 to N_2 as key intermediate in the overall process. Hence, the presence of metallic and electrophilic gold and silver species on alumina would be needed to catalyze the NO oxidation to NO_2 and the subsequent reduction of NO_2 via the SCR process respectively [23]. Such behavior should be likely true over bimetallic Au-Ag catalysts since similar catalytic features can be observed compared to those reported elsewhere [7, 20-21, 23]. The presence of hydrogen in the feed and extra *in situ* production as observed in Fig. 1-3 might be of capital importance to increase the oxidation of NO to NO_2 [34] or to assist the SCR process via the stabilization of nitrates species [33] on the support via the occurrence of spillover processes from the metal to the support. It is also noticeable that the relative rates for these chemical processes are likely intimately related to the structure of the active sites with crystalline metallic silver particles for the NO/O_2 reaction and highly active Ag^+ cations for N_2 production under SCR operating conditions [28] which means a more complex description for bimetallic Au-Ag catalysts taking into account the inhomogeneity in surface composition. Arve et al. [32] pointed out from HRTEM the importance to get 3 nm diameter particles to activate the SCR reactions. However, it seems not the sole parameter to be considered since the balance between Ag^0 and $Ag^{\delta+}$ species may drive the selectivity of the reaction which was previously found insensitive to the particle size [32]. Based on the above-mentioned statements, the difficulty to understand surface processes for further optimization of single Au and Ag based catalysts is likely related to the versatile properties of the surface

which can stabilize differently according to the selected preparation methods, the pre-activation thermal treatments and reaction conditions (temperature, chemical nature of the reducing agent and presence of hydrogen in the feed or *in situ* produced). All these experimental factors could influence, through surface reconstructions, the particle size, the atomic Ag^0 to $Ag_n^{\delta+}$ ratio and the metal/support interface involve in the overall SCR process.

Up to now, significant attention was not paid to the utilization of bimetallic Au-Ag catalyst for $DeNO_x$ applications. The utilization of these materials is more widespread for oxidative reactions [15, 28, 35-38]. Hence, tuning their oxidative/reductive properties according to the selected method for their preparation is an important outcome. Fig. 1-3 provide important information showing that co-impregnation leads essentially to oxidation reactions, no extra CO formation is observed on the aged sample with a rise in temperature. It is remarkable that a poor activity for NO_x conversion characterises this catalyst. Subsequent ageing overnight at 500 ºC (Fig. 1b) accentuates this trend with the disappearance of broad and weak low temperature range for NO conversion. This can be easily explain by a total oxidation of decane, propene, CO and H_2 into CO_2 and H_2O by oxygen which occurs more readily than the SCR process, then no reducing agent could be available for the parallel reduction of NO. All these trends seem in correct agreement with an accentuation of the metallic character of Ag and Au evidenced from XPS analyses and likely in connection to a greater sensibility to particle sintering. Contrarily to co-impregnated, the activity of prereduced bimetallic Au-Ag catalysts prepared by successive impregnation in NO_x conversion develops especially after activation overnight in the reaction mixture at 500 ºC (in an excess of oxygen) could be ascribed in a first approximation to an equilibration of the oxidation state of Au and/or Ag starting with a pre-reduced Au-Ag/Al_2O_3 catalyst. These samples differ from their surface composition with a systematic surface silver enrichment which could be explain by a greater affinity of Ag to oxygen adsorption than gold and a higher mobility of oxidic silver species [39].

Hence, a first objective of this chapter was to relate the different catalytic properties of Au-Ag/Al_2O_3 prepared by successive and co-impregnation to their peculiar surface properties. Secondly, up to now there is no observation of rate enhancement in NO conversion reported in the literature on modified-silver based catalysts as exemplified in Fig. 2 and 3 on aged Au-Ag/Al_2O_3 samples. Recent investigations on single gold catalysts report such observations but in lower extent and at much higher temperature [28]. Hence, an

important issue was to describe straight forwardly the different surface reconstructions taking place on the bimetallic samples depending on the protocol aged for gold and silver deposition and to correlate this information to a bi-functional catalysis involving a two-step process with initial NO oxidation to NO_2 and then the SCR process [35]. As mentioned above previous investigations emphasized the fact that particle size and shape is not trivial to explain the kinetics and activity of silver based catalysts. However, in the case of bimetallic catalyst, the surface composition should be considered and would depend on the type of interactions between Au and Ag.

Regarding the impact of alloying effects or segregation in case of bimetallic particles, it was previously reported for the CO/O_2 reaction that their behavior is drastically different. This is particularly true for CO oxidation at low temperature in which small gold particles (2-5 nm) are generally considered as the most active while larger ones become inactive. On the other hand, Au-Ag particles with particle sizes in the range 20-50 nm after pre-reduction in H_2 at 550-650 ºC become exceptionally active [36]. Returning to our observations, they do not allow to state on possible particle size dependency of the rate of NO conversion. This can be consistent with previous observations related to the weak particle size dependency of the $Ag^0/Ag_n^{\delta+}$ ratio [23]. The most prominent observation is related to a promotional effect of re-dispersion process on the activity taking place at 500 ºC under reactive conditions. Hence, both particle size and in homogeneity in surface composition are probably responsible of the gain in activity. Indeed, DRS analysis of aged AgAuAl reveals that cationic Ag species are still detected after reaction at 500 ºC suggesting the preservation of Ag^+ and $Ag_n^{\delta+}$ clusters and no significant strengthening of the metallic character compared to previous observations on co-impregnated sample due to thermal sintering. On the other hand, the shift observed on the characteristic UV-vis absorption band of Ag^+ compared to Tof-SIMS analysis, show that the nature and the distribution of Ag^+ species would drastically change on the aged AgAuAl catalyst. Indeed, instead of large particle ascribed to the aggregation of AgCl [40] significant re-dispersion would occur through reaction described in Eq. (3) possibly into Ag_2O clusters. Changes in spectral features observed on AgAuAl could be related to Ag_2O decorating gold particles as earlier proposed for explaining the drastic rate enhancement of large bimetallic having particle in the CO/O_2 reaction. This type of configuration has been already envisioned where Au particles would be decorated by a discontinuous surface oxide layer [42]. Ag_2O would strongly interact with gold particle preventing their agglomeration/aggregation and preserving low-coordinated Au atoms interacting with AgO_x patches [41]. While such an

explanation could be valid, it cannot completely rationalize results obtained from LEIS analysis showing a preferential Ag enrichment of the outermost surface. Such an observation could be consistent with the formation of core-shell structures with surface Ag enriched Au-Ag particles on AgAuAl with a core mainly composed of gold. This configuration could be in agreement with the explanation provided by Wang et al. [42] involving a close interaction between metallic and electrophilic Ag sites for the activation of the NO reduction to nitrogen. Such an explanation seems consistent with earlier investigation reporting that Ag^+ can adsorb preferentially onto gold surface rather than onto alumina support on the basis of the strong electrostatic attraction between Au and Ag^+ [42]. Such statement is supported by DFT calculation revealing that gold particles are slightly negatively charged [43]. Hence, the synergistic effect observed on freshly-prepared further strengthened on aged bimetallic catalyst could be related to the creation of active site at the interface of metallic gold particles and AgO_x patches.

4. Conclusion

The catalytic performances of bimetallic Au-Ag/Al_2O_3 catalysts are sensitive to the preparation protocol. Optimal surface properties involve the participation of metallic and electrophilic sites to catalyse respectively NO oxidation to NO_2 and its subsequent reduction to nitrogen. Different parameters can contribute to get such an optimal balance taking into account the size and shape of the particle and inhomogeneity in surface composition in the case of bimetallic catalysts. It was found that co-impregnation leads to the preferential formation of alloyed particles more active for oxidative reaction than reductive ones and resulting in a poor conversion of NO_x to nitrogen. Subsequent exposure at high temperature in reactive conditions has a strong detrimental effect due to particle sintering altering the metal/support interface and a strengthening of the metallic character which favor the total oxidation of reducing agents. For catalysts prepared by successive impregnation, starting from Au/Al_2O_3 or Ag/Al_2O_3 and then introducing respectively silver or gold leads inevitably to a significant surface silver enrichment. However the creation of active site at the interface of metallic gold and AgOx patches is the key for higher activity. This option considerably improves NO conversion which was ascribed to synergistic effect between Au and Ag with re-dispersion processes of large AgCl particles into Ag_2O interacting with gold particles preserving their sintering after ageing.

5. References

[1] M. Iwamoto, H. Yahiro, Catal. Today, 22 (1994) 5-18.

[2] M. Koebel, M. Elsener, M. Kleemann Catal. Today, 59, (2000) 335-345.

[3] J. Oh, K. Lee, Fuel, 119 (2014) 90-97.

[4] F. Birkhold, U. Meingast, P. Wassermann, O. Deutschmann, Appl. Catal. B 70 31 (2007) 119-127.

[5] J. A. Sullivan, O. Keane, Appl. Catal. B 70 (2007) 205-214.

[6] M. Colombo, I. Nova, E. Tronconi, V. Schmeißer, B. Bandl-Konrad, L. Zimmermann, Appl. Catal. B.142–143(2013) 861-876.

[7] D.L. Nguyen, S.B. Umbarkar, M.K. Dongare, C. Lancelot, J.S. Girardon, C. Dujardin, P. Granger, Catal.Catal. Comm.26 (2012) 225-230; Top. Catal. 56 (2013) 157-164.

[8] N. Jagtap, S.B. Umbarkar, P. Miquel, P. Granger, M. Dongare, Appl. Catal. B.90 (2009) 416-425.

[9] B. Wichterlová, P. Sazama, J.P. Breen, R. Burch, C.J. Hill, L. Čapek, Z. Sobalík, J. Catal. 235 (2005) 195-200.

[10] Ueda, T. Oshima, M. Haruta,Appl. Catal. B. 12 (1997) 81-93.

[11] K. Arve, Adam O. Simakova, L. Capek, K. Eranen, D. Yu. Murzin, Top. Catal. 52 (2009) 1762-1765.

[12] C. Hamill, R. Burch, A. Goguet, D. Rooney, H. Driss, L. Petrov, M. Daous, Appl. Catal. B. 147 (2014) 864-870.

[13] A. Wang, X.Y. Liu, C.Y. Mou, T. Zhang, J. Catal. 308 (2013) 258-271.

[14] X.Y. Liu, A.Q. Wang, L. Li, T. Zhang, C.Y. Mou, J.F. Lee, J. Catal. 278 (2011) 288-296.

[15] A. Sandoval, A. Aguilar, C. Louis, A. Traverse, R. Zanella, J. Catal. 281 (2011) 40-49.

[16] Z. Qu, G. Ke, Y. Wang, M. Liu, T. Jiang, J. Gao, Appl. Surf. Sci. 277 (2013) 293-301.

[17] A.-Q. Wang, J.-H. Liu, S.D. Lin, T.-S. Lin, C.-Y. Mou, J. Catal. 233 (2005) 186-197.

[18] D.A. Shirley, Phys. Rev. B. 5(12) (1972) 4709-4714.

[19] H.H. Brongersma, T. Grehl, P.A. van Hal, N.C.W. Kuijpers, S.G.J. Mathijssen, E.R.Schofield, R.A.P. Smith, H.R.J. ter Veen, Vacuum 84 (2010) 1005–1007.

[20] D.L. Nguyen, S. Umbarkar, M.K. Dongare, C. Lancelot, J.S. Girardon, C. Dujardin, P. Granger, Catal. Comm. 26 (2012) 225-230.

[21] P. Miquel, P. Granger, N. Jagtap, S. Umbarkar, M. Dongare, C. Dujardin. J. Mol. Catal. A. 322 (2010) 90–97.

[22] R. Burch, T.C. Watling, J. Catal. 169 (1997) 45-54.

[23] V.I. Parvulescu, B. Cojocaru, V. Parvulescu, R. Richards, Z. Li, C. Cadigan, P. Granger, P. Miquel, J. Catal. 272 (2010) 92-100.

[24] T. Déronzier, F. Morfin, M. Lomello, J.L. Rousset, J. Catal. 311 (2014) 221-229.

[25] J. Zheng, H. Lin, Y.N. Wang, X. Zheng, X. Duan, Y. Yuan, J. Catal. 297 (2013) 110-118.

[26] C. A. Foss, G.L. Hornyak, J.A. Stockert, C.R. Martin, J. Phys. Chem. 98 (1994) 2963-2971.

[27] B.M.I. van der Zande, M.R. Bohmer, L.G.J. Fokkink, C.J. Schnenberger, J. Phys. Chem. B. 101 (1997) 852-854

[28] N. Bogdanchikova, F.C. Meunier, M. Avalos-Borja, J. P. Breen, A. Pestryakov, Appl. Catal. B. 36 (2002) 287-297.

[29] L. Zhang, C. Wang, Y. Zhang, Appl. Surf. Sci. 258 (2012) 5312-5318.

[30] J. Zheng, H. Lin, Y.N. Wang, X. Zheng, X. Duan, Y. Yuan, J. Catal. 297 (2013) 110-118.

[31] W.L. Dai, Y. Cao, L.P. Ren, X.L. Yang, J.H. Xu, H.X. Li, H.Y. He, K.N. Fan, J. Catal. 228 (2004) 80–91.

[32] K. Arve, J.R. Hernandez Carucci, K. Eränen, A. Aho, D.Y. Murzin, Appl. Catal. B. 90 (2009) 603-612.

[33] S. Tamm, N. Vallim, M. Skoglundh, L. Olsson, J. Catal. 307 (2013) 153-161.

[34] S. Tamm, S. Fogel, P. Gabrielsson, M. Skoglundh, L. Olsson, Appl. Catal. B. 136-137 (2013) 168-176.

[35] H. Zhang, N. Toshima, Appl. Catal. A. 447-448 (2012) 81-88.

[36] X. Huang, X. Wang, X. Wang, X. Wang, M. Tuan, W. Ding, X. Lu, J. Catal. 301 (2013) 217-226.

[37] X. Liu, Y. Li, J.W. Lee, C. Y. Hong, C.Y. Mou, B.W.L. Jang, Appl. Catal. A. 439-440 (2012) 8-14.

[38] A.Q. Wang, J.H. Liu, T.S. Lin, C.Y. Mou, J. Catal. 223 (2005) 186-197.

[39] N. Toreis, X.E. Verykios, S.M. Khalid, G.B. Bunker, Surf. Sci. 197 (1988) 415-429.

[40] A.Q. Wang, Y. Hsieh, Y.F. Chen, C.Y. Mou, J. Catal. 237 (2006) 197-206.

[41] J. H. Liu, A.Q. Wang, Y. S. Shi, H. P. Lin, C.-Y. Mou, D. S. Su, J. Phys. Chem. B. 109 (2005) 40-43.

[42] A. Wang, X.Y. Liu, C.-Y. Mou, T. Zhang, J. Catal. 308 (2013) 258-271.

[43] X. Y. Liu, A. Q. Wang, X. F. Yang, T. Zhang, C. -Y. Mou, D. S. Su, J. Li, Chem. Mat. 21 (2009) 410-418.

Chapter 4: Effect of metal loading on SCR of NO_x by hydrocarbon using bimetallic catalysts.

Abstract:- Bimetallic Ag-Au/Al_2O_3 catalyst with varying Au or Ag loading (1 and 2 wt%) on in house prepared high surface area alumina (450 m^2g^{-1}) were synthesized by successive impregnation method and by changing the order of metal impregnation. For comparison the bimetallic catalysts were also prepared with 1% Ag and 1% Au loading on the same high surface area alumina using different sequence of impregnation. The catalysts were characterised by various physico-chemical techniques and tested for SCR activity under lean burn engine exhaust condition. 1 wt% Au-2 wt% Ag/Al_2O_3 catalyst showed better SCR activity (50% NO conv. at 234 ºC) compared to 1Au-1Ag/Al_2O_3 (50% NO conv. at 273 ºC). The effect of metal loading on SCR activity of Ag-Au/Al_2O_3 was studied and catalysts with higher silver loading (2 wt%) was found to give the best results with wide temperature window for NO conversion to N_2. Further ageing of the catalyst under reaction feed at 500 ºC resulted in considerable increase in low temperature activity of bimetallic catalyst with higher silver loading (2 wt%) compared to catalyst with higher gold loading. Detailed investigation of the textural properties of the pretreated and aged catalysts showed presence of well dispersed metallic Au and $Ag_n^{\delta+}$ clusters.

1. Introduction

The use of diesel engine have significant advantages over their counterpart gasoline spark ignition (SI) engines due to the enhanced fuel economy and high efficiency. The selective catalytic reduction (SCR) using HC is a promising technique for nitrogen oxides (NO_x) abatement in excess oxygen from diesel engine exhaust. Among various catalyst studied for HC-SCR, Ag/Al_2O_3 was found to be the most promising and is considered as benchmark catalyst since it exhibits high activity for NO reduction and high selectivity for N_2. However the major drawback of this system is poor low temperature activity and sulfur tolerance in temperature range of 300 – 400 ºC [1-5]. Improvement in both low temperature activity and the sulfur tolerance of Ag/Al_2O_3 catalyst by support modification has been studied previously [1, 6]. Addition of second metal attracted special attention for improvement in activity of Ag/Al_2O_3. Due to the formation of synergistic effects between two metallic components, the activity of bimetallic catalyst may be greater than the sum of two separated monometallic catalysts. Bimetallic catalysts have also shown better reducing activity and water resistance could be improved due to the synergistic effect between metals [7-10]. Ag/Al_2O_3 showed SCR activity at low temperature with narrow temperature window whereas Au/Al_2O_3 showed maximum activity at higher temperature [6]. In previous chapter we have seen considerable change in SCR activity of Ag/Al_2O_3 after addition of Au. The effect of different pretreatment and preparation method on SCR activity of bimetallic Ag-Au/Al_2O_3 has been reported in previous chapter [11]. The improvement in low temperature activity and widening of temperature window of bimetallic catalysts is highly desired. Effect of increase in silver loading is reported elsewhere, silver loading could be responsible for the increase in low temperature activity (200 to 350 ^oC) whereas high temperature activity was declined [12, 13]. Ueda et al. [14] have studied the effect of gold loading on NO_x reduction activity. The result showed decrease in NO_x reduction activity with increase in gold content from 0.5 to 5 wt% in the temperature range of 300 to 500 ºC. The effect of metal loading on NO_x reduction activity of bimetallic silver-gold catalyst was analyzed by Arve et al. [15], and result showed higher NO conversion (45%) at lower wt% loading of Au on Al_2O_3. Among bimetallic Au-Ag catalyst 0.3 wt% Au-1.9 wt% Ag/Al_2O_3 showed higher NO reduction activity compared to the catalyst with lower silver loading. With this background the effect of amount of metal loading in AgAuAl catalyst was studied for selective reduction of NO_x into N_2.

2. Experimental

2.1. Catalysts preparation

Chemicals and Reagents: $AgNO_3$ (99.8%,Thomas Baker) and $HAuCl_4$ (49% Au, LOBA Chemie) were used without further purification. Alumina (γ-Al_2O_3) was prepared by solgel method by dissolving 248.96 g aluminium tri-sec-butoxide (97%,Aldrich) in 300 g isopropanol and stirring it at room temperature for 2 h to get transparent solution. Isopropanol solution (50 mL) of NH_4OH (5 mL) was added dropwise with constant stirring till the gel was formed. Gel was dried in air for 12 h and calcined at 500 ºC for 4 h. This alumina was further used as support for loading of Ag and Au. Bimetallic catalyst with different amount of Ag and Au were prepared by two different methods.

In first method, initially Au/Al_2O_3 was prepared by deposition-precipitation method using urea. $HAuCl_4$ solution was added dropwise to a slurry of alumina in water at 80 ºC with constant stirring. Urea solution was added dropwise to the above solution in order to promote the precipitation of $Au(OH)_3$ on the surface of alumina. The solid thus obtained was filtered and washed with water to remove chloride as checked by silver chloride test. This 1 wt% Au/Al_2O_3 catalyst (dried at 80 ºC for 12 h) was further impregnated with $AgNO_3$ solution to get bimetallic 1% Ag-1% Au/Al_2O_3 catalyst. The catalyst was dried at 80 ºC for 12 h followed by calcination at 500 ºC for 6 h and labeled as AgAuAl.

In second method, bimetallic catalysts were prepared by reversing the order of metal impregnation. In this method starting material was Ag/Al_2O_3 which was prepared by impregnating aqueous $AgNO_3$solution on alumina. After drying the catalyst at 80 ºC for 12 h, gold was added via the above mentioned deposition precipitation method using urea. The obtained sample was filtered and washed with water till complete removal of chloride. Finally sample was dried at 80 ºC for 12 h and then calcined in air at 500 ºC for 6 h. The bimetallic Au–Ag/Al_2O_3 and Ag–Au/Al_2O_3 were labeled as AuAgAl and AgAuAl respectively. The amount of Au and Ag loading of these catalysts is shown in table 1.

Table 1. Catalysts prepared with different metal loading

Catalyst	Metal loading (Wt%)		Order of metal loading on alumina	
	Ag	Au	First	Second
AgAuAl	1	1	Au	Ag
AuAgAl	1	1	Ag	Au
Ag2AuAl	1	2	Au	Ag
2AgAuAl	2	1	Au	Ag
Au2AgAl	1	2	Ag	Au
2AuAgAl	2	1	Ag	Au

2.2. Catalyst characterisations

2.2.1. Powder X-ray diffraction studies

The powder X-ray diffraction data was collected on a Philips (Xpert) equipped with a Ni filtered Cu Kα radiation (λ=1.5406 Å, 40 kV, 30 mA). The data was collected in the 2θ range 20-80º with a stepsize of 0.02º and scan rate of 4º min^{-1}.

2.2.2. Nitrogen adsorption studies

The BET surface area of the calcined samples was determined by N_2 sorption at 77 K using NOVA 1200 (Quanta Chrome) equipment. Prior to N_2 adsorption, the material was evacuated at 300 ºC under vacuum. The specific surface area was determined according to the BET equation.

2.2.3. UV-vis diffuse reflectance studies (UV–vis DRS)

The characterizations of pretreated (pretreatment at 250 ºC in H_2 for overnight) and aged (overnight ageing under reaction feed at 500 ºC) catalyst were carried out. UV–vis DRS spectra were recorded with a UV–vis spectrophotometer (PerkinElmer, Lambda 650) in the diffuse reflectance mode between 200 and 800 nm at a step of 0.2 nm with a slit width of 1 nm. $BaSO_4$ was used as a reference sample to confirm the baseline spectrum.

2.2.4. X-ray photoelectron spectroscopy study (XPS)

X-ray photoelectron spectroscopy (XPS) was used for the characterization of surface of pretreated and aged catalysts. XPS experiments were performed using an ESCA 3000 spectrometer equipped with a magnesium source for excitation in the analysis chamber under ultrahigh vacuum (10^{-10}Torr). Binding energy (B.E.) values were referenced to the binding energy of the O1s core level (531.3 eV).

2.2.5. Energy dispersive X-ray spectroscopy (EDS)

The dispersion of metal on the catalyst surface was measured by EDS elemental mapping images taken by Quanta FEI 200 3D equipped with tungsten filament as source of electron.

2.3. Catalytic activity

The selective catalytic reduction (SCR) of NO_x under realistic synthetic exhaust condition corresponding to lean engine exhaust was carried out at atmospheric pressure in quartz tubular down flow reactor (inner diameter 20 mm). Catalyst powder (360 mg) diluted with commercial silicon carbide (2 g) was placed in the reactor and a thermocouple was inserted in the center of the catalyst bed to measure the temperature. Typical reaction feed used for SCR activity was 300 ppm NO, 300 ppm CO, 300 ppm C_3H_6, 2000 ppm H_2, 100 ppm $C_{10}H_{22}$, 10% CO_2, 10% O_2, 5% H_2O, He balance. The total flow rate of the gas mixture was 300 mL min^{-1} to obtain a gas hourly space velocity of 50,000 $mL.g^{-1}.h^{-1}$. The flow rate was monitored by mass flow controller.

Prior to the reaction catalyst was pretreated at 250 ºC in hydrogen flow for 12 h. After pretreatment, the catalyst was cooled to 80 ºC and the reaction feed was passed on catalyst surface with increasing the temperature from 80 ºC to 500 ºC with heating rate of 2 ºC min^{-1}. The reaction feed was stabilized on the catalyst at 500 ºC for 12 h for catalyst ageing. Later the catalyst was cooled to 80 ºC and in the last stage the catalytic activity was monitored under reaction feed with increasing the temperature from 80 to 500 ºC with heating rate of 2 ºC min^{-1}.

The concentrations of the inlet and outlet gases were simultaneously monitored using Micro GC (Varian, CP 4900) with TCD detector and NO_x analyzer (Environment SA MIR

9000). The micro GC has two columns to detect different gases: molecular sieves (MS 5A) for H_2, N_2, O_2, NO and CO and Porapak Q for H_2, CO_2, N_2O, C_3H_6 and H_2O.

The NO conversion was calculated from outlet molar flow rates of N_2 + N_2O formation (F_{N_2}, F_{N_2O}) and inlet molar flow rate of NO ($F_{0,\,NO}$) using the following Eq. (1):

$$\%NO\ Conv. = 100 \times \frac{2 \times \left(F_{N_2} + F_{N_2O}\right)}{F_{0,\,NO}} \qquad (1)$$

N_2 selectivity was calculated using following Eq. (2) :

$$S_{N_2} = 100 \times \frac{F_{N_2}}{F_{N_2} + F_{N_2O}} \qquad (2)$$

3. Result and discussion

3.1. Catalytic activity

The series of bimetallic catalysts were prepared by increasing the amount of Ag or Au to 2 wt% by successive impregnation method and also by changing the sequence of metal impregnation on alumina support. The catalytic activity of the prepared catalyst was tested under lean burn condition.

3.1.1. Activity comparison of Ag2AuAl, 2AgAuAl and AgAuAl

All the catalysts were pretreated in H_2 at 250 ºC (Fig. 1A). The effect of metal loading on catalytic activity was analyzed by comparing NO conversion with AgAuAl. The SCR activity of AgAuAl catalyst initiated at 200 ºC with maximum conversion at 366 ºC (100%) which decreased concomitantly to 52% when temperature was increased to 500 ºC. After increasing the silver loading (2AgAuAl), activity initiated at 150 ºC with maximum NO conversion (91%) at 325 ºC which further decreased to 15% at 500 ºC. This indicates that increase in silver amount significantly improves the NO conversion in low temperature (100 to 350 ºC). When the gold loading was increased (Ag2AuAl), the activity initiated at 150 ºC and showed maximum NO conversion (73%) at 305 ºC. However NO conversion decreased to 30% with increase in temperature to 500 ºC, indicating detrimental effect of increase in gold loading. AgAuAl catalyst showed maximum activity (100%) at higher temperature (366

ºC) as compared to Ag2AuAl (305 ºC) and 2AgAuAl (325 ºC). The temperature of 50% NO conversion (T_{50}) was in the order of 2AgAuAl (216 ºC) < Ag2AuAl (244 ºC) < AgAuAl (284 ºC).

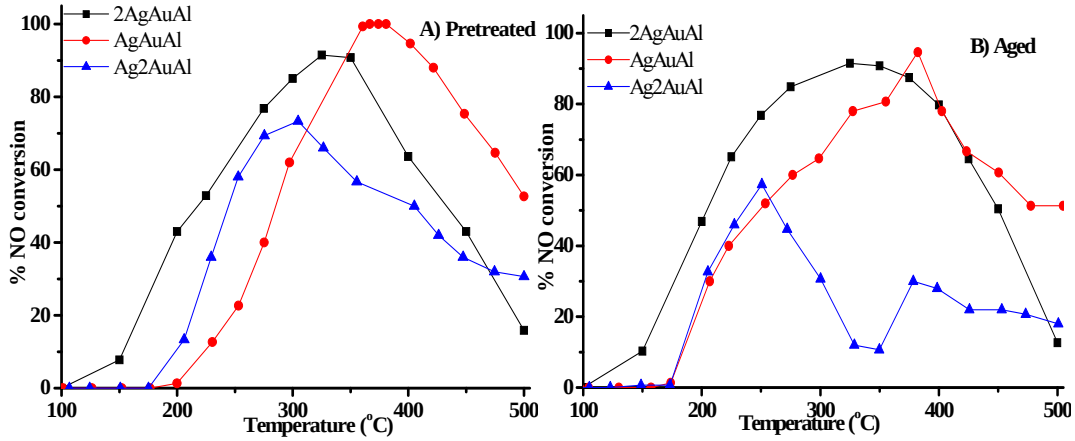

Fig. 1. SCR activity of impregnated bimetallic catalyst (a) pretreated b) aged. Reaction feed:- 300 ppm NO, 300 ppm CO, 300 ppm C_3H_6, 2000 ppm H_2, 100 ppm $C_{10}H_{22}$, 10% CO_2, 10% O_2, 5% H_2O, He balance, GHSV=50,000 $mL.g^{-1}.h^{-1}$.

SCR activity of catalysts after ageing under reaction feed for 12 h is shown in Fig. 1B. In case of AgAuAl catalyst low temperature activity increased from 13 to 40% at ~225 ºC whereas high temperature activity decreased from 64 to 50% at 400 ºC. Catalyst with increased silver loading (2AgAuAl) after ageing showed increase in low as well as high temperature NO conversion from 52 to 65% and 63 to 78% at 225 ºC and 400 ºC respectively. The catalyst with higher gold loading (Ag2AuAl) showed increase in NO conversion from 35 to 45% at low temperature (225 ºC) with significant decrease in high temperature activity from 50 to 28% at 400 ºC. Monometallic Au/Al_2O_3 did not show improvement in low temperature activity after ageing as mentioned in previous chapter. Hence increase in NO conversion after ageing of 2AgAuAl can be attributed to synergisitic effect of Ag and Au present in catalyst, the temperature for 50% NO conversion (T_{50})decreased for all catalyst though order remains same 2AgAuAl (204 ºC) < Ag2AuAl (235 ºC) < AgAuAl (248 ºC) respectively. All catalyst showed 100% selectivity for N_2.

Increase in low temperature activity was observed after ageing in all catalysts. Only 2AgAuAl showed increase in high temperature activity as well, whereas remaining catalysts

showed decrease in high temperature (400 ºC) activity. These results indicate that increase in silver loading in bimetallic catalyst significantly improve the low and high temperature activity.

3.1.2. Activity comparison of Au2AgAl, 2AuAgAl and AuAgAl

The effect of increasing Ag or Au (2 wt%) loading on catalytic activity was also analyzed by changing the sequence of metal impregnation on alumina (Fig. 2). All catalysts were pretreated in H_2 at 250 ºC. The AuAgAl catalyst showed12% NO conversion at 150 ºC with maximum conversion at 325 ºC (94%) which decreased with increase in temperature to 69% at 500 ºC. The SCR activity of catalysts after increasing silver loading (Au2AgAl) initiated at 150 ºC with maximum conversion (95%) at 325 ºC which further decreased to 69% at 500 ºC. When the gold loading was increased (2AuAgAl), activity was initiated at 250 ºC with maximum conversion of 58% at 325 ºC. Further activity declined to 19% with increase in temperature to 500 ºC. Catalysts showed T_{50} is in order of Au2AgAl (234 ºC) < AuAgAl (273 ºC) < 2AuAgAl (316 ºC).

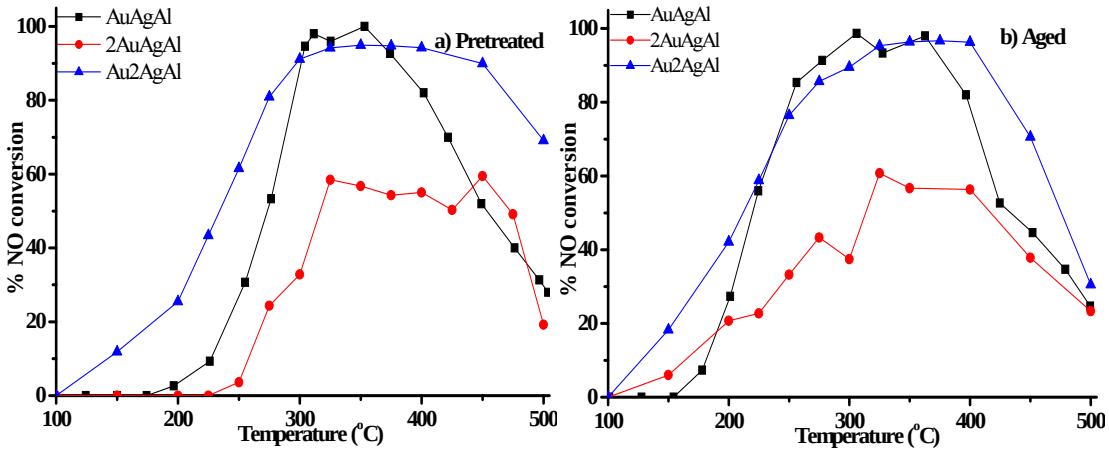

Fig. 2. SCR activity of catalysts a) pretreated at 250 ºC in H_2, b) after overnight ageing at 500 ºC in the reaction feed. Reaction feed:- 300 ppm NO, 300 ppm CO, 300 ppm C_3H_6, 2000 ppm H_2, 100 ppm $C_{10}H_{22}$, 10% CO_2, 10% O_2, 5% H_2O, He balance, GHSV=50,000 $mL.g^{-1}.h^{-1}$.

The low temperature activity of aged catalysts increased in the temperature range of 100-300 ºC as shown in Fig. 2B. AuAgAl catalyst showed increase in activity at low temperature from 3 to 27% at 200 ºC which decreased at high temperature (500 ºC) from 28

to 25%. However the selectivity for N_2 at low temperature (<200 ºC) was decreased as mentioned in previous chapter. Increase in low temperature NO conversion from 26 to 42% was observed at 200 ºC with increase in silver amount after ageing (Au2AgAl), however high temperature (500 ºC) activity decreased from 69 to 30%. When gold loading was increased (2AuAgAl), the low temperature activity increased (1 to 21% at 200 ºC) with decrease in high temperature (500 ºC) activity from 22 to 18%. Such improvement in low temperature activity after ageing was not observed in case of monometallic Au/Al_2O_3. Hence the improvement in low temperature activity can be attributed to the synergistic effect between Ag and Au. The T_{50} of all catalysts shifted to lower temperature and its order was Au2AgAl (211 ºC) > AuAgAl (220 ºC) > 2AuAgAl (312 ºC). The low temperature activity increased significantly with increase in silver loading. However pretreated AuAgAl catalyst showed maximum activity at higher temperature compared to Au2AgAl and 2AuAgAl. The catalytic activity is comparable with literature report [16, 17].

3.2. *Catalyst characterisation*

3.2.1. Powder X-ray diffraction analysis

The XRD patterns of all the catalysts are given in Fig. 3. The broad XRD peaks (Fig. 1A) observed at 2θ 32.2, 38.01, 46.02 and 66.7º confirmed formation of γ-Al_2O_3 (JCPDS, 29-0063). The XRD pattern of pretreated bimetallic catalyst showed peaks (Fig. 3A) at 2θ 38.2, 44.2, 64.4º corresponding to metallic silver (JCPDS, 04-0783). Metallic gold crystallites were detected on Au catalyst with characteristic XRD peaks (Fig. 3A) at 2θ 38.18, 44.39, 64.57º (JCPDS, 04-784). However peaks of metallic Ag and Au could not be differentiated in case of all catalysts due to very small difference in d value. Similar characteristics were shown by other catalyst also, AgAuAl showed peak correspond to the metallic silver and gold (32.2 and 32.18º). The intensity of Ag and Au peaks increased with increasing in silver loading (2AgAuAl), indicating that increase in silver loading increases the crystalline nature of metal particle. AgAuAl catalyst showed less intense peaks compared to 2AgAuAl and Ag2AuAl after ageing the catalyst under reaction feed for 12h. The presence of broad and low intensity peaks suggested the improved dispersion of silver and gold particles on alumina support with formation of smaller metallic particles.

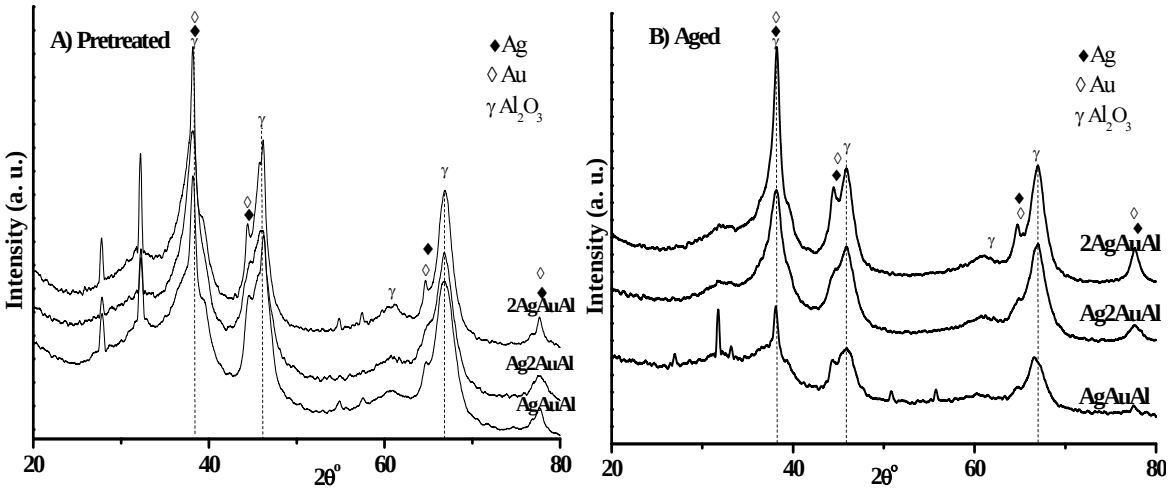

Fig. 3. XRD pattern of A) pretreated and B) aged bimetallic catalysts.

Fig. 4 shows XRD pattern of catalysts prepared by reversing the order of impregnation. AuAgAl showed peaks at 2θ 38.2, 44.2, 64.4º for metallic silver and gold which overlapped with peaks of γ-Al_2O_3 due to the small difference in d-spacing.

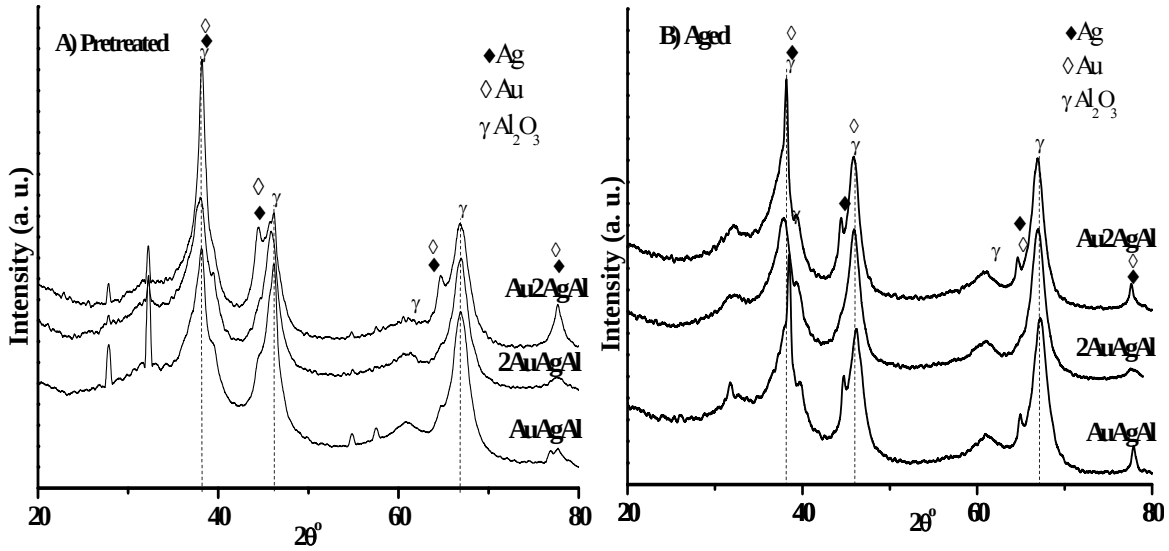

Fig. 4. XRD pattern of A) pretreated and B) aged bimetallic catalysts.

The intensity of peak corresponds to the metallic Ag and Au (44.4, 64.5 and 77.7º) increased with increase in silver loading (Au2AgAl), indicates the agglomeration of Ag and Au. The intensity of alumina, Ag and Au peaks decreased after ageing of AgAuAl.

However sharpness of the peak increased with increase in silver loading in Au2AgAl, whereas such sharp peaks were not observed after increasing the gold loading (2AuAgAl).

3.2.2. UV- visible diffuse reflectance analysis (UV-vis DRS)

The UV-vis spectra of pretreated and aged bimetallic catalysts are shown in Fig. 5A and 5B respectively. For clarity in distinguishing the peaks for different species of active component, UV spectrum of Al_2O_3 was subtracted from UV of all the catalyst samples. Catalyst pretreated at 250 ºC in H_2 showed strong absorption bands in the range of 215 nm and 250 to 280 nm due to the small Ag^+ ion and $Ag_n^{\delta+}$ clusters respectively. The band at 450 nm can be assigned for the larger metallic silver particle. The absorption band at 525 nm (500-600) can be attributed to metallic Au [2, 5, 7-11]. Pretreated AgAuAl catalyst showed presence of $Ag_n^{\delta+}$ clusters (280 nm) with presence of ionic and metallic silver (215 nm, 430 nm) and metallic gold (550 nm) particles. Increase in silver loading (2AgAuAl) showed shift in band of $Ag_n^{\delta+}$ clusters to lower wavelength (250 nm) with increase in intensity of metallic Ag band (450 nm). The ionic silver was observed at the same position (215 nm) with no significant change in band correspond to the metallic gold (525 nm). Same position of band was observed after increase in gold loading (Ag2AuAl). There was no change in the position of metallic and ionic Ag and Au species after ageing.

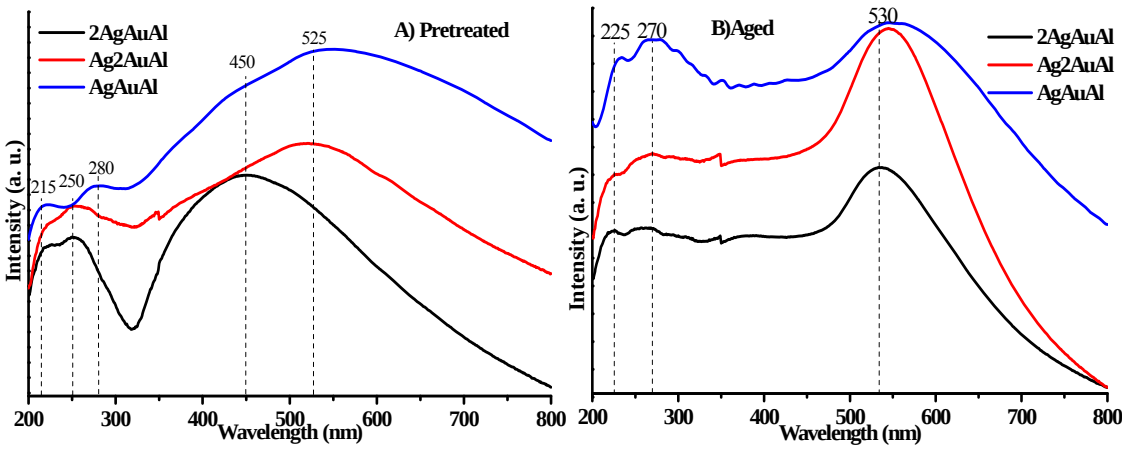

Fig. 5. UV-vis DRS study of A) pretreated and B) aged bimetallic catalysts.

The effect of ageing in reaction feed at 500 ºC was studied by UV-vis DRS for all the catalysts after pre-treating in presence of H_2 at 250 ºC (Fig. 5B). The intensity of $Ag_n^{\delta+}$ species (275 nm) increased considerably on aged AgAuAl catalyst compared to pretreated

catalyst. At the same time the band corresponding to the metallic silver (450 nm) disappeared. There was no change in band position of Au^{o} (550 nm) after ageing indicating no agglomeration of gold particles due to ageing at 500 ºC. The hump between 225 and 260 nm for $Ag_n^{\delta+}$ clusters was observed when silver loading (2AgAuAl) was increased, whereas the band of metallic Ag (450 nm) disappeared indicating the conversion of metallic Ag into $Ag_n^{\delta+}$ clusters after ageing. There was no considerable change in the position of band for metallic gold (530 nm) indicating no agglomeration of gold particles due to ageing at 500 ºC. The intensity of band of gold increased with increase in gold loading (Ag2AuAl).

The catalyst with higher silver loading (2AgAuAl) showed absence of band for metallic silver after ageing with increase in the intensity of band for Ag^{+} and $Ag_n^{\delta+}$ clusters, indicating the oxidation of metallic silver. The metallic gold band shifted to slight higher wavelength and shifting is more pronounced (525 to 550 nm) in case of catalyst with higher gold loading (Ag2AuAl), which confirmed the agglomeration of gold. Increase in the intensity of $Ag_n^{\delta+}$ clusters, could be correlated to the improvement in low temperature activity of aged catalysts (2AgAuAl) with higher silver loading. The agglomeration of gold has lead to the decrease in activity of Ag2AuAl after ageing.

The UV-vis DRS spectra of catalysts prepared by reversing the order of metal impregnation are shown in Fig. 6A (pretreated) and 6B (aged). AuAgAl shows presence of metallic gold at 525 nm whereas the band at 255 nm corresponds to the $Ag_n^{\delta+}$ clusters. After increasing the silver loading catalyst (Au2AgAl) showed hump of metallic (450 nm) and ionic Ag (255 nm) and metallic Au at 525 nm. Same band were observed in catalyst with increased gold loading (2AuAgAl) however the intensity of gold band (525 nm) increased due to the increased loading of gold. The AuAgAl catalyst after ageing under reaction feed at 500 ºC showed band at 214, 255 nm for ionic Ag and $Ag_n^{\delta+}$ clusters respectively. The gold band shifted to the higher wavelength from 525 to 540 nm, indicating the slight agglomeration of gold particles. The intensity of the $Ag_n^{\delta+}$ band (255 nm) increased after increase in silver loading (Au2AgAl) with disappearance of metallic Ag band (450 nm), indicating partial oxidation of metallic Ag. However the wavelength of gold band was not shifted. When the gold loading was increased (2AuAgAl), UV band was observed at 214 and 255 nm attributed to the presence of ionic Ag and $Ag_n^{\delta+}$ clusters respectively. However the band for metallic Au shifted from 525 nm to 564 nm after ageing, which suggested the significant agglomeration of Au.

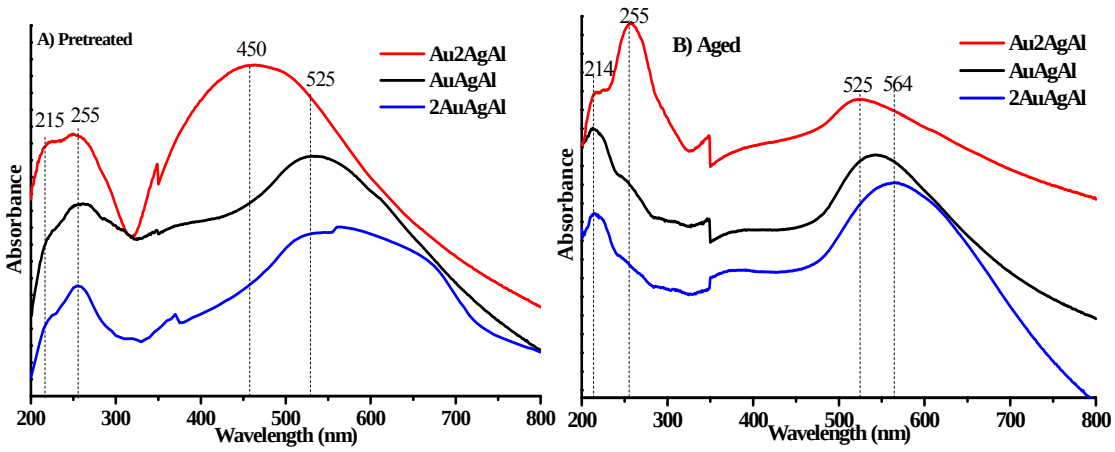

Fig. 6. UV-vis DRS study of A) pretreated and B) aged catalyst prepared by reversing the order of metal impregnation.

Formation of more $Ag_n^{\delta+}$ clusters was observed after increase in the Ag loading (2AgAuAl and Au2AgAl, 255 nm) which is known to be more active for SCR of NO_x. The clusters of $Ag_n^{\delta+}$ species (n<8) are reported to be active species for SCR of NOx and the species are chracterised by the UV band around 270 nm [18]. Hence in the present work also the formation of more $Ag_n^{\delta+}$ species are observed in UV analysis, which improved the activity of catalyst after ageing can be attributed to the formation of more $Ag_n^{\delta+}$ species. These catalysts also showed absence of metallic Ag band after ageing indicating the oxidation of Ag. The shifting of gold band to higher wavelength indicates the agglomeration of gold in 2AuAgAl and Ag2AuAl catalysts. The formation of more $Ag_n^{\delta+}$ clusters could be responsible for improved low temperature activity of catalyst after ageing.

3.2.3. X-ray photoelectron spectroscopy study (XPS)

Fig. 7 shows the comparison of XPS data for pretreated and aged bimetallic 2AgAuAl, Au2AgAl catalysts plotted on the common scale of intensity. Table 3 summarizes the binding energy of Ag and Au on 2AgAuAl and Au2AgAl catalyst.

XPS analysis did not show peak correspond to Au, indicating availability of very low concentration of Au on the surface. The concentration of gold on the surface is negligible, hence not detected. The catalyst reduced at 250 ºC showed considerably lower intensity of silver species on the surface compared to aged catalyst (Fig. 7). XPS data clearly revealed increased intensity of silver species on aged catalyst compared to pretreated 2AgAuAl and

Au2AgAl catalyst.

Table 3. Binding energy and surface composition

Catalyst	Binding energy (eV.)			
		$Ag3d_{5/2}$		
		$Au4f_{7/2}$	Ag^0	Ag^+
2AgAuAl	Pretreated	NA	368.4	367.2
	Aged	NA	368.1	367.1
Au2AgAl	Pretreated	NA	368.5	367.3
	Aged	NA	368.4	367.3

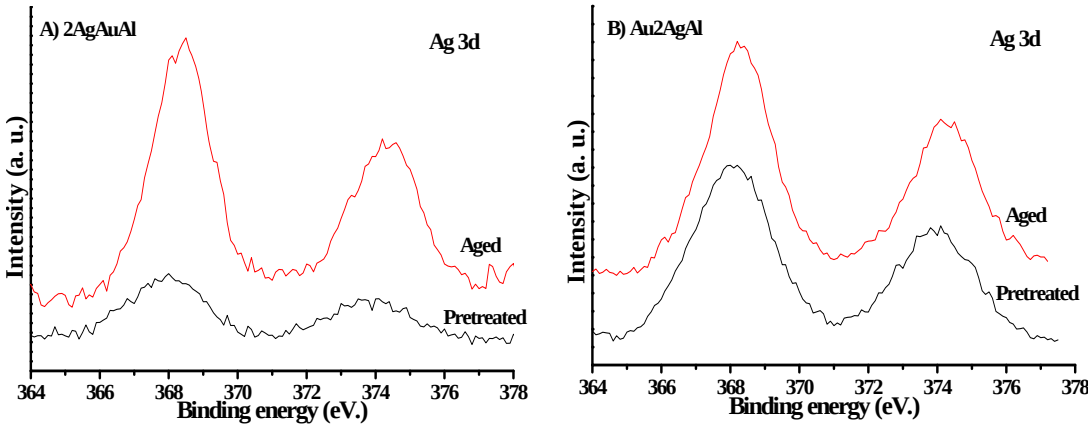

Fig. 7. XPS comparison of pretreated and aged A) 2AgAuAl and B) Au2AgAl catalysts.

The BE for Ag^+ was observed at 367.2 eV in pretreated 2AgAuAl catalyst which decreased after ageing to 367.1 eV, however the BE for Ag^0 was observed at 368.4 eV which shifted to 368.1 eV after ageing (Fig. 8). No significant change in binding energy of Ag^+ was observed, whereas Ag^0 showed decrease in binding energy due to ageing which is in well agreement with UV results where the peak corresponding to Ag^0 at 450 nm diminished after

ageing. Au2AgAl catalyst showed similar change, binding energy of Ag^0 slightly decreased with no change in binding energy of Ag^+ species. The area of Ag ($3d_{5/2}$) species increased after ageing (4395 to 16055), indicating the surface enrichment of silver species in 2AgAuAl catalyst. In case of Au2AgAl catalyst showed slight increase in area (14788 to 16023). These results are in accordance with UV results. The UV spectrum of the samples after subtraction of alumina also showed formation of more $Ag_n^{\delta+}$ species after ageing. Hence the XPS and UV-vis data is in agreement with catalytic activity results.

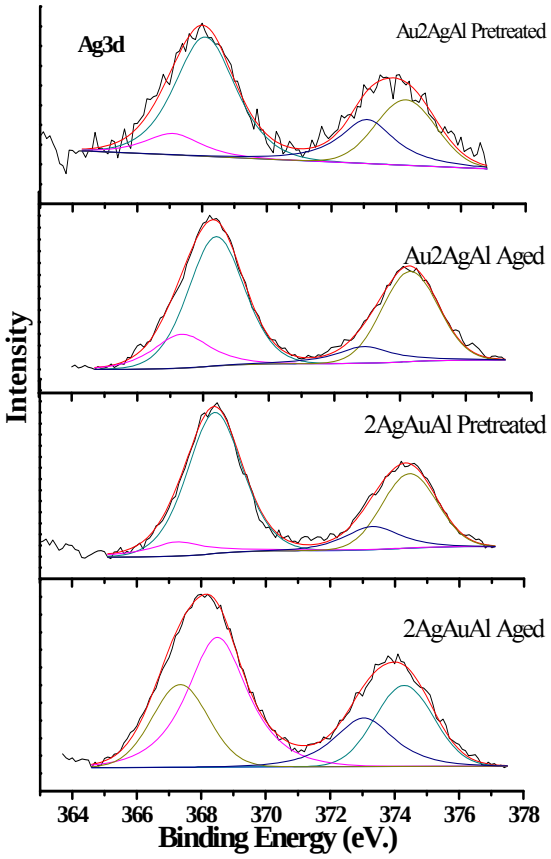

Fig. 8. XPS spectra of pretreated and aged bimetallic catalysts.

3.2.4. Energy dispersive studies (EDS studies)

The metal dispersion after pretreatment and ageing was studied by EDAX in 7.5 x 7.5 μm^2 area of catalysts (Fig. 9). Bimetallic catalyst with increased silver loading (2AgAuAl, Au2AgAl) showed improved dispersion of silver and gold particles after ageing compared to freshly pretreated catalyst. Whereas the catalysts with higher gold loading (Ag2AuAl and 2AuAgAl) showed decrease in dispersion after ageing. Agglomeration of metal particle

increased with increase in gold loading which causes the decrease in activity. AgAuAl, 2AgAuAl, AuAgAl catalysts showed less amount of the gold on the surface (table 4) which could be responsible for maximum activity.

Table 4. Wt% analysis by EDS

Sr No.	Catalysts (Wt%)	Wt% by EDS	
		%Ag	%Au
1	Ag2AuAl	0.90	1.41
2	2AgAuAl	1.99	0.65
3	Au2AgAl	1.98	0.85
4	2AuAgAl	0.90	1.90
5	AgAuAl	1.04	0.60
6	AuAgAl	1.01	0.80

a) 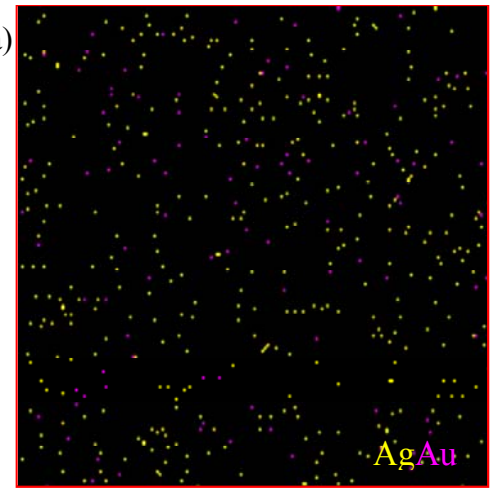

g) 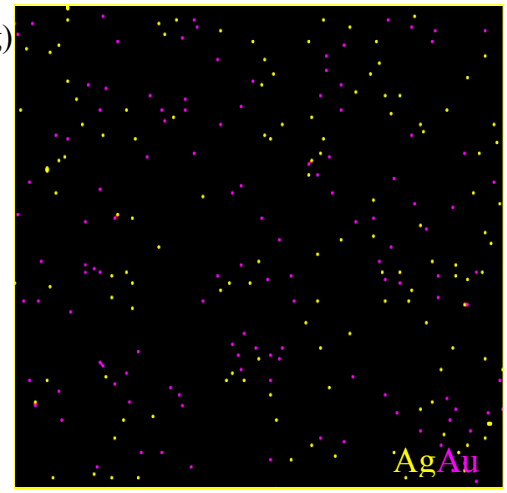

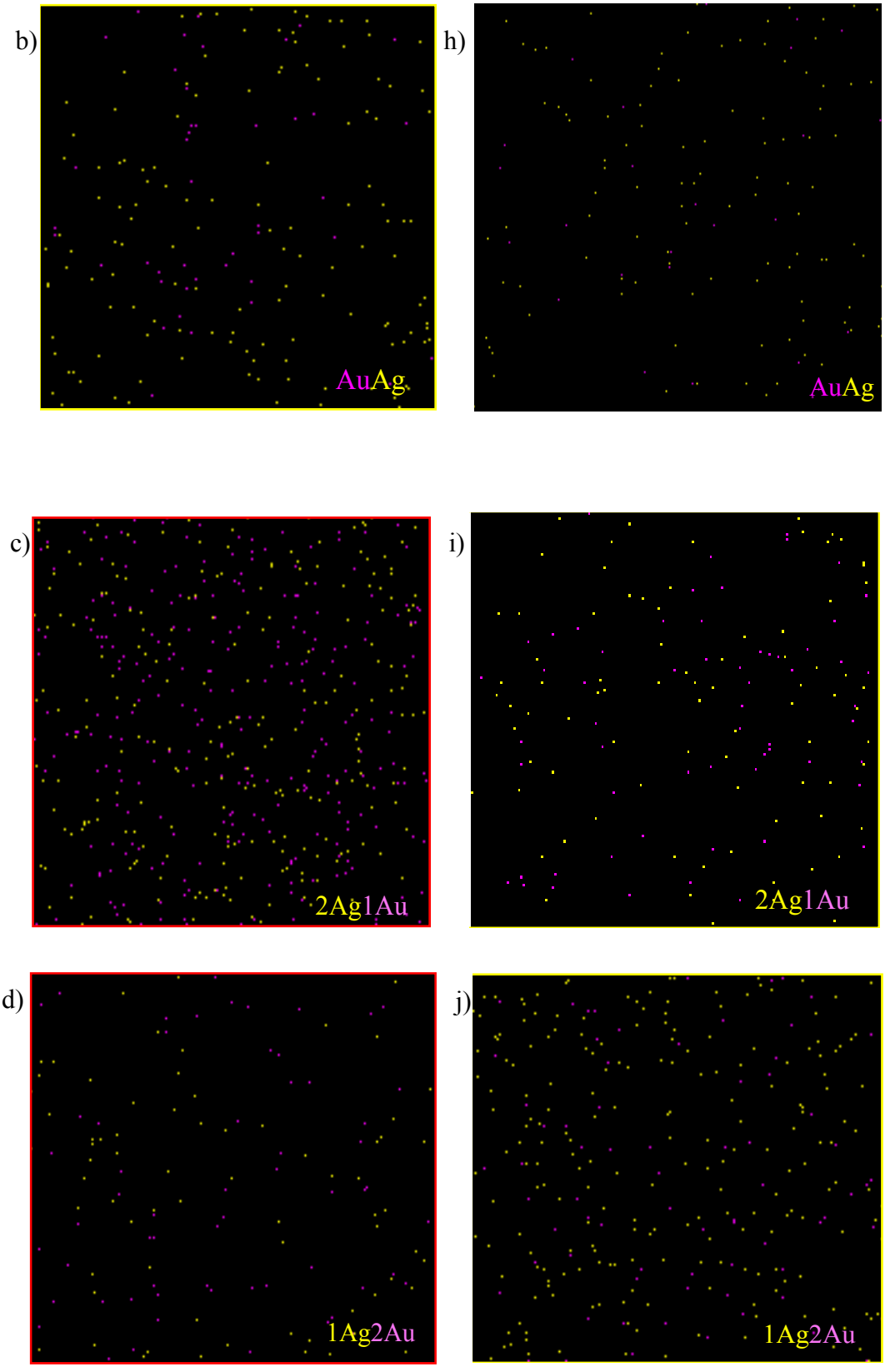
b)
AuAg
h)
AuAg
c)
2Ag1Au
i)
2Ag1Au
d)
1Ag2Au
j)
1Ag2Au

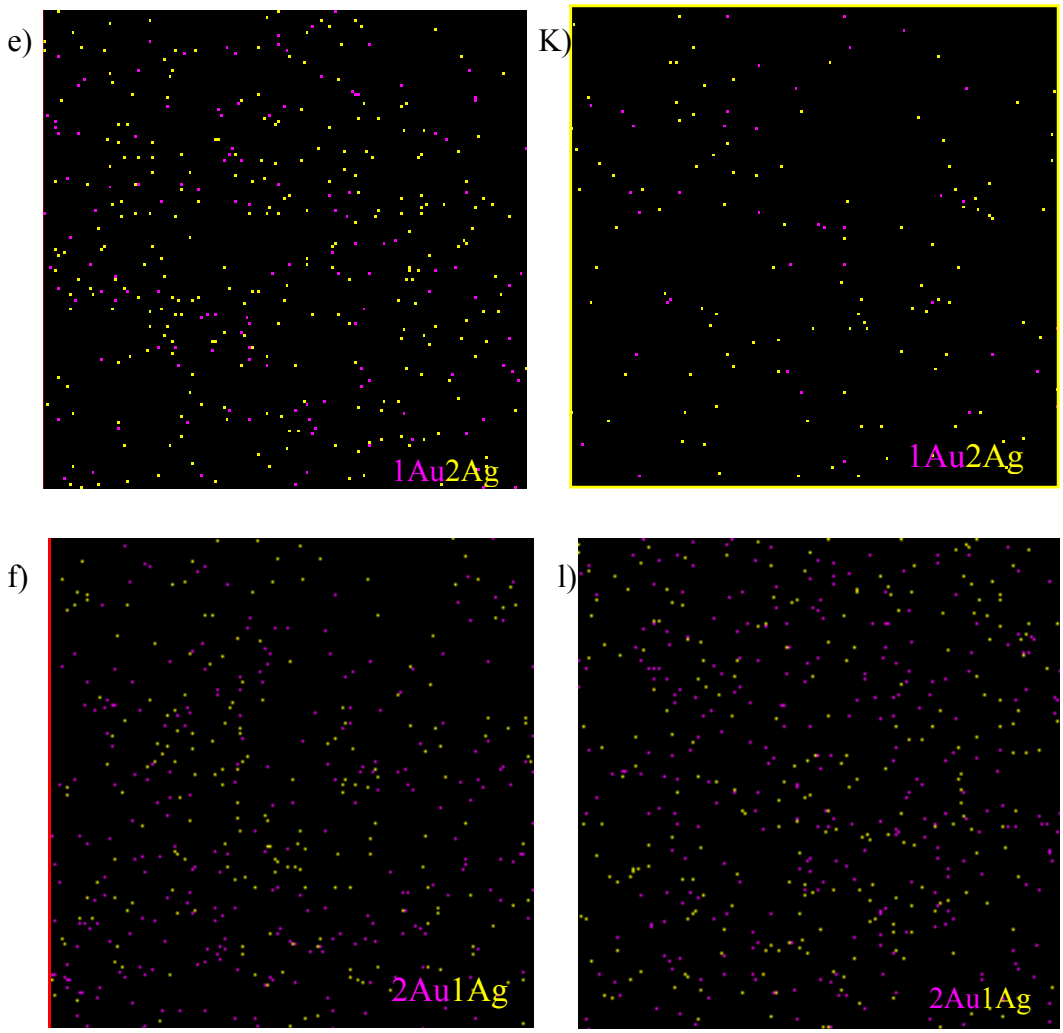

Fig. 9. Elemental mapping images of impregnated and reverse impregnated catalysts. a, b, c, d, e, f- pretreated, g, h, i, j, k, l - aged.

Total six composition of Ag-Au bimetallic catalysts were prepared by successive impregnation method. The catalysts with higher silver loading showed increase in low temperature NO_x conversion (2AgAuAl, Au2AgAl). Fig 1B and 2B shows a broadening in the NO_x reduction temperature window to lower temperatures range (150 to 280 ºC) after ageing. This low temperature conversion could be due to the increased Ag surface density (Ag loading) as confirmed by XPS. Increasing Ag loading could utilize maximum HC for NO reduction leading to the higher SCR activity [19]. Martinez et al. [20] reported that Ag/Al_2O_3 catalyst with higher silver (6 wt%) loading showed increase in the low temperature NO conversion, whereas activity decreased at high temperature (> 225 ºC). Same observation is reported by Thomas et al. [16] in SCR of NO_x by propene and H_2 with detail kinetic study.

The improvement in activity was also attributed to the presence of well dispersed Ag and Au as confirmed by XRD and EDS data. Improvement in NO_x conversion after ageing can be correlated to the formation of more $Ag_n^{\delta+}$ clusters as demonstrated by UV-vis data. Gunnarson et al. [19] explained the enhancement in activity of Ag/Al_2O_3 after ageing due to the mild hydrothermal treatment resulting in reconfiguration of the silver particles. This increased their ability to partially oxidize the hydrocarbon that can facilitate the selective NO_x reduction into N_2.

The catalyst with lower gold loading and higher Ag loading (Au2AgAl, 2AgAuAl) showed maximum NO_x conversion attributed to the maximum dispersion of Ag as confirmed by EDS. The catalysts have shown significant widening of temperature window (150 - 450 ºC) for SCR activity. In present work, the catalyst with higher silver loading after changing the sequence of metal impregnation (Au2AgAl) has shown conspicuous effect on SCR activity. When first Ag was impregnated on alumina (Au2AgAl), low temperature activity considerably improved with widening of temperature window compared to first deposition of Au on alumina (2AgAuAl). It could be proposed that lower loading of Au (1 wt%) helps the dispersion of Ag. Whereas at higher loading of Au leads to the agglomeration as demonstrated by UV and EDS result. Hence activity of the catalysts Ag2AuAl and 2AuAgAl decreased after ageing. Same observation was reported by He et al. [21] that addition of 0.01 wt% of Au to the Ag/Al_2O_3 catalyst also led to the increase of NO_x reduction activity at 220–380 ºC. However, when the Au content was increased to 0.05 wt%, NO_x reduction was greatly suppressed at 410–600 ºC.

4. Conclusion

The effect of amount of silver and gold loading on alumina, prepared by successive impregnation method showed improvement in low temperature activity. The low temperature activity increased with increase in silver loading correlated to the high dispersion of silver whereas increased gold loading showed agglomeration after ageing. The agglomeration of gold showed detrimental effect on activity. The presence of gold was responsible for dispersion of silver as demonstrated by various characterisations. More number of $Ag_n^{\delta+}$ clusters could be responsible for improvement in low temperature activity after ageing. Considerable widening of temperature window (150 - 450 ºC) SCR activity was achieved with increasing the Ag loading to 2 wt% with 1wt% Au loading.

5. References

[1] T. Chaieb, L. Delannoy, C. Louis, C. Thomas, Appl. Catal. B. 142– 143 (2013) 780 – 784.

[2] J. Lee, S. Song, K. M. Chun, Ind. Eng. Chem. Res. 49 (2010)3553 – 3560.

[3] V. I. Pârvulescu, B. Cojocaru, V. Pârvulescu, R. Richards, Z. Li, C. Cadigan, P. Granger, P. Miquel, C. Hardacre, J. Catal. 272 (2010) 92 – 100.

[4] P. S. Kim, M. K. Kim, B. K. Cho, I. -S. Nam, S. H. Oh, J. Catal. 301 (2013) 65 – 76.

[5] P. M. More, N. Jagtap, A. B. Kulal, M. K. Dongare, S. B. Umbarkar, Appl. Catal. B. 144 (2014) 408 – 415.

[6] N. Jagtap, S. B. Umbarkar, P. Miquel, P. Granger, M. K. Dongare, Appl. Catal. B.90 (2009) 416 – 425.

[7] L. Guczi, D. Bazin, Appl. Catal. A. 188 (1999) 163 – 174.

[8] C. Hamill, R. Burch, A. Goguet, D. Rooney, H. Driss, L. Petrov, M. Daous, Appl. Catal. B. 147 (2014) 864–870.

[9] L. Gutierrez, E.A. Lombardo, Appl. Catal. A. 360 (2009) 107 –119.

[10] S. G. Aspromonte, E. E. Miró, A. V. Boix, Catal. Comm. 28 (2012) 105 – 110.

[11] P. M. More, D. L. Nguyen, M. K. Dongare, S. B. Umbarkar, N. Nuns, J.-S. Girardon, C. Dujardin, C. Lancelot, A.-S. Mamede, P. Granger, Appl. Catal. B. 162 (2015) 11–20.

[12] Y. Guo, J. Chen, H. Kameyama, Appl. Catal. A, 397 (2011) 163–170.

[13] M. K. Kim, P. S. Kim, J. H. Baik,1, I. –S. Nam, B. K. Cho, S. H. Oh, Appl. Catal. B. 105 (2011) 1–14.

[14] A. Ueda, T. Oshima, M. Haruta, Appl. Catal. B. 12 (1997) 81-93.

[15] K. Arve, J. Adam, O. Simakova, L. Capek, K. Eranen, D. Yu. Murzin, Top. Catal. (2009) 52:1762 – 1765.

[16] T. Chaieb, L. Delannoy, G. Costentin, C. Louis, S. Casale, Ruth, L. Chantry, Z.Y. Li, C. Thomas, Appl. Catal. B. 156–157 (2014) 192–201.

[17] H. He, Y. Yu, Catal. Today. 100 (2005) 37–47.

[18] U. Kamolphop, S. Chansai, S. F. R. Taylor, C. Hardacre, J. P. Breen, R. Burch, S. Hengrasmee, J. J. Delgado, S. L. James, ACS Catal. 1 (2011) 1257–1262.

[19] F. Gunnarsson, J. Zheng, H. Kannisto, C. Cid, A. Lindholm, M. Milh, M. Skoglundh, H. Ha¨relind, Top. Catal. 56 (2013) 416–420.

[20] A. Martınez-Arias, M. Fernández-Garcıa, A. Iglesias-Juez, J. A. Anderson, J. C. Conesa, J. Soria, Appl. Catal, B. 28 (2000) 29–41.

[21] J. Wang, H. He, Q. Feng, Y. Yu, K. Yoshida, Catal. Today. 93–95 (2004) 783–789.

Chapter 5: Summary and Conclusions

This chapter delivers the overall summary of the results and highlights the key findings.

Applications of catalysis are well known in many fields, including energy, industry, environment and life sciences. Whether homogeneous or heterogeneous (or even enzymatic), catalysis primarily is a molecular phenomenon since it involves the chemical transformation of molecules into other molecules. Present thesis is mainly focused on the heterogeneous catalysis for environmental applications specifically for NO_x emission control from diesel engine exhaust. The NO_x is emitted from different sources like vehicles (mobile) as well as boilers and coal fired power plant (stationary). NO_x emission has harmful effect on human. For abatement of NO_x emission and its effect on the environment, various legislation norms are introduced. It also gives information about the various emission control strategies that are used for the reduction of NO_x. The different technologies used for the abatement of NO_x are discussed in chapter 1. The use of "three-way catalysts" in stoichiometric engines (gasoline) and their ineffectiveness in the reduction of NO_x in diesel engines, which operates under lean-burn condition. Finally the scope and objective of the present thesis work with a clear emphasis on the selective catalytic reduction of NO_x with hydrocarbons as reductant is highlighted.

The selective catalytic reduction (SCR) of NO_x using hydrocarbon (HC-SCR) is considered as the most promising alternative technology for removal of NO_x from diesel automobile engine exhaust compared to urea SCR and lean NO_x trap (LNT). Among the various catalyst compositions investigated for HC-SCR of NO_x, Ag/Al_2O_3 (2 wt% Ag) has shown promising results and is being considered as a benchmark catalyst for HC-SCR of NO_x for diesel engine exhaust. However Ag/Al_2O_3 catalyst is not efficient for practical application at lower temperature of diesel engine exhaust due to narrow temperature window, low sulfur and water tolerance. The improvement in low temperature deNO_x activity of Ag/Al_2O_3 catalyst is being investigated by varying the catalyst composition and the method of preparation. Sulphur and water tolerance of Ag/Al_2O_3 has been improved by modification of support by SiO_2, TiO_2 and MgO previously. Activity of Ag/Al_2O_3 can be improved by addition of second metal (Au), as small amount of Au which significantly improved the activity of bimetallic catalyst and it also showed activity at higher temperature which is reported in literature.

In present work we have prepared the bimetallic Ag-Au catalyst supported on in house prepared high surface area alumina (450 m^2g^{-1}) by different methods like successive impregnation and co-impregnation. In successive impregnation method the order of metal

impregnation was also changed. In first method, Au was deposited on alumina using urea followed by impregnation of Ag after drying AuAl at 80 ºC (AgAuAl). In second method, first Ag was impregnated on alumina followed by Au using urea as precipitating agent (AuAgAl) and later Au and Ag were impregnated simultaneously on alumina (Au-Ag/Al). The effect of amount of metal loading on SCR activity of bimetallic Ag-Au/Al_2O_3 catalyst has been also studied by varying Au or Ag loading (1 and 2 wt%) on alumina which was synthesized by successive impregnation method and by changing the order of metal impregnation.

The effect of different thermal pretreatment was analyzed on bimetallic catalyst prepared by successive impregnation method. Pretreatment at 250 ºC in flow of hydrogen was found to give the best results compared to pretreatment at 500 ºC in H_2 or air. When effect of preparation methods was studied, Ag-Au/Al_2O_3 (AgAuAl) catalyst prepared by successive impregnation method, showed higher NO conversion to N_2 at lower temperature compared to 1Ag/Al_2O_3 and 1Au/Al_2O_3. Further ageing of the catalyst under reaction feed at 500 ºC resulted in considerable increase in low temperature activity of bimetallic catalyst. Even though the SCR activity of pretreated AgAuAl (Ag-Au/Al_2O_3) and AgAl (Ag/Al_2O_3) were comparable, after ageing the Ag-Au/Al_2O_3 showed significantly higher NO conversion compared to AgAl (Ag/Al_2O_3) and AuAl (Au/Al_2O_3). In case of bimetallic AuAgAl (Au-Ag/Al_2O_3) catalyst prepared by reversing the order of metal impregnation, showed maximum activity at lower temperature. Catalytic performance of bimetallic AuAgAl (Au-Ag/Al_2O_3) catalyst was to be sensitive to the preparation protocol. Optimal surface properties involve the participation of metallic and electrophilic sites to catalyze respectively NO oxidation to NO_2 and its subsequent reduction to nitrogen. Different parameters can contribute to get such an optimal balance taking into account the size and shape of the particle and inhomogeneity in surface composition in the case of bimetallic catalysts. It was found that co-impregnation leads to the preferential formation of alloyed particles more active for oxidative reaction than reductive ones resulting in a poor conversion of NO_x to nitrogen. Subsequent exposure at high temperature in reactive conditions has a strong detrimental effect due to particle sintering altering the metal/support interface and a strengthening of the metallic character which favor the total oxidation of reducing agents. For catalysts prepared by successive impregnation, starting from Au/Al_2O_3 or Ag/Al_2O_3 and then introducing respectively silver or gold leads inevitably to a significant surface silver enrichment. This option considerably improve NO conversion which was ascribed to synergistic effect between Au and Ag with re-

dispersion processes of large AgCl particles into Ag_2O interacting with gold particles preventing their sintering after ageing. An optimal balance between oxidative and reductive surface properties was obtained when Au and Ag were successively introduced. Significant re-dispersion processes took place when the catalyst was aged at 500 ºC leading to a gain in activity at low temperature which was ascribed to a better interaction between Au and Ag species. Co-impregnation led to a preferential formation of intermetallic Au–Ag particles which was detrimental to the catalytic performances. Ageing at 500 ºC led to a significant particle sintering and a strengthening of the metallic character.

Further more to analyze the effect of amount of metal loading, either Ag or Au was increased to 2 wt% by successive impregnation (2AgAuAl, Ag2AuAl, Au2AgAl, 2AuAgAl). Catalyst with higher Ag loading showed considerable improvement in SCR activity especially increases in low temperature activity. The effect was further improved when order of metal loading was reversed (Au2AgAl) with considerable widening of the temperature range of SCR activity from 150 to 450 ºC.

The catalyst prepared by successive impregnation method (AgAuAl, 2AgAuAl, Ag2AuAl) and by reversing the order of impregnation (AuAgAl, Au2AgAl, 2AuAgAl) showed considerable improvement in SCR activity compared to the catalyst prepared by co-impregnation (Au-Ag/Al). All catalyst prepared by successive impregnation showed enhancement in low temperature SCR activity after ageing. The catalyst with higher silver loading (2AgAuAl, Au2AgAl) showed significant improvement in low temperature activity with widening of temperature window (150 -450ºC). Detailed investigation of the textural properties of the pretreated and aged catalysts showed presence of well dispersed metallic Au and $Ag_n^{\delta+}$ clusters. Low amount of gold assisted for improving the dispersion of Ag after ageing, as well as more formation of $Ag_n^{\delta+}$ species which helped in enhancing low temperature activity. Whereas increased gold loading showed agglomeration after ageing, which has detrimental effect on activity. In conclusion by varying the method of preparation, catalyst pretreatment and amount of metal loading, considerable improvement in low temperature SCR activity is achieved with significant widening in temperature range from 150 to 450 ºC for SCR of NO_x from lean burn diesel engine exhaust.

List of Publications

Patent

1. **Non noble metal based diesel oxidation catalyst,** Shubhangi B. Umbarkar, Mohan K. Dongare, Pavan M. More, Ankush V. Biradar,Patent filed (NCL No. INV-2013-144).

Publications from the thesis

1) **Ag-Au/Al_2O_3 Bimetallic Catalysts for Improved Low Temperature HC-SCR of NO_x for Lean Burn Engine Exhaust: Influence of thermal activation pretreatment**
P. M. More, D.L. Nguyen, M. K. Dongare, S.B. Umbarkar, P. Granger, C. Dujardin. Applied Catalysis B: Environmental 174 (2015) 145–156.

2) **Rational preparation of Ag and Au bimetallic catalysts for the hydrocarbon-SCR of NOx: Sequential deposition vs. co-precipitation method**
P. M. More, D.L. Nguyen, M. K. Dongare, S.B. Umbarkar, N. Nuns, J.-S. Girardon, C. Dujardin, C. Lancelot, A.-S. Mamede, P. Granger, Applied Catalysis B: Environmental 162 (2015) 11–20.

2) **Effect of metal loading on SCR of NO_x by hydrocarbon using bimetallic catalysts.**
P. M. More, M. K. Dongare, S. B. Umbarkar, P. Granger, C. Dujardin. Manuscript under preparation

Other publications

1) **Magnesia doped Ag/Al_2O_3– Sulfur tolerant catalyst for low temperature HC-SCR of NOx** Pavan M. More, Neelam Jagtap, Atul B. Kulal, Mohan K. Dongare, Shubhangi B. Umbarkar. Applied Catalysis B: Environmental 144 (2014) 408– 415.

2) **A Greener route for synthesis of efficient solid base catalyst by covalently grafting organoamines onto carbon microspheres**
Doke Dhananjay; More Pavan; Umbarkar Shubhangi; Biradar Ankush**,** Accepeted in Applied catalysis A

Presentations at Symposia

1. Magnesia doped Ag/Al_2O_3- sulphur tolerant catalyst for low temperature HC-SCR of NOx, in workshop on catalysis for sustainable development held at CSIR-National Environmental engineering research institute, Nagpur, India. Feb-2014 **"Best poster award".**

2.Oral Presentation on "Bimetallic Catalyst for HC-SCR of NO_x under lean burn condition" in catalysis for sustainable and environmental chemistry held at Lille University, France, in June-2012.

3. Oral Presentation on "$Ag\text{-}Au/Al_2O_3$ Bimetallic Catalysts for Improved Low Temperature HC-SCR of NO_x for Lean Burn Engine Exhaust: Influence of thermal activation pretreatment" in catalysis for sustainable and environmental chemistry held at CSIR-National Chemical Laboratory, India, in Oct-2014.